Global Forest Monitoring from Earth Observation

Earth Observation of Global Changes

Series Editor
Chuvieco Emilio

Global Forest Monitoring from Earth Observation
edited by Frédéric Achard and Matthew C. Hansen

Global Forest Monitoring from Earth Observation

Edited by

Frédéric Achard • Matthew C. Hansen

CRC Press
Taylor & Francis Group
Boca Raton London New York

CRC Press is an imprint of the
Taylor & Francis Group, an **informa** business

Joint Research Centre, Institute for Environment and Sustainability

CRC Press
Taylor & Francis Group
6000 Broken Sound Parkway NW, Suite 300
Boca Raton, FL 33487-2742

International Standard Book Number: 978-1-1380-7447-7 (Paperback)
International Standard Book Number: 978-1-4665-5201-2 (Hardback)

Library of Congress Cataloging-in-Publication Data

Global forest monitoring from earth observation / edited by Frederic Achard and Matthew C. Hansen.
p. cm.
Includes bibliographical references and index.
ISBN 978-1-4665-5201-2
1. Forests and forestry--Remote sensing. 2. Forest monitoring. I. Achard, Frédéric. II. Hansen, Matthew C.

SD387.R4G56 2012
333.75--dc23 2012018562

Visit the Taylor & Francis Web site at
http://www.taylorandfrancis.com

and the CRC Press Web site at
http://www.crcpress.com

Contents

Preface..vii
Editors...ix
Contributors...xi

1. **Why Forest Monitoring Matters for People and the Planet**..................1
   Ruth DeFries

2. **Role of Forests and Impact of Deforestation in the Global Carbon Cycle**...15
   Richard A. Houghton

3. **Use of Earth Observation Technology to Monitor Forests across the Globe**..39
   Frédéric Achard and Matthew C. Hansen

4. **Global Data Availability from U.S. Satellites: Landsat and MODIS**...55
   Thomas R. Loveland and Matthew C. Hansen

5. **Sampling Strategies for Forest Monitoring from Global to National Levels**...65
   Stephen V. Stehman

6. **Use of Coarse-Resolution Imagery to Identify Hot Spots of Forest Loss at the Global Scale**..93
   Matthew C. Hansen, Peter Potapov, and Svetlana Turubanova

7. **Use of a Systematic Statistical Sample with Moderate-Resolution Imagery to Assess Forest Cover Changes at Tropical to Global Scale**..111
   Frédéric Achard, Hans-Jürgen Stibig, René Beuchle, Erik Lindquist, and Rémi D'Annunzio

8. **Monitoring Forest Loss and Degradation at National to Global Scales Using Landsat Data**..129
   Peter Potapov, Svetlana Turubanova, Matthew C. Hansen, Ilona Zhuravleva, Alexey Yaroshenko, and Lars Laestadius

9. **The Brazilian Amazon Monitoring Program: PRODES and DETER Projects** ... 153
Yosio Edemir Shimabukuro, João Roberto dos Santos, Antonio Roberto Formaggio, Valdete Duarte, and Bernardo Friedrich Theodor Rudorff

10. **Monitoring of Forest Degradation: A Review of Methods in the Amazon Basin** ... 171
Carlos Souza, Jr.

11. **Use of Wall-to-Wall Moderate- and High-Resolution Satellite Imagery to Monitor Forest Cover across Europe** ... 195
Jesús San-Miguel-Ayanz, Daniel McInerney, Fernando Sedano, Peter Strobl, Pieter Kempeneers, Anssi Pekkarinen, and Lucia Seebach

12. **Monitoring U.S. Forest Dynamics with Landsat** ... 211
Jeffrey G. Masek and Sean P. Healey

13. **Long-Term Monitoring of Australian Land Cover Change Using Landsat Data: Development, Implementation, and Operation** ... 229
Peter Caccetta, Suzanne Furby, Jeremy Wallace, Xiaoliang Wu, Gary Richards, and Robert Waterworth

14. **Assessment of Burned Forest Areas over the Russian Federation from MODIS and Landsat-TM/ETM+ Imagery** ... 245
Sergey Bartalev, Vyacheslav Egorov, Victor Efremov, Evgeny Flitman, Evgeny Loupian, and Fedor Stytsenko

15. **Global Forest Monitoring with Synthetic Aperture Radar (SAR) Data** ... 273
Richard Lucas, Ake Rosenqvist, Josef Kellndorfer, Dirk Hoekman, Masanobu Shimada, Daniel Clewley, Wayne Walker, and Humberto Navarro de Mesquita, Jr.

16. **Future Perspectives (Way Forward)** ... 299
Alan Belward, Frédéric Achard, Matthew C. Hansen, and Olivier Arino

Index ... 307

Preface

Forest resources are crucial in the context of sustainable development and climate change mitigation. Dynamic information on the location and evolution of forest resources are needed to properly define, implement, and evaluate strategies related to multilateral environmental agreements such as the UN Framework Convention on Climate Change (UNFCCC) and the Convention on Biological Diversity. For the global change scientific community and the UNFCCC process, it is important to tackle the technical issues surrounding the ability to produce accurate and consistent estimates of greenhouse gas emissions and removals from forest area changes worldwide and at the country level.

The following compilation of chapters constitutes a review of why and how researchers currently use remotely sensed data to study forest cover extent and loss over large areas. Remotely sensed data are most valuable where other information, for example, forest inventory data, are not available, or for analyses of large areas for which such data cannot be easily acquired. The ability of a satellite sensor to synoptically measure the land surface from national to global scales provides researchers, governments, civil society, and private industry with an invaluable perspective on the spatial and temporal dynamics of forest cover changes. The reasons for quantifying forest extent and change rates are many. In addition to commercial exploitation and local livelihoods, forests provide key ecosystem services including climate regulation, carbon sequestration, watershed protection, and biodiversity conservation, to name a few. Many of our land use planning decisions are made without full understanding of the value of these services, or of the rate at which they are being lost in the pursuit of more immediate economic gains through direct forest exploitation. Our collection of papers begins with an introduction on the roles of forests in the provision of ecosystem services and the need for monitoring their change over time (Chapters 1 and 2).

We follow this introduction with an overview on the use of Earth observation datasets in support of forest monitoring (Chapters 3 through 5). General methodological differences, including wall-to-wall mapping and sampling approaches, as well as data availability, are discussed. For large-area monitoring applications, the need for systematically acquired low or no cost data cannot be overstated. To date, data policy has been the primary impediment to large-area monitoring, as national to global scale forest monitoring requires large volumes of consistently acquired and processed imagery. Without this, there is no prospect for tracking the changes to this key Earth system resource.

The main section of the book covers forest monitoring using optical data sets (Chapters 6 through 14). Optical datasets, such as Landsat, constitute the longest record of the Earth surface. Our experience of using them in mapping and monitoring forest cover is greater than that of other datasets due to the relatively rich record of optical imagery compared to actively acquired data sets such as radar imagery. The contributions to this section range from indicator mapping at coarse spatial resolution to sample-based assessments and wall-to-wall mapping at medium spatial resolution. The studies presented span scales, environments, and themes. For example, forest degradation, as opposed to stand-replacement disturbance, is analyzed in two chapters. Forest degradation is an important variable regarding biomass, emissions, and ecological integrity, as well as being a technically challenging theme to map. Chapters 6 through 14 also present a number of operational systems, from Brazil's PRODES and DETER products, to Australia's NCAS system. These chapters represent the maturity of methods as evidenced by their incorporation by governments into official environmental assessments. The fourth section covers the use of radar imagery in forest monitoring (Chapter 15). Radar data have a long history of experimental use and are presented here as a viable data source for global forest resource assessment.

We believe that this book is a point of departure for the future advancement of satellite-based monitoring of global forest resources. More and more observing systems are being launched, methods are quickly maturing, and the need for timely and accurate forest change information is increasing. If data policies are progressive, users of all kinds will soon have the opportunity to test and implement forest monitoring methods. Our collective understanding of forest change will improve dramatically. The information gained through these studies will be critical to informing policies that balance the various demands on our forest resources. The transparency provided by Earth observation data sets will, at a minimum, record how well we perform in this task.

We deeply thank Prof. Emilio Chuvieco from the University of Alcalá (Spain) who gave us the opportunity to publish this book and supported and encouraged us in its preparation. We also sincerely thank all the contributors who kindly agreed to take part in this publication and who together have produced a highly valuable book.

Frédéric Achard and Matthew C. Hansen

Editors

Dr. Frédéric Achard is a senior scientist at the Joint Research Centre (JRC), Ispra, Italy. He first worked in optical remote sensing at the Institute for the International Vegetation Map (CNRS/University) in Toulouse, France. Having joined the JRC in 1992, he started research over Southeast Asia in the framework of the TREES (TRopical Ecosystem Environment observations by Satellites) project. His current research interests include the development of Earth observation techniques for global and regional forest monitoring and the assessment of the implications of forest cover changes in the tropics and boreal Eurasia on the global carbon budget. Frédéric Achard received his PhD in tropical ecology and remote sensing from Toulouse University, Toulouse, France, in 1989. He has coauthored over 50 scientific peer-reviewed papers in leading scientific journals including *Nature*, *Science*, *International Journal of Remote Sensing*, *Forest Ecology and Management*, *Global Biogeochemical Cycles*, and *Remote Sensing of Environment*.

Dr. Matthew C. Hansen is a professor in the Department of Geographical Sciences at the University of Maryland, College Park, Maryland. He has a bachelor of electrical engineering degree from Auburn University, Auburn, Alabama. His graduate degrees include a master of engineering in civil engineering and a master of arts in geography from the University of North Carolina at Charlotte and a doctoral degree in geography from the University of Maryland, College Park, Maryland. His research specialization is in large-area land cover monitoring using multispectral, multitemporal, and multiresolution remotely sensed data sets. He is an associate member of the MODIS (Moderate Resolution Imaging Spectroradiometer) Land Science Team and a member of the GOFC-GOLD (Global Observations of Forest Cover and Land Dynamics) Implementation Working Group.

Taylor & Francis
Taylor & Francis Group
http://taylorandfrancis.com

Contributors

Frédéric Achard
Institute for Environment
and Sustainability
Joint Research Centre of
the European Commission
Ispra, Italy

Olivier Arino
Earth Observation Directorate
European Space Agency
Frascati, Italy

Sergey Bartalev
Space Research Institute
Russian Academy of Sciences
Moscow, Russian Federation

Alan Belward
Institute for Environment
and Sustainability
Joint Research Centre of
the European Commission
Ispra, Italy

René Beuchle
Institute for Environment
and Sustainability
Joint Research Centre of
the European Commission
Ispra, Italy

Peter Caccetta
Mathematics, Statistics
and Informatics
Commonwealth Scientific and
Industrial Research Organisation
Floreat, Western Australia,
Australia

Daniel Clewley
Institute of Geography and Earth
Sciences
Aberystwyth University
Aberystwyth, United Kingdom

Rémi D'Annunzio
Forestry Department
Food and Agriculture Organization
of the United Nations
Rome, Italy

Ruth DeFries
Department of Ecology, Evolution
and Environmental Biology
Columbia University
New York, New York

Valdete Duarte
Remote Sensing Division
Brazilian Institute for Space
Research
São Paulo, Brazil

Victor Efremov
Space Research Institute
Russian Academy of Sciences
Moscow, Russian Federation

Vyacheslav Egorov
Space Research Institute
Russian Academy of Sciences
Moscow, Russian Federation

Evgeny Flitman
Space Research Institute
Russian Academy of Sciences
Moscow, Russian Federation

Antonio Roberto Formaggio
Remote Sensing Division
Brazilian Institute for Space Research
São Paulo, Brazil

Suzanne Furby
Mathematics, Statistics
and Informatics
Commonwealth Scientific
and Industrial Research
Organisation
Floreat, Western Australia, Australia

Matthew C. Hansen
Department of Geographical
Sciences
University of Maryland
College Park, Maryland

Sean P. Healey
Rocky Mountain Research Station
U.S. Forest Service
Ogden, Utah

Dirk Hoekman
Department of Environmental
Sciences, Earth System Science
and Climate Change Group
Wageningen University
Wageningen, The Netherlands

Richard A. Houghton
Woods Hole Research Center
Falmouth, Massachusetts

Josef Kellndorfer
Woods Hole Research Center
Falmouth, Massachusetts

Pieter Kempeneers
Earth Observation Department
Flemish Institute for Technological
Research
Mol, Belgium

Lars Laestadius
People and Ecosystems
Department
World Resources Institute
Washington, DC

Erik Lindquist
Forestry Department
Food and Agriculture Organization
of the United Nations
Rome, Italy

Evgeny Loupian
Space Research Institute
Russian Academy of Sciences
Moscow, Russian Federation

Thomas R. Loveland
Earth Resources Observation
and Science Center
U.S. Geological Survey
Sioux Falls, South Dakota

Richard Lucas
Institute of Geography
and Earth Sciences
Aberystwyth University
Aberystwyth, United Kingdom

Jeffrey G. Masek
NASA Goddard Space Flight Center
Greenbelt, Maryland

Daniel McInerney
Institute for Environment
and Sustainability
Joint Research Centre of the
European Commission
Ispra, Italy

Humberto Navarro de Mesquita, Jr.
National Forest Registry
Brazilian Forest Service
Brasilia, Brazil

Anssi Pekkarinen
Forestry Department
United Nations Food and Agriculture Organization
Rome, Italy

Peter Potapov
Department of Geographical Sciences
University of Maryland
College Park, Maryland

Gary Richards
Department of Climate Change and Energy Efficiency
Canberra, Australia
and
Fenner School of Environment and Society
Australian National University
Canberra, Australia

Ake Rosenqvist
solo Earth Observation
Tokyo, Japan

Bernardo Friedrich Theodor Rudorff
Remote Sensing Division
Brazilian Institute for Space Research
São Paulo, Brazil

Jesús San-Miguel-Ayanz
Institute for Environment and Sustainability
Joint Research Centre of the European Commission
Ispra, Italy

João Roberto dos Santos
Remote Sensing Division
Brazilian Institute for Space Research
São Paulo, Brazil

Fernando Sedano
Institute for Environment and Sustainability
Joint Research Centre of the European Commission
Ispra, Italy

Lucia Seebach
Department of Forest and Landscape
University of Copenhagen
Copenhagen, Denmark

Yosio Edemir Shimabukuro
Remote Sensing Division
Brazilian Institute for Space Research
São Paulo, Brazil

Masanobu Shimada
Earth Observation Research Center
Japan Aerospace Exploration Agency
Tokyo, Japan

Carlos Souza, Jr.
Amazon Institute of People and the Environment
Belém, Pará, Brazil

Stephen V. Stehman
College of Environmental Science and Forestry
State University of New York
Syracuse, New York

Hans-Jürgen Stibig
Institute for Environment and Sustainability
Joint Research Centre of the European Commission
Ispra, Italy

Peter Strobl
Institute for Environment and Sustainability
Joint Research Centre of the European Commission
Ispra, Italy

Fedor Stytsenko
Space Research Institute
Russian Academy of Sciences
Moscow, Russian Federation

Svetlana Turubanova
Department of Geographical Sciences
University of Maryland
College Park, Maryland

Wayne Walker
Woods Hole Research Center
Falmouth, Massachusetts

Jeremy Wallace
Mathematics, Statistics and Informatics
Commonwealth Scientific and Industrial Research Organisation
Floreat, Western Australia, Australia

Robert Waterworth
Department of Climate Change and Energy Efficiency
Canberra, Australia

Xiaoliang Wu
Mathematics, Statistics and Informatics
Commonwealth Scientific and Industrial Research Organisation
Floreat, Western Australia, Australia

Alexey Yaroshenko
Greenpeace Russia
Moscow, Russian Federation

Ilona Zhuravleva
Greenpeace Russia
Moscow, Russian Federation

6

Use of Coarse-Resolution Imagery to Identify Hot Spots of Forest Loss at the Global Scale

Matthew C. Hansen, Peter Potapov, and Svetlana Turubanova
University of Maryland

CONTENTS

6.1 Introduction 93
6.1.1 MODIS 93
6.1.2 Global Forest Cover Mapping to Date 94
6.1.3 Global Forest Cover Loss Mapping Using MODIS 94
6.2 Data 96
6.3 Algorithm 96
6.4 Results 97
6.5 Conclusion 105
Acknowledgment 106
About the Contributors 107
References 107

6.1 Introduction

6.1.1 MODIS

The MODIS (Moderate Resolution Imaging Spectroradiometer) sensor onboard NASA's Terra spacecraft has advanced large-area land monitoring during its 10-plus years of operation. Compared to heritage instruments such as the advanced very high-resolution radiometer (AVHRR) meteorological sensor, MODIS represented a significant gain in global land mapping and monitoring capabilities. First, the MODIS sensor has a finer instantaneous field of view compared to other global daily observing systems, including bands with 250, 500, and 1000 m spatial resolutions. Second, MODIS was built with seven bands specifically designed for land cover monitoring by avoiding wavelengths affected by atmospheric scattering and absorption. Third, the 250 m spatial resolution of the red and near-infrared bands was designed specifically to enable the monitoring of land cover change (Justice et al. 1998). Other sensors with global land monitoring capabilities, including SPOT VEGETATION and ENVISAT MERIS, with 1 km and 300 m spatial resolutions, respectively, have also been designed for land monitoring applications. However, MODIS retains the finest spatial resolution observational capability for this class of sensors. While a second MODIS sensor onboard NASA's Aqua spacecraft was launched in 2002, MODIS Terra data have been more widely used in land cover analyses and are the data used in the study presented here.

6.1.2 Global Forest Cover Mapping to Date

A viable solution to examining trends in forest cover change over large areas is to employ remotely sensed data. Satellite-based monitoring of forest clearing can be implemented consistently across large regions at a fraction of the cost of obtaining extensive ground inventory data. Forest inventories are typically unable to quantify forest dynamics at annual intervals due to the costs and logistical challenges of frequently revisiting plots. On the other hand, remotely sensed data enable the synoptic quantification of forest cover and change at regular intervals, providing information on where and how fast forest change is taking place at annual or finer time scales (INPE 2008). While numerous national-scale forest change products exist, global forest change characterizations are comparatively rare. Initial global forest mapping efforts focused on static map products of forest cover, typically as part of multiclass land cover classifications. The IGBP DISCover project (Loveland et al. 2000) used 1 km AVHRR data to produce a global land cover product that included forest leaf type and longevity classes, as did Hansen et al. (2000) with the University of Maryland (UMD) land cover map. Friedl et al. (2002) advanced these efforts in creating the standard MODIS land cover product (MOD12Q1), and Bartholomé et al. (2005) used SPOT VEGETATION data to produce the Global Landcover 2000 (GLC2000) product, both of which contained multiple forest type/density classes. Similarly, the Globcover initiative used 300 m ENVISAT MERIS data to produce a global multiforest class land cover map for 2005–2006 (Arino et al. 2007). Forests as a specific target have been mapped at the global scale as well. Global subpixel percent tree cover maps have been generated using AVHRR data (Hansen and DeFries 2004) and as a standard product using MODIS data, the vegetation continuous field (VCF) of percent tree cover (Hansen et al. 2003). Regarding global forest change, the 8 km AVHRR Pathfinder data set was used to estimate tree cover change from 1982 to 1999 from time-sequential percent tree cover maps (Hansen and DeFries 2004).

6.1.3 Global Forest Cover Loss Mapping Using MODIS

A more recent global forest cover change assessment employed MODIS data to quantify gross forest cover loss (Hansen et al. 2010). In this study, MODIS 500 m forest cover loss indicator maps were used to stratify biomes into homogeneous regions with respect to change (high, medium, and low forest cover loss strata). Within each stratum, samples of Landsat data were drawn and analyzed in order to estimate forest cover extent in 2000 and forest cover loss from 2000 to 2005. Stratum-specific regression estimators incorporating the MODIS-derived forest cover loss data as an auxiliary variable were applied to generate the final forest cover loss estimates. These results demonstrated the effectiveness of using the MODIS forest cover loss data to provide a spatially fine-grained stratification that offered an improvement over more generalized hot spot stratifications subjectively delineated to define low and high forest clearing strata (Achard et al. 2002).

The focus of this study is to extend this previous MODIS work and map indicated forest cover loss at 250 m spatial resolution over the 2000–2010 period. To do so, a turn-key algorithm is run on the 2000–2005 and 2005–2010 epochs. Previous work on multiyear forest cover change quantification using AVHRR data employed a recalibrated model for each year of analysis (Hansen and DeFries 2004). However, as MODIS data feature consistent radiometric calibration (Vermote et al. 2002), it is expected that the change signal being trained upon may be reliably and repeatedly captured over time. Our previous work with MODIS has employed turn-key models applied annually to identify change (Hansen et al. 2008; Potapov et al. 2008). For this study, we employ a fixed characterization algorithm for the 2000–2005 and 2005–2010 epochs. Calibration issues with MODIS have been studied, and a degradation of the near-infrared band quantified for MODIS Terra (Wang et al. 2012).

Given this fact, the use of turn-key approaches to repeatedly mapping land cover with the Terra instrument has come into question (Vermote E., personal communication). We present the following results more as a demonstration of global change mapping methods and not as a definitive long-term environmental change record. MODIS data are imaged nearly daily at the global scale, improving the probability of cloud-free acquisitions. This high-temporal acquisition frequency ensures a consistent and largely cloud-free image feature space at annual time scales. However, the moderate spatial resolution of MODIS is a limitation for area estimation of forest cover loss as much forest disturbance occurs at sub-MODIS pixel scales. The most appropriate use of MODIS for forest monitoring is as an alarm or hot spot indicator (INPE 2008; Hansen et al. 2010; Shimabukuro et al. 2012). Area estimation requires the integration of MODIS with a higher spatial resolution sensor, such as Landsat or another medium spatial resolution data source. MODIS-only products such as the ones presented in this study capture relative rates of forest cover loss across space and through time, with a considerable omission rate for small-scale forest disturbances.

The method presented here demonstrates a global assessment of forest cover loss using MODIS data from 2000 to 2010. For this study, forest clearing equals gross forest cover loss during the study period without quantification of contemporaneous gains in forest cover due to reforestation or afforestation. Forest cover loss is defined as a stand-replacement disturbance of a forest, where forest is defined as an assemblage of trees having a height of 5 m or greater and a canopy crown cover in excess of 25% at the MODIS pixel scale. The method could be implemented repeatedly for both forest cover loss and gain in establishing internally consistent biome-scale trends in both gross and net forest cover loss and gain.

6.2 Data

The 2000–2011 global Terra/MODIS 250 m data 16-day composite data set (MOD44C, collection 5) from the University of Maryland was used. This data set was originally created as an input to the vegetative continuous fields and vegetative cover conversion product and is described in Carroll et al. (2010). Four reflective bands—band 1/red (620–670 nm), band 2/near infrared (841–876 nm), band 6/shortwave infrared (1,628–1,652 nm), and band 7/shortwave infrared (2,105–2,155 nm), along with band 31/thermal (10,780–11,280 nm) and computed normalized difference vegetation index (NDVI)—were used.

Six-year MODIS metrics were derived for 2000 through 2005 and 2005 through 2011. Metrics have been shown to enable large-area mapping by generalizing the multispectral feature space, enabling signature extension over large areas (Reed et al. 1994; DeFries et al. 1995; Hansen et al. 2005). Each band was ranked individually and by temperature and NDVI. Ranked metrics calculated for all bands included 0, 10, 25, 50, 75, 90, and 100 percentiles. Averages between percentiles were also calculated. Annual metrics were generated and used as metrics and as inputs to a time-series regression calculation. Means of the three values corresponding to highest annual NDVI and band 31 brightness temperature were derived and used as the annual inputs and for the regression calculation.

An extensive Landsat-scale training data set was produced for calibrating the algorithm. National-scale products for Indonesia (Broich et al. 2011); the Democratic Republic of the Congo (Potapov et al. in press); European Russia (Potapov et al. 2011); Quebec, Canada; and Brazil, along with an additional 203 image pairs, were used as training data. The majority of the training data were from the 2000 to 2005 epoch. Only the Indonesia and Democratic Republic of the Congo data included 2005–2010 change data. The Landsat-scale forest cover loss maps were aggregated to the MODIS grid as percent forest cover loss. A total of over 23,000,000 pixels at MODIS scale were available as training data.

6.3 Algorithm

Decision trees are a type of distribution-free machine learning tool appropriate for use with remotely sensed data sets (Michaelson et al. 1994;

Hansen et al. 1996; Freidl and Brodley 1997). They are the primary algorithmic tool used in the standard MODIS land VCF products (Hansen et al. 2003). The VCF products depict the per pixel percent cover of basic vegetation traits, such as herbaceous and tree cover. As trees are distribution free, they allow for the improved representation of training data within the multispectral space. The relationship between the independent and dependent variables need not be monotonic or linear. This allows for more flexible subsetting of the multispectral image space not feasible with many other methods and is most appropriate for large-area studies that feature complicated multispectral signatures. In addition, the tree structure enables the interpretation of the explanatory nature of the independent variables.

Trees can accept either categorical data in performing classifications (classification trees) or continuous data in performing subpixel percent cover estimations (regression trees) (Breiman et al. 1984). For this study, we used the regression tree algorithm of the S-Plus statistical package (Clark and Pergibon 1992) to depict percent forest cover loss. Methods to avoid overfitting of tree models are available. One such approach entails performing multiple, independent runs of decision trees via sampling with replacement. This procedure is called bagging (Breiman 1996). A 10% sample of the training data was used to create each tree, which related the dependent percent forest cover loss variable to the set of MODIS-independent variables. Eleven trees were generated, and the median percent forest cover loss from all bagged trees was retained as the per pixel result. To reduce errors of commission, we thresholded the output product at 30% forest cover loss, converting each map to a yes/no forest cover loss estimate per 250 m MODIS pixel.

6.4 Results

Figure 6.1 shows a global-scale annual growing season metric derived from shortwave infrared, near-infrared, and red growing season imagery from 2000. The spectral feature space is largely cloud free, but persistent haze and partial cloud cover exist in the Andes Mountains of Colombia, northern Brazil, the central African coast along the Gulf of Guinea, and montane Borneo and New Guinea (the haze and residual cloud cover are not visible in the figure). The humid tropics are the only region where atmospheric effects are present in the MODIS metric feature space. Other potential limitations, such as seasonal forests and variable growing season length, are not readily apparent in the metric feature space.

Figures 6.2 and 6.3 provide an example of the derived metric feature space for an area of Mato Grosso, Brazil, and Quebec, Canada, respectively. For these subsets, blue represents year 2000 growing season band 7 shortwave infrared reflectance (mean of the band 7 values corresponding to the three

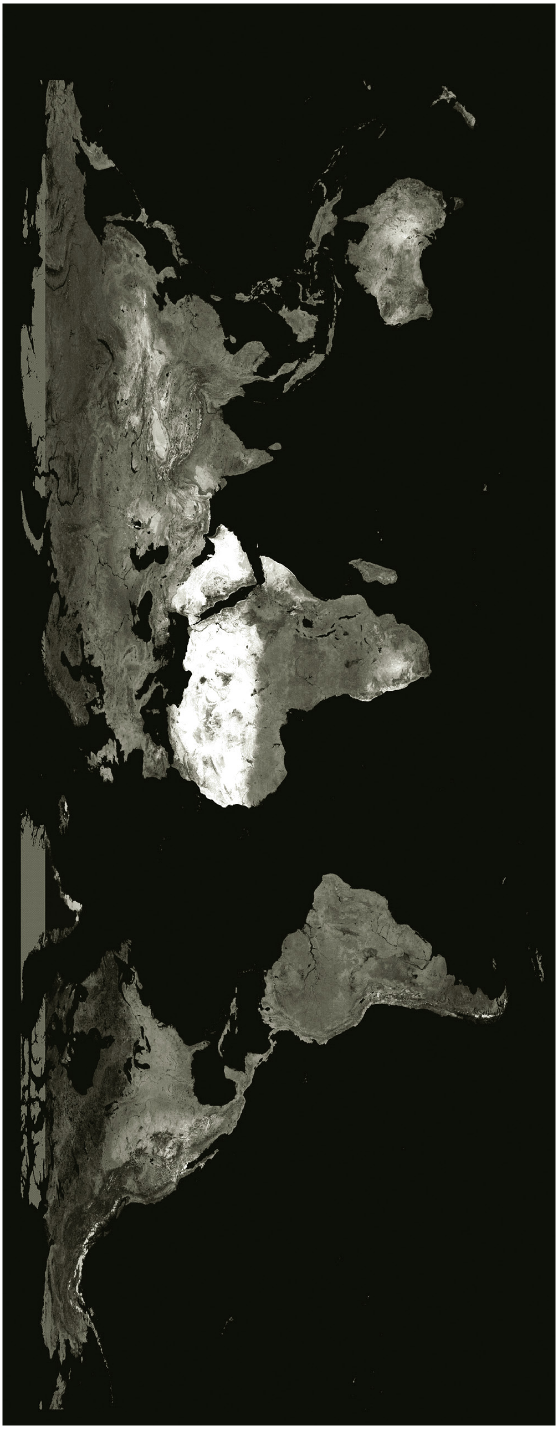

FIGURE 6.1
(See color insert.) MODIS annual growing season image composite of shortwave, near-infrared, and red band, enhanced to appear as true color.

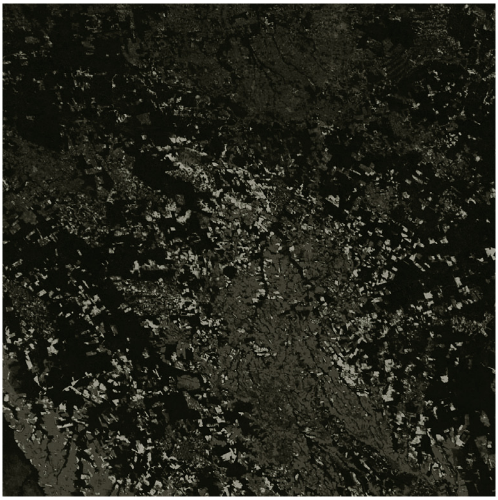

FIGURE 6.2
(See color insert.) 400 km × 400 km subset centered on 12° 4′ S, 55° 59′ W in Mato Grosso, Brazil. False-color composite of MODIS band 7 growing season metrics—*blue*: 2000 mean band 7 shortwave infrared reflectance from the three greenest 16-day composite periods, *green*: difference in the 2000 and 2005 mean band 7 shortwave infrared reflectance from the three greenest 16-day composite periods, and *red*: difference in the 2005 and 2010 mean band 7 shortwave infrared reflectance from the three greenest 16-day composite periods.

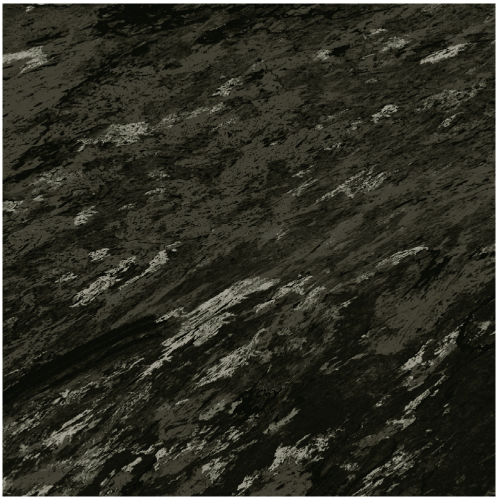

FIGURE 6.3
(See color insert.) 400 km × 400 km subset centered on 51° 45′ N, 72° 8′ W in Quebec, Canada. False-color composite of MODIS band 7 growing season metrics—*blue*: 2000 mean band 7 shortwave infrared reflectance from the three greenest 16-day composite periods, *green*: difference in the 2000 and 2005 mean band 7 shortwave infrared reflectance from the three greenest 16-day composite periods, and *red*: difference in the 2005 and 2010 mean band 7 shortwave infrared reflectance from the three greenest 16-day composite periods.

greenest 16-day composite periods). Areas that are dark in this metric are typically forest (water has been masked out prior to analysis). Green represents the difference for this metric from 2000 to 2005 and red the difference from 2005 to 2010. Pixels that have high increases for this metric, and have an initial dark state (~<5% reflectance), are likely to represent forest disturbance. For the Brazil subset, a dramatic reduction in forest cover loss can be inferred from this false-color composite image. The proportion of 2000–2005 change dwarfs that from 2005 to 2010. For the Canada subset, a less dramatic reduction is observed, related to a predominantly fire-driven dynamic. The tree bagging algorithm formalized the labeling of all forest cover loss pixels.

The global total of MODIS hot spot pixels covered 500,000 km^2 from 2000 to 2005 and 360,000 km^2 from 2005 to 2010. The total MODIS-indicated forest cover loss represents 50% of the total area of gross forest cover loss from the MODIS/Landsat study of Hansen et al. (2010). In other words, the Landsat sample-based area estimate of gross forest cover loss equaled 1,011,000 km^2, while the MODIS hot spot mapped area equaled 500,000 km^2. The MODIS-indicated forest cover loss pixels were aggregated to the same sampling grid as the Hansen et al. study and compared. The following relation yielded an r^2 of 0.64 and a standard error of 1.73%:

$$\text{MODIS/Landsat area} = \text{MODIS-indicated change} \times 0.86 + 0.68$$

Areas from the Hansen et al. (2010) study were reported only for those regions or nations that had sufficient Landsat samples to provide a reasonable uncertainty estimate. These areas included the four major forested biomes (humid tropical, dry tropical, temperate, and boreal), all continents except Antarctica, and countries with over 1,000,000 km^2 of forest cover in 2000. The gross forest cover loss data from Hansen et al. (2010) are plotted against the MODIS-indicated change in Figure 6.4.

The degree of forest cover loss omission in the MODIS data is clear. As stated before, fully half of the global forest cover loss from the Hansen et al. (2010) study is not mapped with MODIS. Regardless, there is a strong overall relationship. Areas where small-scale disturbance predominates, such as Africa, feature the highest proportion of omitted, or cryptic, change. In Figure 6.4 the continent of Africa and the nation of the Democratic Republic of the Congo have the highest ratio of MODIS/Landsat area of forest loss to MODIS-indicated forest loss. This reflects the finer and more diffuse pattern of forest change in Africa where most clearing is performed in swidden agricultural settings too small for quantification using MODIS data. Areas with large agroindustrial clearing, such as Brazil, South America as a whole, and Indonesia, have the lowest omission rates.

The model was applied to the two study intervals, and a comparison of the amount of change hot spots was made. Figures 6.5 and 6.6 illustrate the

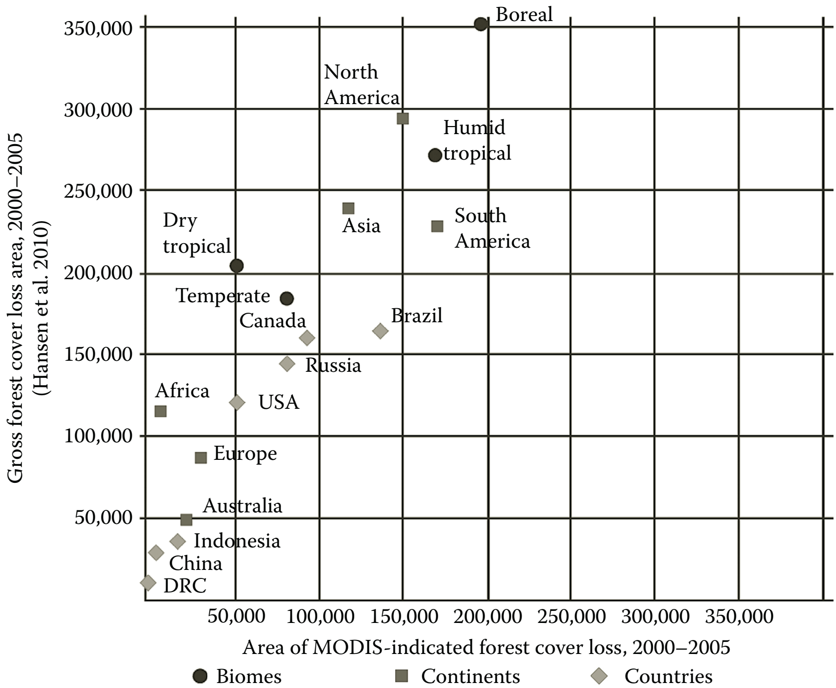

FIGURE 6.4
Plot of area of MODIS-indicated forest cover loss versus gross forest cover loss area for reported regions. (From Hansen, M.C., et al., *Proc. Natl. Acad. Sci.*, 107, 8650, 2010.)

global distribution of MODIS-indicated forest cover loss. The most obvious change in the patterns of forest cover loss is found in Brazil. As Shimabukuro et al. (2012) report, the Brazilian government has sought to reduce the clearing of Amazonian forests, efforts that have included the use of satellite data as an enforcement tool. The global results from Figures 6.5 and 6.6 confirm this reduction. Contrary to this trend is a marked increase in the clearing of the Chaco woodlands of Bolivia, Paraguay, and Argentina between the two periods. Africa is largely absent of large-scale change, with only the agroforestry of South Africa evident at this scale. For tropical Asia, Indonesia exhibits a rise in forest cover loss over the study period. Epochal variation at higher latitudes is less evident and largely due to variations in high latitude fire dynamics as well as storm damage. In general, forest cover losses due to fire appear greater in the 2000–2005 interval than in the 2005–2010 interval (see Alaska, Siberia, and Australia). Areas of active forestry practices feature prominently in both epochs.

Figures 6.7 through 6.9 show the change in MODIS-indicated forest cover loss over the study period. At the biome scale, significant reductions in forest cover loss within the humid tropical and boreal biomes are found.

FIGURE 6.5
(See color insert.) MODIS percent tree cover 2000 and indicated forest cover loss from 2000 to 2005.

FIGURE 6.6
(See color insert.) MODIS percent tree cover 2000 and indicated forest cover loss from 2005 to 2010.

Brazil's reduced clearing drives the humid tropical change, while less forest cover loss due to fire drives the boreal forest change. At the continental scale, the same dynamics are evident, with Europe and Africa exhibiting little or no change in forest cover loss. For countries with greater than 1 Mha of year 2000 forest cover, only Indonesia exhibits a clear increase in forest cover loss.

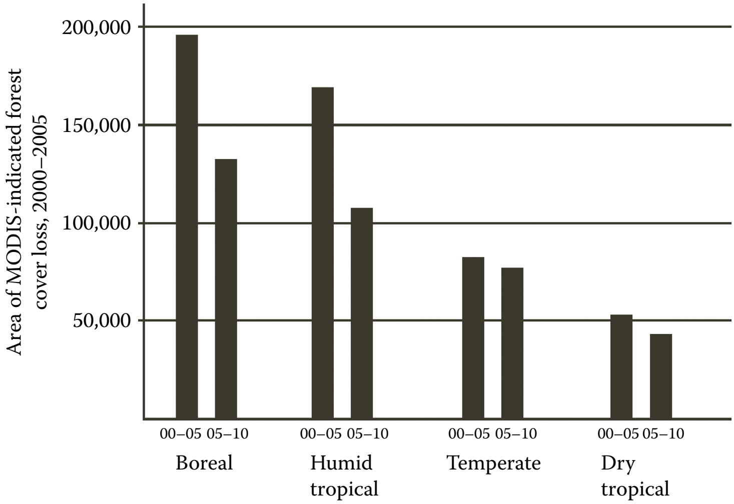

FIGURE 6.7
MODIS-indicated forest cover loss totals per forested biome for the 2000–2005 and 2005–2010 epochs.

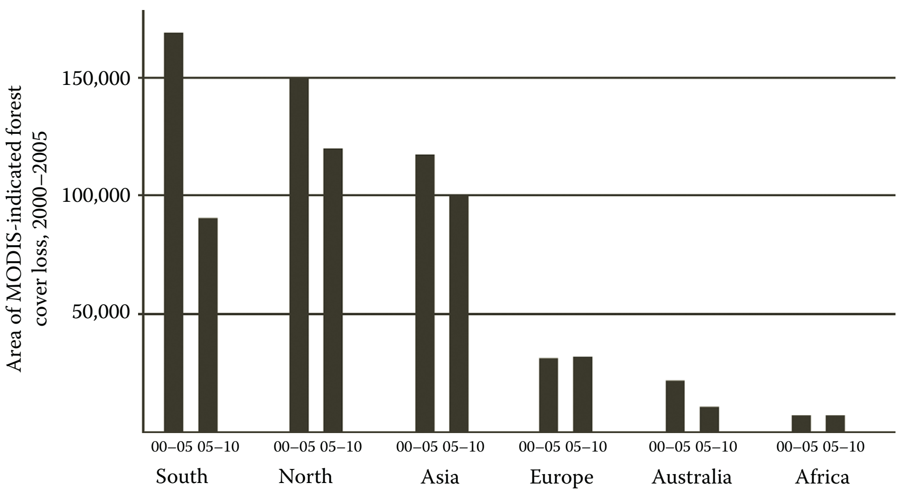

FIGURE 6.8
MODIS-indicated forest cover loss totals per continent for the 2000–2005 and 2005–2010 epochs.

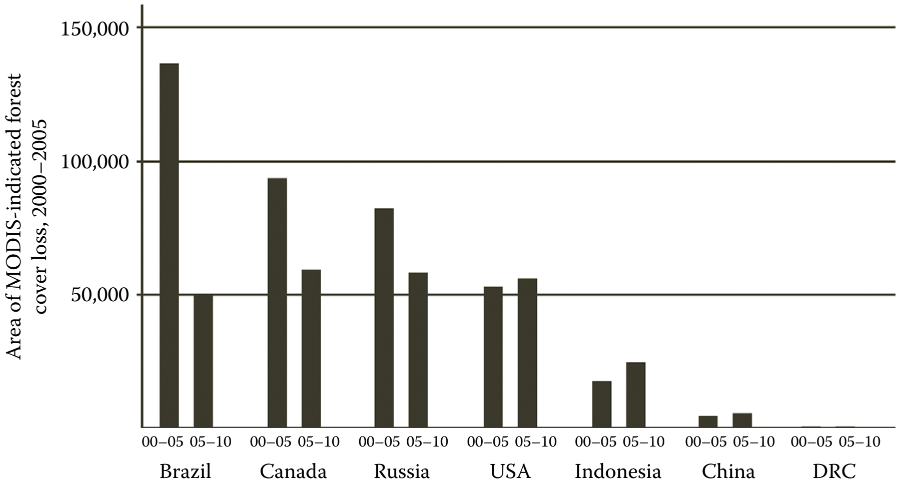

FIGURE 6.9
MODIS-indicated forest cover loss totals per country for the 2000–2005 and 2005–2010 epochs (only countries with greater than 1,000,000 km^2 of forest cover in 2000).

The results, as shown in Figure 6.4, have significant errors of omission, mainly related to the coarse scale of observation, as stated previously. Obvious commission errors are associated largely with two environmental dynamics. First, residual haze and cloud cover impact the metric space and lead to noise-related commission errors in a few humid tropical regions referred to earlier. Second, wetlands are very dynamic in their patterns of spectral change as floods arrive and recede along with attendant vegetation responses. Wetland formations are another source of forest change commission error. Finally, the uncertainty regarding the radiometric stability of the Terra instrument could significantly impact the repeated use of a single model over the two 5-year intervals. Further study is required to resolve the impact of Terra's radiometric degradation on the observed forest extent changes of this study, particularly between the two 5-year epochs.

6.5 Conclusion

The combined high-temporal observation frequency and moderate spatial resolution of MODIS data enable global forest change indicator mapping. The ability to synoptically characterize forest disturbance at the global scale allows for direct comparison of change rates through time and across space. The continuous acquisition of multispectral observations at the global scale for 10+ years illustrates the value of operational systems in quantifying environmental dynamics. As noted, such analyses are dependent on a stable radiometric data source. While MODIS is not an operational system, it enables the development of methods that can be implemented with operational systems such as the recently launched VIIRS (Visible Infrared Imager Radiometer Suite) instrument (Justice et al. 2010). This is a critical monitoring tool of indicators of global change, such as forest dynamics, and its value will only increase with the length of the high-temporal, moderate spatial resolution data record.

Our results document a pervasive and changing global forest disturbance dynamic. Overall, a reduction in stand-replacement forest disturbance from 2000 to 2005 and 2005 to 2010 was found. However, the data represent only indications of forest cover loss, not an estimation of total area, and may also be affected by degradation of the Terra sensor. Differences in epochal change illustrated here are a function of the scale of MODIS observations. Definitive quantification of aerial change over time could be different than that observed with MODIS and would require finer scale time-series imagery for either direct forest area loss estimation or calibration of the MODIS indicator product. The clearest reduction in forest cover loss occurred in Brazil and is related to policy and enforcement efforts to improve regulation of forest clearing in the Brazilian Amazon. Forest cover loss related to fire appeared to decline over the two epochs as well. The drivers of global forest change are many, and the spatial patterns seen in the MODIS change products capture four principle drivers: (1) agroindustrial scale clearing related to land use conversions and forestry practices, (2) fire, (3) disease, and (4) storm damage. Attributing each identified change pixel to a specific driver would greatly enhance the utility of the data for a host of land use and biogeochemical cycle modeling applications.

The ability to quantify both forest cover extent and change independent of land use designations is important in generating a consistent narrative of global forest change. Global observing systems such as MODIS enable such quantifications, but are limited in area estimation. As the discipline moves forward, high-temporal observations will be needed at finer resolutions in order to generate global forest cover extent and change maps that can be used directly in estimating area change. Landsat data, which have included a global acquisition strategy (Arvidson et al. 2001) and are now freely available (Woodcock et al. 2008), will be the data source to extend the methods developed using MODIS to finer spatial scales.

Acknowledgment

Support for this work was provided by the United States National Aeronautics and Space Administration's Land Cover and Land Use Change, MEASURES, and Science of TERRA and AQUA programs under Grants NNG06GD95G, NNX08AP33A, and NNX11AF38G.

About the Contributors

Matthew C. Hansen is a professor in the Department of Geographical Sciences at the University of Maryland, College Park, Maryland. He has a bachelor of electrical engineering from Auburn University, Auburn, Alabama. His graduate degrees include a master of engineering in civil engineering and a master of arts in geography from the University of North Carolina at Charlotte, North Carolina, and a doctoral degree in geography from the University of Maryland, College Park, Maryland. His research specialization is in large-area land cover monitoring using multispectral, multitemporal, and multiresolution remotely sensed data sets. He is an associate member of the MODIS Land Science Team and a member of the GOFC-GOLD Implementation Working Group.

Peter Potapov received a diploma in botany from the Moscow State University, Moscow, Russia, in 2000, and a PhD in ecology and natural resources from the Russian Academy of Science, Moscow, Russia, in 2005. From 1998 to 2006, he was a Geographical Information System (GIS) specialist at Greenpeace (Russian office) where he took part in developing an approach for mapping and monitoring forest degradation using the intact forest landscapes (IFL) method. He was a postdoctoral researcher from 2006 to 2011 at South Dakota State University, Brookings, South Dakota, and currently he is a research associate professor at the University of Maryland, College Park, Maryland. His current research is focused on establishing a global operational forest monitoring algorithm using integration of Landsat and MODIS data.

Svetlana Turubanova received a BSc in geography from the Komi Pedagogical Institute, Syktyvkar, Russia (1996), an MSc in ecology from the Pushchino State University, Pushchino, Russia (1998), and PhD in ecology from the Russian Academy of Science, Moscow, Russia (2002). She started her career as a GIS specialist at Greenpeace Russia in 1999. Later, she was a postdoctoral researcher at South Dakota State University (from 2008 to 2011), Brookings, South Dakota. Currently she is a research associate at the University of Maryland, College Park, Maryland. Her current research interests are focused on national-scale Landsat-based forest mapping, deforestation monitoring, and forest degradation assessment.

References

Arvidson, T., Gasch, J., and Goward, S.N., Landsat 7s long-term acquisition plan—An innovative approach to building a global imagery archive. *Remote Sensing of Environment*, 78, 13, 2001.

Achard, F., et al., Determination of deforestation rates of the world's humid tropical forests. *Science*, 297, 999, 2002.

Arino, O., et al., GlobCover—A global land cover service with MERIS. In *Proceedings of Envisat Symposium 2007*, Montreux, Switzerland, 2007.

Bartholomé, E. and Belward, A.S., GLC2000: A new approach to global land cover mapping from earth observation data. *International Journal of Remote Sensing*, 26, 1959, 2005.

Breiman, L., Bagging predictors. *Machine Learning*, 26, 123, 1996.

Breiman, L., Friedman, J., Olshen, R., and Stone, C. *Classification and Regression Trees*. Monterey, CA: Wadsworth, 1984.

Broich, M., et al., Time-series analysis of multi-resolution optical imagery for quantifying forest cover loss in Sumatra and Kalimantan, Indonesia. *International Journal of Applied Earth Observation and Geoinformation*, 13, 277, 2011.

Carroll, M., et al., Vegetative cover conversion and vegetation continuous fields. In B. Ramachandran, C. Justice, and M. Abrams (Eds.), *Land Remote Sensing and Global Environmental Change: NASA's EOS and the Science of ASTER and MODIS*. New York: Springer, 2010.

Clark, L.A. and Pergibon, D., Tree-based models. In T.J. Hastie (Ed.), *Statistical Models in S*. Pacific Grove, CA: Wadsworth and Brooks, 1992.

DeFries, R., Hansen, M., and Townshend, J., Global discrimination of land cover types from metrics derived from AVHRR Pathfinder data. *Remote Sensing of Environment*, 54, 209, 1995.

Freidl, M.A. and Brodley, C.E., Decision tree classification of land cover from remotely sensed data. *Remote Sensing of Environment*, 61, 399, 1997.

Friedl, M.A., et al., Global land cover mapping from MODIS: Algorithms and early results. *Remote Sensing of Environment*, 83, 287, 2002.

Hansen, M.C. and DeFries, R.S., Detecting long term global forest change using continuous fields of tree cover maps from 8 km AVHRR data for the years 1982–1999. *Ecosystems*, 7, 695, 2004.

Hansen, M.C., DeFries, R.S., Townshend, J.R.G., and Sohlberg, R., Global land cover classification at 1 km spatial resolution using a classification tree approach. *International Journal of Remote Sensing*, 21, 1331, 2000.

Hansen, M., Dubayah, R., and DeFries, R., Classification trees: An alternative to traditional land cover classifiers. *International Journal of Remote Sensing*, 17, 1075, 1996.

Hansen, M.C., Stehman, S.V., and Potapov, P.V., Quantification of global gross forest cover loss, *Proceedings of the National Academy of Sciences*, 107, 8650, 2010.

Hansen, M.C., et al., Global percent tree cover at a spatial resolution of 500 meters: First results of the MODIS vegetation continuous fields algorithm. *Earth Interactions*, 7(10), 15, 2003.

Hansen, M.C., et al., Estimation of tree cover using MODIS data at global, continental and regional/local scales. *International Journal of Remote Sensing*, 26, 4359, 2005.

Hansen, M.C., et al., Humid tropical forest clearing from 2000 to 2005 quantified using multi-temporal and multi-resolution remotely sensed data. *Proceedings of the National Academy of Sciences*, 105, 9439, 2008.

INPE (Instituto Nacional de Pesquisas Espaciais), *Monitoramento da cobertura florestal da Amazônia por satélites: Sistemas PRODES, DETER, DEGRAD E QUEIMADAS 2007–2008*. São José dos Campos, SP, Brazil: Instituto Nacional de Pesquisas Espaciais, 47 p, 2008.

Justice, C.O., et al., The moderate resolution imaging spectroradiometer (MODIS): Land remote sensing for global change research. *IEEE Transactions on Geoscience and Remote Sensing*, 4, 1228, 1998.

Justice C.O., et al., The evolution of U.S. moderate resolution optical land remote sensing from AVHRR to VIIRS. In B. Ramachandran, C.O. Justice, and M.J. Abrams (Eds.), *Land Remote Sensing and Global Environmental Change: NASA's EOS and the Science of ASTER and MODIS*. New York: Springer, 2010.

Loveland, T., et al., Development of a global land cover characteristics database and IGBP DISCover from 1 km AVHRR data. *International Journal of Remote Sensing*, 21, 1303, 2000.

Michaelson, J., et al., Regression tree analysis of satellite and terrain data to guide vegetation sampling and surveys. *Journal of Vegetation Science*, 5, 673, 1994.

Potapov, P., Turubanova S., and Hansen M.C., Regional-scale boreal forest cover and change mapping using Landsat data composites for European Russia. *Remote Sensing of Environment*, 115, 548, 2011.

Potapov, P., et al., Combining MODIS and Landsat imagery to estimate and map boreal forest cover loss. *Remote Sensing of Environment*, 112, 3708, 2008.

Potapov, P.V., et al., Quantifying forest cover loss in Democratic Republic of the Congo, 2000–2010, with Landsat ETM+ data. *Remote Sensing Environment*, in press.

Reed, B.C., et al., Measuring phenological variability from satellite imagery. *Journal of Vegetation Science*, 5, 703, 1994.

Shimabukuro, Y.E., et al., The Brazilian Amazon monitoring program: PRODES and DETER projects. In F. Achard and M.C. Hansen (Eds.), *Global Forest Monitoring from Earth Observations*. Taylor & Francis: Boca Raton, FL, 2012.

Vermote, E.F., El-Saleous, N., and Justice, C.O., Atmospheric correction of MODIS data in the visible to middle infrared: First results. *Remote Sensing of Environment*, 83, 97, 2002.

Wang, D., et al., Impact of sensor degradation on the MODIS NDVI time series. *Remote Sensing of Environment*, 119, 55, 2012.

Woodcock, C., et al., Free access to Landsat imagery. *Science*, 320, 1011, 2008.

7

Use of a Systematic Statistical Sample with Moderate-Resolution Imagery to Assess Forest Cover Changes at Tropical to Global Scale

Frédéric Achard, Hans-Jürgen Stibig, and René Beuchle

Joint Research Centre of the European Commission

Erik Lindquist and Rémi D'Annunzio

Food and Agriculture Organization of the United Nations

CONTENTS

7.1 Introduction 112
7.2 Sampling Strategy 113
7.3 Acquisition of Satellite Imagery 114
7.4 Preprocessing of Satellite Imagery 115
7.5 Segmentation of Satellite Imagery 117
7.6 Definition of Land Cover and Land Use Classes 118
7.7 Supervised Classification of Segmented Satellite Imagery for the Tropical Sample Sites 119
7.8 Visual Verification and Refinement of the Land Cover Classifications 120
7.9 Conversion of the Land Cover Maps into Land Use Maps 121
7.10 Production of Transition Matrices and Correction to Reference Dates and for Missing Data 122
7.11 Production of Statistical Estimates 123
7.12 Perspectives 124
About the Contributors 126
References 127

7.1 Introduction

This chapter presents an operational remote sensing approach for monitoring forest cover at continental and global levels, based on a statistical sampling design and on satellite imagery from optical sensors of moderate spatial resolution (30 m × 30 m resolution).

There are two main approaches to forest characterization and monitoring with remotely sensed data (Achard et al. 2010): analyses that cover the full spatial extent of the forested areas, termed "wall-to-wall" coverage, or those that select a statistical sample of forested areas for careful analysis and extrapolate the findings to the entire area of interest. Wall-to-wall mapping has long been done with relatively coarse spatial resolution satellite data and, currently, moderate spatial resolution wall-to-wall analyses are possible (see following Chapters 9 to 13 for examples of wall-to-wall analyses). However, spatially exhaustive analyses are challenging to operationalize on frequent time intervals and over very large, heterogeneous areas. Statistical sampling approaches, therefore, serve an important role in providing cost-effective, timely, repeatable estimates of forest characteristics over large areas and at frequent time intervals (e.g., Brink and Eva 2009; Broich et al. 2009; Duveiller et al. 2008; Eva et al. 2010). A sampling procedure that adequately represents deforestation events (e.g., through a sufficiently dense systematic or stratified sample in space and time) can capture deforestation trends.

Whichever overall approach is chosen, sampling or wall-to-wall, the spatial unit of analyses or minimum mapping unit (MMU) must also be decided upon. There are two main choices for this. In pixel-based approaches, the smallest unit of analysis is the individual image pixel. Object-based approaches use pixel clustering algorithms to create spectrally homogenous pixel groupings, which are thereafter treated as individual units for analysis.

For the Global Forest Resources Assessment 2010 (FRA 2010), the FAO (Food and Agriculture Organization of the UN) has extended its global and continental monitoring of forest cover changes to include analysis of remotely sensed land cover and land use as a complement to standard national reporting. The survey applies object-based image analysis methods to a globally distributed, systematic sample of moderate-resolution satellite imagery to estimate forest land cover and land use change for the periods 1990–2000 and 2000–2005. The FAO has produced estimates of tropical forest cover changes as part of past assessments (FRA 1990, 2000), but the remote sensing survey (RSS) of FRA 2010 has been extended to all lands (FAO et al. 2009). This survey has been conducted by a partnership between FAO and its member countries, the European Commission Joint Research Centre (JRC) as the main scientific partner, South Dakota State

University, the United States Geological Survey (USGS), and the U.S. National Aeronautics and Space Administration (NASA). Over 200 national experts from 106 countries have participated in the survey.

This chapter presents the scientific and technical methods that have been developed for monitoring forest cover changes in the framework of this global survey.

7.2 Sampling Strategy

The grid system selected for the global systematic sample is a rectilinear grid, based on degrees of geographical latitude and longitude (Figure 7.1), that enables a straightforward implementation, and easy location and understanding (Mayaux et al. 2005). Although stratified sampling is generally preferable for improving the efficiency of land cover change

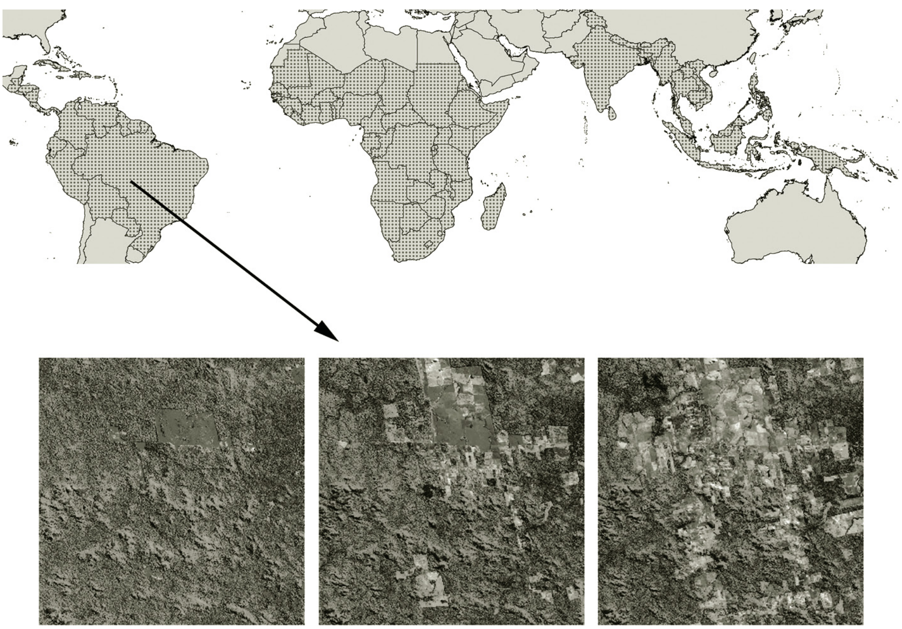

FIGURE 7.1
(See color insert.) Example of time series (for years 1990, 2000, and 2005) of Landsat satellite imagery over one sample site in the Amazon Basin (20 km × 20 km size). Forests appear in dark green, deforested areas (agriculture and pastures) appear in light green or pink.

estimation (Stehman et al. 2011), a systematic, nonstratified sampling has been implemented because:

1. This sampling scheme is intended to be also used for future time periods (for year 2010 and later), and it is impossible to reliably predict where deforestation "hot spots" will be located in future years.
2. The systematic sample scheme can be easily intensified for specific purposes, in particular for assessment at a national level or for a particular ecosystem. Indeed, a number of countries supported by FAO are already carrying out national forest assessments based on an intensification of the global sampling scheme (http://www.fao.org/forestry/nfma).

The global systematic sampling approach has already been tested against wall-to-wall reference data over the Brazilian Amazonia basin (Eva et al. 2010). It has also been intensified and tested for the Congo River basin region for the 1990–2000 period (Duveiller et al. 2008) and for the French Guiana territory (Eva et al. 2010), demonstrating its potential to estimate forest cover changes from continental to regional levels (Broich et al. 2009).

Globally, the survey involved 13,690 sample sites. Sampling has not been performed for latitudes higher than 75° north or south. At most sites, the area surveyed was 10 km × 10 km, which represents approximately 1% of the world's land surface. In the tropics, the area surveyed for each site was 20 km × 20 km for the period 1990–2000, which represents approximately 3.6% of the tropics.

7.3 Acquisition of Satellite Imagery

Nearly complete global coverage from the Landsat satellites is now available at no cost from the Earth Resources Observation Systems (EROS) Data Center (EDC) of the USGS (http://eros.usgs.gov/). A recent product, called the Global Land Survey (GLS), represents a global archive of good quality, orthorectified and geodetically accurate image acquisitions from Landsat Multispectral Scanner (MSS), Landsat Thematic Mapper (TM), and Landsat Enhanced Thematic Mapper (ETM+) sensors focused on the epochs ca. 1975, ca. 1990, ca. 2000, mid-2000s, and ca. 2010 (Gutman et al. 2008). These GLS data sets play a key role in establishing historical deforestation rates (Masek et al. 2008), although in some parts of the tropics (e.g., Western Colombia, Central Africa, and Borneo) persistent cloud cover is a major challenge for using these data (Ju et al. 2009; Linquist et al. 2008). For these regions, the GLS data sets can be complemented by remote sensing data from other satellite sensors with similar characteristics, in particular, optical sensors of moderate spatial resolution. The GLS data sets are described with full details in Chapter 4.

For each sample location of the systematic grid, the available Landsat data (from TM or ETM sensors) were sought from the GLS database (primary data source). These data were downloaded at full resolution (30 m × 30 m). Image subsets of 20 km × 20 km covering the sample sites were extracted in UTM projection (Potapov et al. 2011). The sample site target size is 10 km × 10 km, but a 5 km buffer has been used for data extraction and processing in order to keep contextual information. In the event of the data being unacceptable (due to cloud cover or artifacts from visual screening assessment), replacement data were sought from different sources with the help of the GEOSS (Global Earth Observing System of Systems) Land Surface Imaging Constellation. In particular, for the 4,016 sample sites covering the tropics, 2,868 suitable image pairs were found for the period 1990–2000 from the GLS data sets, representing 71.6% of the tropical sample (Beuchle et al. 2011). Better alternatives could be found for 26.6% of these 4,016 sites, substituting cloudy or missing GLS data sets at one or the other epoch or both (GLS-1990 or GLS-2000). Gaps were filled from the USGS Landsat archives (1,070 samples), data from other Landsat archives (e.g., GISTDA, ACRES, INPE; 53 samples), or with alternatives to Landsat, i.e., 15 samples from SPOT (Satellite Pour l'Observation de la Terre). This increased the effective number of sample pairs to 3,945, representing 98% of all target samples. No suitable image pairs were found for 71 confluence points, which were not randomly distributed, but mostly concentrated in the Congo basin, where around 15% of the region remains unsampled. There is a higher number of missing sites in the second period assessed (2000–2005) in particular for tropical regions, due to the malfunctioning of the line scanner on the Landsat 7 ETM sensor after June 1, 2003, which corrupts around 25% of each image acquisition (Maxwell 2004). The missing sites in the tropics for the 2000–2005 period are mainly located in Central America, Ecuador, the Colombian Choco, the Guianas, the southern ridge of West Africa, the western part of Congo basin (South Cameroon, Equatorial Guinea, Gabon, and Western Congo), Central Democratic Republic of Congo, Eastern Tanzania, and Indonesia (Kalimantan, Sulawesi, and Irian Jaya).

7.4 Preprocessing of Satellite Imagery

For each sample site, satellite image subsets (from 1990, 2000, and 2005) were preprocessed for geometric control, radiometric calibration and normalization, segmentation, and classification. Prior to the object segmentation and classification steps, radiometric correction to a common radiometric scale is required in order to apply standard supervised classification algorithms to the full imagery data set, making use of spectral training data of representative vegetation types. Acquisition errors and irrelevant data (e.g., clouds and cloud shadows) must also be removed in the preprocessing phase. A robust approach applicable to a large amount of multidate and multiscene Landsat imagery has been developed to convert all images into normalized radiometric values (Bodart et al. 2011). The different preprocessing steps were (1) conversion to top-of-atmosphere (ToA) reflectance, (2) cloud and cloud shadow removals, (3) haze correction, and (4) image radiometric normalization. The conversion to ToA reflectance was achieved by first converting raw digital numbers (DN) into at-sensor spectral radiance for each band and subsequently the at-sensor radiance was converted into ToA reflectance. The remaining clouds and cloud shadows in the selected images were masked in two steps. The first step was to detect all potential cloud and cloud shadow pixels using an automatic spectral rule-based mapping approach followed by a second step that consisted of a sequential application of a postprocessing algorithm based on morphological and topological methods designed to create a refined mask for images where clouds were visually identified. Image contamination by haze is relatively frequent in tropical regions (semitransparent clouds and aerosol layers that alter the spectral signatures of objects, especially in the visible bands). Partially contaminated images were corrected on the basis of the method using the fourth component of the tasseled cap transformation (TC4) computed from the six reflective bands of Landsat imagery. The applied image radiometric normalization is a relative normalization of multitemporal imagery covering different areas. Relative normalization adjusts the spectral values of all images to the values of one reference image. Dense evergreen forest pixels have been considered as pseudo-invariant features (PIF), i.e., stable targets between dates, assuming that reflectance differences in these stable targets are due to atmospheric perturbations. This normalization algorithm, referred to as "forest normalization," has been applied to each sample image with significant presence of dense evergreen forests (i.e., more than 2,000 pixels in the image). The median forest value parameter was extracted from a forest mask based on empirically determined thresholds of NDVI and bands 4 and 5 from Landsat imagery from years 1990 and 2000 and intersected with a 250 m forest map derived from the vegetation continuous field (VCF) product (Hansen et al. 2003). For those sites with a lower proportion of dense evergreen forests (i.e., less than 2,000 pixels in the image), a relative normalization has been performed whenever possible by visually selecting an area that did not change between the two dates, using the image of year 2000 as the reference image.

The haze correction algorithm improved the visual appearance of the image and significantly corrected the digital numbers for Landsat visible bands. The normalization procedures (forest normalization and relative normalization) improved the correlation between the spectral values of the same land cover in multidate images. The image subsets from the year 2000 were taken as the reference for geometric and radiometric controls. The preprocessed multitemporal data set constituted the basis for an automatic object-based supervised classification.

7.5 Segmentation of Satellite Imagery

After preprocessing, the image subsets were segmented so as to identify homogenous land units that can then be classified for each date (Raši et al. 2011). This approach comprises two automated steps of multidate image segmentation and object-based land cover classification (based on a supervised spectral library), followed by an intense phase of visual control and expert refinement. Image segmentation is done at two spatial scales, introducing the concept of an MMU via the automated selection of a site-specific scale parameter. The automated segmentation of land cover polygons and the pre-classification of land cover types mainly aim at avoiding manual delineation and at reducing the efforts of visual interpretation of land cover to a reasonable level, making the analysis of 13,000 sample sites feasible.

Several segmentation algorithms were tested. Based on technical performance and visual assessment of the object delineation, the eCognition software (Trimble) was chosen as most suited for our specific purpose. In particular, this software can process large amounts of data and classify objects in one common processing chain. For the purpose of forest cover monitoring, a multidate segmentation approach has been preferred to two separate, single-date image segmentations. Multidate segmentation integrates from the very beginning of the temporal aspect into the generation of spatially and spectrally consistent mapping units. For the tropical 4,000 sites, the segmentation process was initially implemented on two-date imagery (1990 and 2000) in a single operation. The Landsat TM or ETM+ spectral bands 3, 4, and 5 (ToA reflectance values) of both reference years (1990 and 2000) were therefore used as a common input to the segmentation procedure, assigning equal weights for all six bands. The weights of two other parameters in the eCognition software—referred to as "spectral" and "shape"—had to be determined for segmentation. Based on a series of tests with varying settings, the main weight of 0.9 has been empirically assigned to the "spectral" parameter, i.e., the spectral homogeneity accounts for 90% of the merging decision rules. The resulting weight for the "shape" parameter of 0.1 (as sum of the two weights = 1) proved to be sufficient for avoiding very irregular and fringed objects.

The main parameter controlling the size of objects is referred to as the scale parameter. The higher the scale parameter, the larger the average size of image objects, and in particular the maximum object size. We developed a process that automatically determines a specific scale parameter for each sample site in order to reach the desired MMU. This is achieved by increasing the scale parameter through iterative segmentations, until a size threshold for the smallest polygons is reached: the iterative process is stopped when the largest object among the 5% smallest objects reaches the desired MMU, i.e., when at least 95% of the remaining objects in the sample site are larger than the MMU. An initial MMU of 1 ha was set for the segments. This is a compromise between not having segments that are too small, and avoiding segments with mixed land covers. The segments of the individual image subsets are then classified using an automated supervised classification. In a second phase, these classified segments are aggregated into segments of 5 ha by increasing the scale parameter through iterative segmentations. In a final step, the number of the remaining small polygons below 5 ha size was reduced by merging each object smaller than 3 ha (corresponding to ca. 33 Landsat TM pixels) with the object it shared the longest common borderline with. The image objects resulting from the multidate segmentation conform to a standard MMU and exhibit similar spectral characteristics in time and in space. This 3 ha MMU size enables a feasible visual assessment of the classification by local experts.

7.6 Definition of Land Cover and Land Use Classes

Four main land cover categories were defined for labeling the 1 ha MMU segments: "tree cover" (TC), "other wooded land" (OWL), "other land" (OL), and "water" (WA). TC comprises all tree cover where canopy density can be expected to be ≥10% and tree heights to be ≥5 m. Included are natural forests and forest plantations, but also tree cover outside forests, such as in parks or on agricultural lands. OWL comprises all woody vegetation of lower height (<5 m), mainly shrub land, but also shrub-like agricultural crops, vegetation regrowth, or plantations with small trees. OL includes all nonwoody land cover (e.g., herbaceous cover, pastures, nonwoody crops, burnt areas, bare soils, settlements), except for water. The water class consists of rivers and in-land water bodies. The definition for tree cover has been chosen to be compatible with the FAO "forest" definition (FAO 2010). From the spectral and textural information of the moderate-resolution satellite imagery used in this study, one can only infer approximate tree density and broad height categories. The class thresholds served therefore rather as guidance for interpretation and for selection of training areas.

Land cover is the observed biophysical properties of the land surface, whereas land use is defined by the human activities and inputs on a given land area. Four main land use categories have been defined: "forest," "other wooded land," "other land use," and "water." Treating forest as a land use is consistent with the forest definition used in FAO's Global FRA country reports and national reports to the United Nations Framework Convention on Climate Change (UNFCCC). Forest land use may include periods during which the land is devoid of tree cover, for example, during cycles of forest harvesting and regeneration. In such cases, a land use is considered to be forest land use when management or natural processes will, within a reasonable time, restore tree cover to the point where it constitutes a forest.

7.7 Supervised Classification of Segmented Satellite Imagery for the Tropical Sample Sites

Spectral signatures were collected from the preprocessed Landsat ETM+ data of the year 2000 from one common set of training areas representing the main land cover classes within a region (Raši et al. 2011). For the first level classification at 1 ha, a large number of spectral classes were required to cover the variability of spectral reflectance within any particular land cover class, e.g., the TC class consists of 15 spectral classes including dense evergreen forests, degraded evergreen forests, dry deciduous forests in different phenological phases, mangrove, and swamp forest. Only homogeneous land cover units were selected as training areas, using additional references like fine-resolution satellite data (e.g., Google Earth). The number of pixels ultimately used for establishing the spectral signature of a subclass was generally higher than 1,000. Spectral signature statistics (means and standard deviations) were calculated at the level of subclasses.

A generic supervised classification of the 1 ha level segmentation objects was performed uniformly for all sample sites. The classification was based on membership functions established from the spectral signature of each subclass for the Landsat TM/ETM+ spectral bands 3, 4, and 5. The membership functions of each subclass were defined as an approximation of the class probability distribution, represented by isosceles triangles in the feature space of each spectral band. The top of the triangle corresponds to the class mean (m) and represents the spectral value of highest probability for class assignment. The two triangle legs descend from that position up to a spectral distance of $m \pm 3$ sd (sd = standard deviation), linearly decreasing the probability of class assignment to a value of "0" at the positions $m \pm 3$ sd.

The classification process compares the object spectral mean values to the membership functions defined for all subclasses. An object was assigned to the class displaying the highest membership probability for the object spectral mean values. We applied these membership functions to the imagery of all reference years, having performed previous spectral calibration to ToA reflectance values, haze correction, as well as normalization of the satellite imagery. The subclasses resulting from supervised classification served only for the mapping of the four main land cover classes.

The 1 ha level classified segments were automatically aggregated to 5 ha level into the five broad land cover classes based on the proportion of tree cover. The supervised classification result obtained for the 1 ha objects served as direct input to the thematic aggregation done at the second-level segmentation (5 ha MMU). The labeling of the second-level objects was performed by passing through a sequential list of classification criteria, with a main emphasis on tree cover proportions within second-level objects, e.g., TC class is defined as containing more that 70% tree cover within the 5 ha segment. As a consequence of merging objects from a finer scale (1 ha MMU), a "tree cover mosaic" class has been introduced for objects containing partial tree cover at the second level (objects containing an area portion of 40%–70% tree cover).

7.8 Visual Verification and Refinement of the Land Cover Classifications

The resulting land cover multitemporal classifications are then interdependently visually controlled by national experts. A dedicated graphical user interface has been developed for the visual verification and potential reassignment of land cover labels (Simonetti et al. 2011). For a selected sample site, the tool displays simultaneously the pair of image subsets (e.g., of 1990 and 2000) and the corresponding digitally classified land cover maps. The tool offers an optimized set of commands including image enhancement, simultaneous zoom of displayed data, single or multiobject selection and relabeling, specific class selection, and highlighting. The graphical user interface is available in English, Spanish, French, and Russian.

Visual control and refinement of the digital classification results at the 5 ha MMU level were implemented using, whenever available, very high-resolution satellite imagery (e.g., through Google Earth), but also existing vegetation maps and field knowledge as supplementary references: a revision of the mapping results was then carried out by forestry experts from the tropical countries who contributed local forest knowledge to improve the interpretation. During a final phase of regional harmonization, an experienced image interpreter performed a control of the interpretation consistency across the region, applying final corrections where necessary. Figure 7.2 shows a simplified example of the main steps used in visual verification and refinement of the land cover and land cover changes between 1990 and 2000.

The phase of visual control and refinement has been designed as a crucial component for correcting classification errors and for implementing the change assessment. The importance of visual control and correction can be perceived when comparing to the initial automatic classification result: e.g., in South East Asia about 20% of the polygon labels were changed through expert knowledge by visual interpretation (Raši et al. 2011). More than 120 experts from tropical countries have been involved in this verification and refinement phase of the survey.

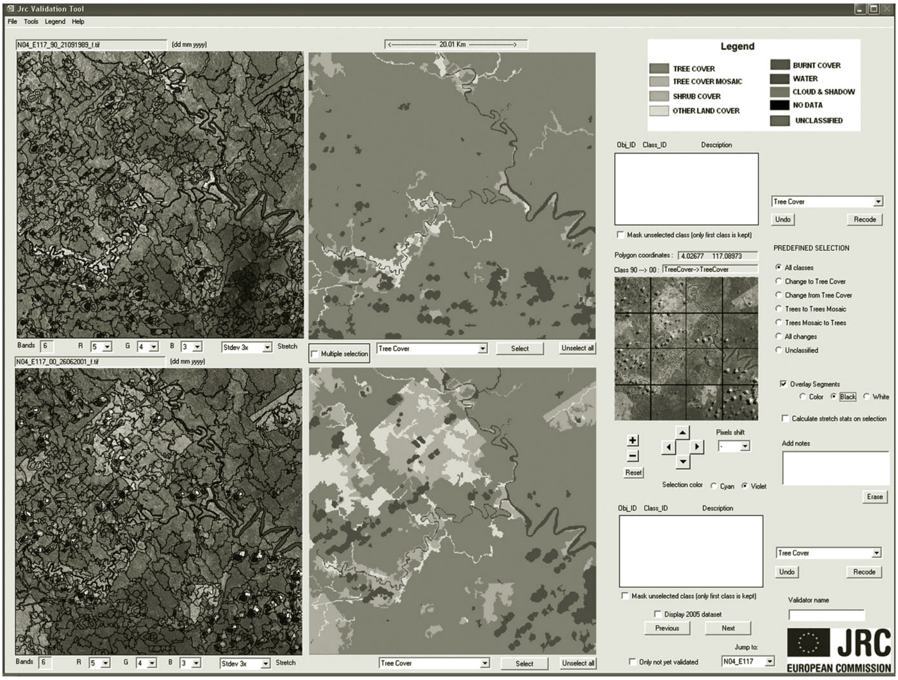

FIGURE 7.2
(See color insert.) Visualization tool used for the process of verification and correction of multitemporal classifications. *Left column*: Segmented Landsat imagery displayed (top: year 1990, bottom: year 2000). *Right column*: Land cover maps produced from satellite imagery.

7.9 Conversion of the Land Cover Maps into Land Use Maps

Land cover maps were first converted automatically into land use maps, and then the conversion results were reviewed through visual control by national experts. The automatic conversion of land cover maps into land use maps uses the following systematic rules:

- Classes TC and tree cover mosaic are converted to forest
- Class OWL remains as OWL
- Class OL is renamed other land use
- Class WA remains as WA

Because a direct translation possible from land cover to land use is not always possible, a visual interpretation and refinement of the land use classifications must be carried out by national experts. For example, when a forest has been

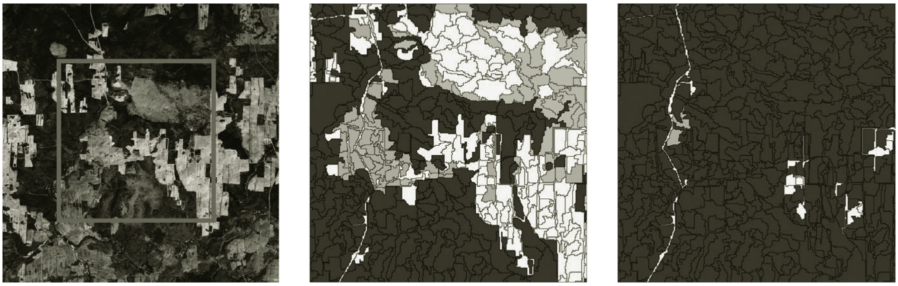

FIGURE 7.3
(See color insert.) The 20 km × 20 km multi-spectral Landsat image (left) for a sample site in the boreal forest showing, for the central 10 km × 10 km portion (red box), the classification of land cover (center) and land use (right). Land cover is classified as TC (green), tree cover mosaic (light green), OWL (orange), and other land cover (yellow). Land use is classified as forest (green), OWL (orange), and other land use (yellow).

clear-cut and is temporally unstocked, the land cover derived from any kind of automatic classification or visual interpretation will indicate something other than tree cover. However, the land use will remain as forest for a temporary clearing caused by timber harvest or fire, and this information can only be inferred by local knowledge of the land use context (Figure 7.3).

7.10 Production of Transition Matrices and Correction to Reference Dates and for Missing Data

For each sample site, land area transition matrices are produced for each period (1990–2000 and 2000–2005) and for both land cover and land use transitions (Table 7.1).

It was not possible to acquire all images at the exact reference date, with acquisitions ranging from 1984 to 1992 for the first reference year (1990), 1997 to 2003 for the second reference year (2000), and 2004 to 2009 for the third reference year (2005) (Beuchle et al. 2011). Each sample site's transition matrix was then adjusted to the baseline dates of June 30, 1990, 2000, and 2005; this was done by assuming that the land cover change rates are constant during the given period. We, therefore, linearly adjusted the land cover change matrices to the three reference dates.

Cloudy areas were considered as an unbiased loss of data and assumed to have the same proportions of land cover as noncloudy areas within the same site. This is achieved by converting the transition matrices 1990–2000 and 2000–2005 to area proportions relative to the total cloud-free land area of the sample site. For the missing sample sites in tropical regions, we

TABLE 7.1

Example of Land Cover Transition Matrix for Site [North 2°; West 074°] (areas in km^2)

Year 2000/Year 1990	Tree Cover (TC)	Tree Cover Mosaic (TCM)	Other Wooded Land (OWL)	Other Land Cover (OLC)	WA	Total Year 1990
TC	44.9	4.4	2.8	9.8	0	61.9
TCM	0	3.4	1.7	5.4	0	10.5
OWL	0	0.6	4.1	3.4	0	8.1
OLC	0	0.3	1.6	17.9	0	19.8
WA	0	0	0	0	0	0
Total year 2000	44.9	8.7	10.2	26.5	0	100.2

used a local average from surrounding sample sites as surrogate results. The following weights ($\delta_{jj'}$) were applied for the local average of missing sites:

$$\delta_{jj'} = \frac{1}{d(j,j')} = \frac{1}{(d(\text{lat}))^4 + (d(\text{long}))^4} \tag{7.1}$$

where the differences in latitude and longitude between two sample sites (j and j') is used with a power of 4.

Small differences may appear between land cover proportions of year 2000 obtained from the successive transition matrices [1900–2000] and [2000–2005] due to the linear temporal extrapolation to the reference dates. To correct for potential inconsistencies for the common year 2000, the land cover proportions of year 2000 from the change matrices for period 2000–2005 are "calibrated" to the land cover proportions of year 2000 from the [1990–2000] transition matrix through a linear adjustment for each sample site.

7.11 Production of Statistical Estimates

For the statistical estimation phase, the sample sites are weighted in relation to their probability of selection (Eva et al. 2012). Indeed the sampling frame, although systematic, does not give equal probability because the distance between sites along a parallel is not the same as the distance along a meridian. All sample units were given a weight, equal to the cosine of the latitude, to account for this unequal probability. The impact of these weights is moderate in tropical areas. The sample sites that contain a proportion of sea compensate for unselected sample sites that contain a proportion of land (when the center of the site is located in the sea) because they were considered as full sites.

The area change proportions of all sample sites are then extrapolated to the study area using the Horvitz–Thompson direct expansion estimator. The estimator for each area class transition is the mean proportion of that change per sample site, given by Equation 7.2:

$$\bar{y}_c = \frac{1}{m}\sum_{i=1}^{n} w_i \cdot y_{ic} \tag{7.2}$$

where y_{ic} is the proportion of area change for a particular class transition in the ith sample site. The weight of the sample unit is w_i and m is the sum of the sample weights. The total area of change for this class transition Z_c is obtained from:

$$Z_c = D \cdot \bar{y}_c \tag{7.3}$$

where D is the total area of the study region.

The usual variance estimation of the mean is known to have a positive bias. Alternative estimators based on a local estimation of the variance have been shown to reduce the bias. We use an estimator of the standard error based on local variance estimation:

$$s^2 = (1-f)\frac{\sum_{j \neq j'} w_{jj'}\delta_{jj'}(y_j - y_{j'})^2}{2\sum_{j \neq j'} w_{jj'}\delta_{jj'}} \tag{7.4}$$

where

f is the sampling rate

weight $w_{jj'}$ is an average of the weights w_j and $w_{j'}$

$\delta_{jj'}$ is a decreasing function (7.1) of the distance between j and j'.

The standard error is then calculated from this local variance using the total number of available sample sites, i.e., not accounting for the missing sites even if they are replaced by a local average.

The observations (source data sets) that are used to produce these results are derived from satellite interpretations. These surrogates to ground observations may be subject to uncertainty (bias). The use of such surrogate data for assessing area change is inevitable in many areas of the tropics where no ground observations exist and where large areas of inaccessible forests can only be monitored at affordable costs by using satellite data.

7.12 Perspectives

An operational system for processing and analysis of a global sample of moderate-resolution satellite imagery has been developed to produce maps and estimates of forest area changes in the periods 1990–2000 and 2000–2005 at tropical to global scale (Figure 7.4).

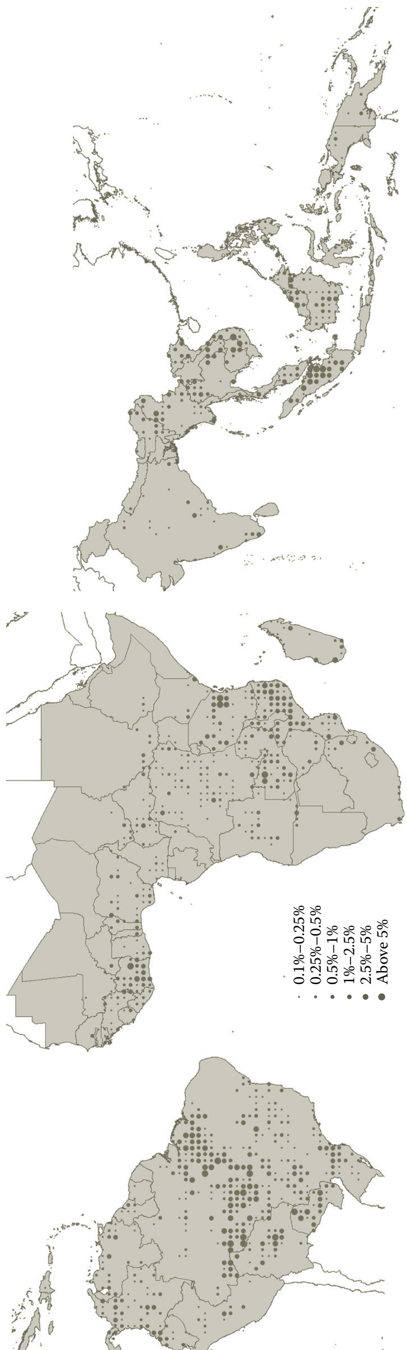

FIGURE 7.4
(See color insert.) Annual rate of gross forest cover loss during the period 2000–2005 for the tropical sample units of the global systematic sample.

The preliminary findings of an in-depth analysis of forest land-use change globally (FAO and JRC 2011) can be summarized as follows:

- The area in forest land use declined between 1990 and 2005, with global mean rates of loss between 1990 and 2000 of 2.7 (±0.9) million ha/year, rising to a mean annual loss of 6.3 (±1.4) million ha/year between 2000 and 2005.
- Just over half the world's forests are in tropical or subtropical climatic domains.
- There were important regional differences in forest loss and gain. In particular, forest loss was highest in the tropics going from –5.7 (±0.8) million ha/year in the 1990s to –9.1 (±1.2) million ha/year between 2000 and 2005.

The methods developed through the survey will be used to improve the measurement and reporting of forest area and change in forest area over time as part of the continual improvement of the FAO FRA process.

These results can be an important input to national and international reporting processes where forest area and change statistics are needed, such as the Convention for Biological Diversity and the emerging initiative for Reducing Emissions from Deforestation and Forest Degradation in Developing countries (REDD+) under the UNFCCC.

About the Contributors

Frédéric Achard is a senior scientist at the JRC, Ispra, Italy. His current research interests include the development of earth observation techniques for global and regional forest monitoring and the assessment of the implications of forest cover changes in the tropics and boreal Eurasia on the global carbon budget. Achard received his PhD in tropical ecology and remote sensing from Toulouse University, France, in 1989. He has coauthored over 50 scientific peer-reviewed papers in leading scientific journals.

Hans-Jürgen Stibig is a senior scientist at the JRC, Ispra, Italy. He received his PhD in forestry and remote sensing from the University of Freiburg, Germany, and has then been working in the field of forest inventory, mapping, and monitoring in several tropical countries, particularly in Southeast Asia. His current research interests is on global and regional forest monitoring by remote sensing, analyzing the impact and drivers of forest change in the tropics, with a geographical focus on Southeast Asia.

Erik Lindquist is a remote sensing specialist with the Food and Agriculture Organization. He is the coordinator of remote sensing activities within the Global FRA team based in Rome, Italy. He is completing his PhD in geospatial science and engineering from South Dakota State University, Brookings, South Dakota.

René Beuchle is a scientist at the JRC, Ispra, Italy. He has specialized in remote sensing, geoinformation systems, and cartography. He received a degree in cartography from the Karlsruhe University of Applied Sciences, Karlsruhe, Germany, in 1991. His current research activities are related to the assessment of tropical forest cover change by remote sensing with a geographical focus on South and Central America.

Rémi d'Annunzio is an forestry officer at the Food and Agriculture Organization (FAO) of the United Nations where he has been working since 2009, within the remote sensing team of the FRA team. He has an MSc in image analysis and segmentation and a PhD in forest science from AgroParistech, Paris, France.

References

Achard, F. et al., Estimating tropical deforestation. *Carbon Management*, 1, 271, 2010.

Beuchle, R. et al., A satellite data set for tropical forest area change assessment. *International Journal of Remote Sensing*, 32, 7009, 2011.

Bodart, C. et al., Pre-processing of a sample of multi-scene and multi-date Landsat imagery used to monitor forest cover changes over the tropics. *ISPRS Journal of Photogrammetry and Remote Sensing*, 66, 555, 2011.

Brink, A. and Eva, H.D., Monitoring 25 years of land cover change dynamics in Africa: A sample based remote sensing approach. *Applied Geography*, 29, 501, 2009.

Broich, M. et al., A comparison of sampling designs for estimating deforestation from Landsat imagery: A case study of the Brazilian legal Amazon. *Remote Sensing of Environment*, 113, 2448, 2009.

Duveiller, G. et al., Deforestation in Central Africa: Estimates at regional national and landscape levels by advanced processing of systematically distributed Landsat extracts. *Remote Sensing of Environment*, 112, 1969, 2008.

Eva, H.D. et al., Monitoring forest areas from continental to territorial levels using a sample of medium spatial resolution satellite imagery. *ISPRS Journal of Photogrammetry and Remote Sensing*, 65, 191, 2010.

Eva, H.D. et al., Forest cover changes in tropical South and Central America from 1990 to 2005 and related carbon emissions and removals. *Remote Sensing*, 4, 1369, 2012.

FAO, *Global Forest Resources Assessment 2010: Main Report*, FAO Forestry Paper 163, FAO, Rome, 2010.

FAO and JRC, *Global Forest Land-Use Change from 1990 to 2005*, FAO, Rome, 2011 (available at: http://www.fao.org/forestry/fra/remotesensingsurvey/en/).

FAO, JRC, SDSU, and UCL, *The 2010 Global Forest Resources Assessment Remote Sensing Survey: An Outline of the Objectives, Data, Methods and Approach*, Forest Resources Assessment Working Paper 155, FAO, Rome, 2009.

Gutman, B.G. et al., Towards monitoring land-cover and land-use changes at a global scale: The global land survey 2005. *Photogrammatic Engineering and Remote Sensing*, 74, 6, 2008.

Hansen, M.C. et al., Development of 500 meter vegetation continuous field maps using MODIS data. *International Geoscience and Remote Sensing Symposium*, 1, 264, 2003.

Ju, J., The availability of cloud-free Landsat ETM+ data over the conterminous United States and globally. *Remote Sensing and Environment*, 112, 1196, 2008.

Lindquist, E.J., et al., The suitability of decadal image data sets for mapping tropical forest cover change in the Democratic Republic of Congo: Implications for the global land survey. *International Journal of Remote Sensing*, 29, 7269, 2008.

Masek, J. et al., North American forest disturbance mapped from a decadal Landsat record. *Remote Sensing and Environment*, 112, 2914, 2008.

Maxwell, S., Filling Landsat ETM+ SLC-off gaps using a segmentation model approach. *Photogrammatic Engineering and Remote Sensing*, 70, 1109, 2004.

Mayaux, P. et al., Tropical forest cover change in the 1990s and options for future monitoring. *Philosophical Transactions of the Royal Society B: Biological Science*, 360, 373, 2005.

Potapov, P. et al., The global Landsat imagery database for the FAO FRA remote sensing survey. *International Journal of Digital Earth*, 4, 2, 2011.

Raši, R. et al., An automated approach for segmenting and classifying a large sample of multi-date Landsat-type imagery for pan-tropical forest monitoring. *Remote Sensing and Environment*, 115, 3659, 2011.

Simonetti, D., Beuchle, R., and Eva, H.D., *User Manual for the JRC Land Cover/Use Change Validation Tool*. EUR 24683 EN, Luxembourg: Publications Office of the European Union, 2011.

Stehman, S.V. et al., Adapting a global stratified random sample for regional estimation of forest cover change derived from satellite imagery. *Remote Sensing and Environment*, 115, 650, 2011.

8

Monitoring Forest Loss and Degradation at National to Global Scales Using Landsat Data

Peter Potapov, Svetlana Turubanova, and Matthew C. Hansen
University of Maryland

Ilona Zhuravleva and Alexey Yaroshenko
Greenpeace Russia

Lars Laestadius
World Resources Institute

CONTENTS

8.1 Introduction 129
8.2 Landsat Data Processing 133
8.3 National-Scale Forest Cover Extent and Loss Mapping 138
    8.3.1 European Russia Forest Cover and Change Mapping 139
    8.3.2 Forest Cover Monitoring in the DRC 142
8.4 Global- and National-Scale Forest Degradation Monitoring 145
8.5 Conclusion 148
Acknowledgments 150
About the Contributors 150
References 151

8.1 Introduction

Information on the extent and change of forest cover at the national to global scale is important for many reasons. At the national level, it provides a basis for terrestrial carbon accounting, land use management, monitoring of forest resources, and conservation planning. Many international processes use it too. It helps improve the forest cover change reporting of the United Nations Food and Agriculture Organization (FAO), which serves as the baseline reference for global-scale environmental accounting and modeling. It provides keystone variables for international initiatives to reduce deforestation, such as the process of reducing emissions from deforestation and degradation in developing countries (REDD+) of the United Nations Framework Convention on Climate Change (UNFCCC), which requires developing countries to have robust and transparent national forest monitoring systems. It is important to assess the status and threats for biological diversity as required by the Programme of Work on Forest Biological Diversity within the United Nations Convention on Biological Diversity. Environmental nongovernmental organizations such as World Wide Fund, Conservation International, and Greenpeace depend on forest degradation data to design forest conservation campaigns and combat illegal logging.

Ideally, such information should be comprehensive and consistent across the relevant space and time. Currently, the primary source of global forest cover extent and change is data from national forest inventories (NFIs), which are aggregated by FAO to form a series of Global Forest Resources Assessments (FRA). The usefulness of these assessments is reduced, however, by a number of factors that are inherent in the aggregation approach: (1) NFI data from different countries differ in terms of quality and age (update rates), and data from developing countries are often incomplete and inconsistent; (2) despite the efforts of FAO, countries de facto apply different definitions of forest cover and use, different forest accounting and change detection methods, thus making it difficult to synthesize results; (3) forest cover and change information are only provided in a tabular numerical format without any spatial disaggregation. The FRA process has started to incorporate remotely sensed data through the remote sensing survey, a sample-based assessment of global and biome-level forest extent dynamics (FAO 2009). However, for many applications, a spatially exhaustive map product is required.

Satellite remote sensing provides a viable data source to supplement NFIs and global forest monitoring initiatives. Forest cover extent and timely change estimates can be successfully retrieved from medium spatial resolution optical satellite data (Williams et al. 2006). These data are invaluable for the quantification of forest cover within the vast extent of remote and inaccessible forest landscapes, as well as for developing countries where lack of transportation infrastructure coupled with political instability often limit data collection and forest mapping on the ground.

During the last decade, a number of forest monitoring projects have been developed and implemented at the national level using satellite data. Major timber-producing countries, such as Finland (Tomppo 1993), Sweden (Willén et al. 2005), and Canada (Wulder et al. 2008), use optical satellite imagery as a standard source of information to supplement and extrapolate field plot measurements and to monitor forest management. Among developing countries, the Brazilian system on mapping annual deforestation (PRODES) is the largest and most robust operating forest monitoring system (INPE 2002). However, to expand these efforts to the biome and global scales, three major problems need to be solved: (1) methodological consistency must be improved (so that the results obtained at the national scale are directly comparable); (2) cost-effective monitoring methods must be developed (so that the cost of source data and data analysis will be low enough to allow national- to global-scale implementation); and (3) open data access must be ensured (so that various international and nongovernmental organizations and experts are able to analyze, review, and validate the monitoring results).

There are two main strategies for satellite-based forest monitoring at a large scale: sampling and wall-to-wall mapping. Several sample-based approaches have been successfully implemented during the last decade at biome (Achard et al. 2002) and global levels (FAO 2009; Hansen et al. 2010). Different sampling designs were used to select classified imagery subsets, including regular sampling (FAO 2009) and stratified sampling (Achard et al. 2002; Hansen et al. 2010). Both approaches, however, are challenged by low estimate precision due to the uneven distribution of change within forest landscapes (Tucker and Townshend 2000), and neither produces a spatially explicit result. This limits their usefulness for many applications.

Wall-to-wall coverage of satellite data with sufficient spatial resolution differs from sample-based approaches in that it allows for direct mapping of forest cover and change and for a spatially complete quantification of forest dynamics at the national scale. Low spatial resolution data of the kind produced by the MODIS or MERIS sensors are inadequate for direct estimation of forest change, as much of it occurs at subpixel scales (Jin and Sader 2005). Medium spatial resolution data, such as that produced by the Landsat sensor, do allow for accurate forest cover and change area measurement (Williams et al. 2006). The use of medium spatial resolution data for national-scale forest monitoring has been limited until recently by the high data costs, the difficulty of handling large data volumes, and data analysis problems in regions with persistent clouds, such as the humid tropics. Recently, however, changes in data distribution policies and data-processing algorithms have enabled fast and cost-effective national-scale forest cover and change assessment.

Undoubtedly, the most important enabling factor for large-scale satellite-based forest monitoring is free-of-charge data availability. While low spatial resolution data (AVHRR, MODIS) were freely available for decades, medium-resolution data have been costly until recently. In January 2008, the U.S. Geological Survey (USGS) implemented a new Landsat data distribution policy that provides Landsat data free of charge. The free-of-charge data allows financially constrained developing countries to use it for wall-to-wall forest mapping. For example, purchasing the 2000–2010 Landsat data for a country like the Democratic Republic of the Congo (DRC) would have cost more than 6 million U.S. dollars at the pre-2008 price. These resources can now be spent on data processing, analysis, and validation of results. Medium-resolution Landsat imagery provides the best balance between acquisition cost and spatial resolution, despite the fact that it is inadequate for the detection of small-scale forest change (e.g., low-intensity selective logging). Even when a complete national coverage of higher spatial resolution imagery is available, the high data cost will restrict its use by developing countries for national monitoring purposes.

Another important factor increasing the feasibility of using national wall-to-wall medium-resolution imagery for forest monitoring is the progress in computing capacity and data-processing algorithms. Modern computing hardware allows for rapid processing of Landsat data at the national scale (from several weeks to a month). Recent progress in automated Landsat data processing and mosaicing has made it possible to produce cloud-free annual or epochal composite images for persistently cloudy areas (Hansen et al. 2008; Potapov et al. 2011). Nonparametric classifiers (e.g., *k*-nearest neighbor, decision tree, support vector machines, and neural networks) allow for fast and precise mapping and change detection of heterogeneous land cover types such as forest cover (Hansen et al. 1996).

The rapid development in the quality and access to satellite imagery has widened the circle of actors that can monitor forests beyond national forest administrations, thereby enhancing transparency. Civil society, private industry, and researchers can now monitor forests in support of conservation, business, science, and other forest resource assessment and management applications. NFI and monitoring data provided by national governments can be validated by in-country and international nongovernmental organizations and expert groups, highlighting any data quality issues. This creates a competitive environment that stimulates the improvement of governmental policies and NFI methods. Forest monitoring transparency, however, requires that the source satellite data remain in the public domain and can be freely redistributed. Currently, only a few image data providers, including USGS and INPE, deliver satellite imagery under liberal licensing conditions that allow for sharing and redistribution of the data and derived monitoring products.

Our approach to national-scale forest cover loss monitoring is an evolution of an algorithm developed by Hansen et al. (2008). Data from the MODIS sensor were used to preprocess Landsat time-series images that in turn were used to characterize forest cover extent and loss. Our approach is based on a fully automated Landsat data processing, including scene selection, per-pixel quality assessment (QA), and normalization. The Landsat data archive was exhaustively mined, and all data that satisfied our selection criteria were used for the analysis. Individual Landsat images were normalized using MODIS-derived surface reflectance target and used to derive multitemporal metrics and time-sequential composites. These metrics, along with the MODIS data time series, were used as independent variables to build supervised decision tree models for mapping forest cover and change. Mapping and monitoring forest degradation, which include assessment of low-intensity disturbance and fragmentation, required an alternative method based on manual interpretation of time-sequential Landsat image composites following an approach developed by Potapov et al. (2008).

The objective of the forest assessment and monitoring method presented in this chapter is to provide regular national forest cover updates at 5- and 10-year intervals. The same algorithm can be used to produce results at finer temporal steps (e.g., annually), assuming that enough cloud-free observations are available; however, providing annual forest cover updates was beyond the objectives of this study. Further evaluation and evolution of the system will allow for more rapid updating of continental and global forest cover in the near future.

The forest cover loss and degradation assessment algorithms have been applied to different forest biomes, testing and illustrating their capability to be implemented at the global scale. Mapping and monitoring results have been published online along with Landsat image composites for use by national governmental and civil society organizations (European Russia data: http://globalmonitoring.sdstate.edu/projects/boreal/; the DRC data: http://congo.iluci.org/carpemapper/; Intact Forest Landscapes data: http://intacforests.org).

8.2 Landsat Data Processing

The Landsat remote sensing satellite program operated by the USGS provides free-of-charge data with a medium spatial resolution (30 m/pixel for reflective bands) suitable for the full spectra of forest monitoring studies from a local to the global scale (Williams et al. 2006). The Landsat program is unique due to its global image acquisition strategy, allowing land cover monitoring over the last three decades. Landsat ETM+ reflective spectral bands, which include visible (band 1, 450–515 nm; band 2, 525–605 nm; band 3, 630–690 nm), near infrared (band 4, 760–900 nm), and short infrared (band 5, 1,550–1,750 nm; band 7, 2,080–2,350 nm), provide a sufficient spectral profile for vegetation-type mapping and land cover change detection. The thermal infrared data (band 6, 10,400–12,500 nm) enable automatic cloud cover detection. One of the main advantages of the Landsat spectral bands is its radiometric consistency and continuity between Landsat sensors (TM, ETM+, and future LDCM) and with the MODIS sensor, allowing intercalibration of Landsat and MODIS datasets.

The complete global Landsat data archive is available through the USGS National Center for Earth Resources Observation and Science (EROS) from their Web portals: GLOVIS (http://glovis.usgs.gov) and Earth Explorer (http://earthexplorer.usgs.gov). The Earth Explorer data portal allows users to perform advanced archive inventory search as well as bulk Landsat data order and download. Image metadata browsing and selection is guided by the Worldwide Reference System-2 (WRS2) of path (ground track parallel) and row (latitude parallel) coordinates defining scene footprints.

In our study, to reduce computational time for Landsat data processing, only images having less than 50% cloud cover for any scene quarter, as estimated by the automatic cloud cover assessment (ACCA), were selected. However, the cloud cover threshold has been expanded to include images with 70%–80% cloud cover for scene footprints with low numbers of 50% cloud-free images. For boreal regions, only growing season images were selected. The annual growing season start/end dates were established for each Landsat WRS2 footprint using annual time series of MODIS-derived NDVI over a MODIS-derived forest cover mask. Image metadata analysis, scene selection, and bulk data ordering were performed using an automated metadata search tool.

The Landsat images are normally processed as Level 1 terrain (L1T) corrected data by the USGS EROS. The L1T corrected data product provides systematic geometric accuracy by incorporating ground control points and a digital elevation model (DEM) for topographic accuracy. However, if insufficient ground control points or elevation data necessary for terrain correction were available, images can be delivered as Level 1 systematic correction (L1G). Because L1G data often feature low geometric accuracy and require further geocorrection, only images processed as L1T, ensuring a high geolocation precision, were used for the subsequent data processing save for the few coastal scene footprints where L1T corrected data were not available at all.

Our fully automated Landsat data process included two main steps: (1) per-image processing including image resampling, applying at-sensor calibration, per-pixel observation QA, and radiometric normalization and (2) per-pixel observation coverage analysis, production of image composites, and derivation of multitemporal metrics for forest extent and change mapping (Figure 8.1).

To facilitate image processing and enable per-pixel compositing, all image data for the nation (region) were resampled to a predefined pixel grid. The pixel grid was specified separately for each continent in equal-area map projections chosen to reduce geometric distortion. The following examples of national-scale forest monitoring were prototyped using pixel grids with 60 m spatial resolution to reduce data volumes and computation time. The 30 m spatial resolution pixel grid will be used for future continental- to global-scale processing.

At-sensor calibration was applied to convert raw image digital numbers to top-of-atmosphere (TOA) reflectance (for reflective bands) and brightness temperature (for thermal infrared band) in order to minimize differences in sensor calibration, between sensors (TM, ETM+, and MODIS), in the sun–earth distance, and in the elevation of the sun. To calculate TOA reflectance and brightness temperature, we used the approach described in Chander et al. (2009), with coefficients taken from image metadata.

The purpose of per-pixel observation QA was to select cloud-free and cloud shadow-free land and water observations for subsequent image compositing. To automatically map clouds and cloud shadows, we used a set

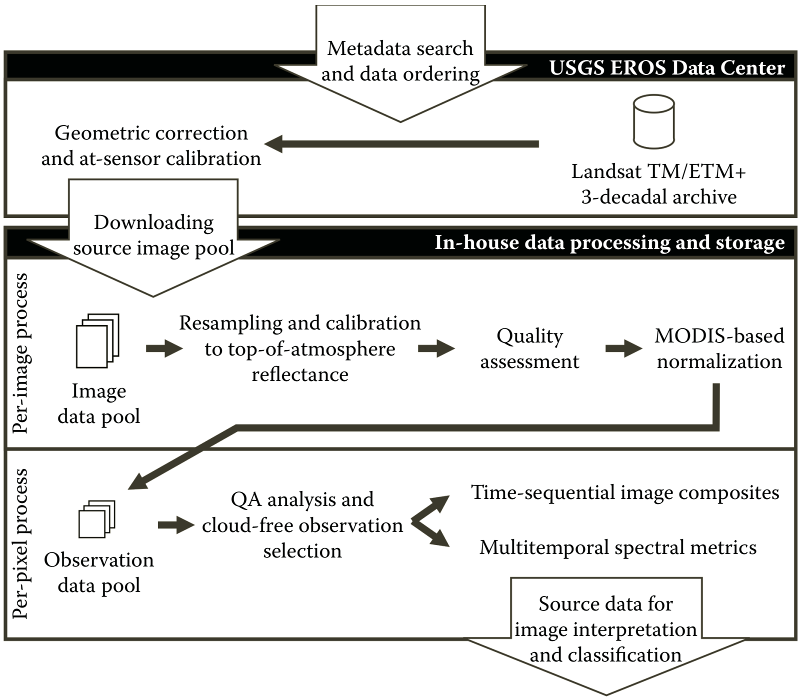

FIGURE 8.1
Landsat data-processing workflow.

of cloud, haze, shadow, and water detection models. The models correspond to a set of classification tree models (Breiman et al. 1984) derived from training data that were collected from a large sample of Landsat imagery. The Landsat training data and derived QA models are biome specific (separate models are used for tropical, temperate, and boreal forests). Training images were manually classified into land, water, cloud, haze, and shadow classes. From these images, 10% samples were randomly selected, aggregated for all images, and used to create generalized classification tree models. Each model was applied per Landsat image, yielding class probability values. Based on these values, a QA code was assigned to each pixel reflecting the probability of the pixel to be a land or water cloud-free observation, using the method described in Potapov et al. (2011).

Relative radiometric normalization of Landsat imagery was used to reduce reflectance variations between image dates due to atmospheric conditions and surface anisotropy. Only reflective bands used for image compositing (bands 3, 4, 5, and 7) were normalized. The shortwave visible bands (bands 1 and 2) were not used due to their sensitivity to atmospheric haze and water vapor, precluding correct normalization. The thermal infrared band 6 was used for the cloud screening model but was not included in the final image composite. The atmospheric correction of Landsat-derived TOA reflectance using time-synchronous atmospheric data and 6S radiative transfer code is a state-of-the art method (Masek et al. 2006) that should be implemented for obtaining consistent surface reflectance. However, simple techniques for relative image normalization using radiometrically consistent sets of moderate spatial resolution data could be successfully employed to facilitate image compositing over large regions (Olthof et al. 2005; Hansen et al. 2008). Our approach relied on the correlation between Landsat TOA and MODIS atmospherically corrected top-of-canopy (TOC) reflectance. MODIS normalization target reflectance data were collected from 2000 to 2009 (10-year) global Terra/MODIS 250 m data 16-day composites (MOD44C, collection 5), provided by the University of Maryland. The MODIS spectral bands 1, 2, 6, and 7 were chosen to correspond with Landsat bands 3, 4, 5, and 7. To reduce the presence of clouds and shadows, the mean surface reflectance corresponding to the three highest NDVI values from observations with the lowest cloud probability over the 2000–2009 interval were used as the normalization target. We calculated a mean bias between MODIS TOC and Landsat TOA reflectance for each spectral band over the land area and used it to adjust Landsat reflectance values. A simple empirically derived reflectance difference threshold was used to avoid areas of rapid land cover or phenological change. For tropical areas where the surface anisotropy effect significantly hindered image interpretation (Hansen et al. 2008), an additional correction for surface anisotropy was implemented. A simple linear regression between the MODIS/Landsat reflectance bias (dependent variable) and distance from orbit ground track (independent variable) was derived for each reflective band and then applied to correct band reflectance values within the entire Landsat image. Image normalization was performed independently for each spectral band and Landsat image. This fully automated image processing approach allowed us to use parallel computing methods, reducing the average image processing time to 12 s/image.

Our approach for image time-series analysis integrates the classic, multidate image compositing method (Holben 1986), with the novel approach of using multitemporal metrics to characterize reflectance variation within a given time interval (Hansen et al. 2003). Image time series were analyzed at per-pixel level using all processed Landsat observations for the entire time interval. For decadal forest monitoring, two sets of metrics were created for two 5-year time intervals: 2001–2005 and 2006–2010. To facilitate data management and to allow parallel computing, compositing was performed independently for a set of rectangular tiles dividing the entire area of analysis. To create an observation "data pool" from which time-sequential composites and spectral metrics could be derived, we preferentially selected observations with the least cloud/shadow contamination within the growing season. Growing season images are more appropriate for forest cover mapping than imagery captured during senescence or dormant periods. Preferential growing season boundaries can be defined either on a per-scene basis (Potapov et al. 2011) or on a per-pixel basis using MODIS-derived annual NDVI profiles. To create a "data pool," we analyzed QA flags for all available observations for the pixel. A set of criteria were designed to identify observations with the least cloud/shadow contamination to be included in the "data pool." Because the cloud shadow classification model was not tuned to water bodies, pixels with high water probability were selected separately. For land pixels, the number of growing season cloud/shadow-free observations for each 5-year interval (for decadal analysis) was calculated. If no cloud-free observations were found for any 5-year time interval, search boundaries were extended first to out-of-season observations, then to observations with moderate cloud/shadow probabilities. After the "data pool" pixels were selected, all other data (flagged as having higher cloud/shadow probability or out of season) were excluded from further processing.

The time-sequential image composites derived from the "data pool" observations represent start/end points for forest cover monitoring analysis and have been used for ca. year 2000 forest mapping, for change detection (for boreal regions), and for visual image interpretation and mapping of forest degradation. Several approaches for image compositing have been tested, including single-date compositing and multidate compositing using mean (or median) value or NDVI (or selected band reflectance) value ranking (Hansen et al. 2008; Potapov et al. 2011). We found that different approaches are appropriate for different applications. For change detection, the first/last single-date observation compositing was found to be the most suitable as it represents the land cover status for the first and last cloud-free image date in the "data pool." For visual interpretation, on the other hand, multidate composites were found to be more suitable due to low noise levels and consistent reflectance values within the area of analysis (Potapov et al. 2011). Our current automatic image compositing method produces a set of different time-sequential composites for use as classification metrics and for visual analysis.

While the time-sequential image composites are invaluable for visual image interpretation and for creating classification training sets, they are inadequate for forest cover change monitoring in tropical forests. This is because the rapid establishment of regrowth obscures the change signal over decadal and mid-decadal time intervals. To highlight reflectance variation within the analyzed time interval, a set of spectral metrics were created from the "data pool" observations. These metrics were designed to capture a generic feature space that facilitates regional-scale mapping and have been used extensively with MODIS and Landsat data (Hansen et al. 2003, 2008, 2010). Three groups of per-band metrics were created: (1) reflectance values representing 6-year maximum, minimum, and selected percentile values (10%, 25%, 50%, 75%, and 90% percentiles); (2) mean reflectance values for observations between selected percentiles (for the min-10%, 10%–25%, 25%–50%, 50%–75%, 75%–90%, 90%–max, min–max, 10%–90%, and 25%–75% intervals); and

(3) the value of the slope of a linear regression of band reflectance versus image date. Multitemporal metrics were used for forest cover and change classification, and selected metrics were employed for visual image analysis and creation of training data.

8.3 National-Scale Forest Cover Extent and Loss Mapping

Forest cover mapping and change detection was carried out on the basis of wall-to-wall image composites using a single national-scale supervised classification model. The classification model was built using an extensive set of training data collected within the entire area of analysis. This approach helped to avoid the problems that arise when a classification model based on local training data is extrapolated to neighboring images (Wulder et al. 2008). The classification and regression tree (CART) algorithm was used as the main tool for image classification and change detection. CART is a nonparametric supervised classification model constructed to predict the class membership by recursively splitting the feature space into a set of nonoverlapping subsets and then reporting the class probability within each subset. The CART algorithm has been shown to have a high precision for land cover mapping (Hansen et al. 1996). To improve the CART model stability and accuracy, a bootstrap aggregation (bagging) algorithm was used that corresponds to a set of trees created using random training data subsamples and taking the median class likelihood as the final result. Bagged classification tree models for forest cover and change mapping were generated using the training data as the dependent variable and multitemporal metrics plus time-sequential image composites as independent variables.

For the purpose of the regional-scale monitoring examples described below, forest was defined as having 30% or greater canopy cover for trees of 5 m or more in height. Forest cover and forest types were mapped for the year 2000, the first year of monitoring. All events resulting in stand replacement at the 60 m pixel scale within the analyzed time interval, including clearings (even if followed by forest regrowth within the same time interval), logging, fire, flooding, and storm damage, were mapped together as a gross forest cover loss class. Forest cover loss was mapped within the year 2000 forest mask. For the decadal monitoring, forest cover loss was mapped independently for each 5-year interval. To build the classification tree models for forest cover extent and forest cover loss mapping, a training set was manually created by visual interpretation of the region-wide time-sequential image composites. A number of additional datasets, including freely available QuickBird images from GoogleEarth™ and expert information, were used as reference materials to aid interpretation.

Two examples of region-wide Landsat forest cover mapping and change detection projects are briefly described below: one within the boreal and temperate forests of European Russia, another within the humid tropical forests and dry tropical woodlands of the DRC.

8.3.1 European Russia Forest Cover and Change Mapping

The forest cover change analysis from 2000 to 2005 was performed within the northern and central administrative regions of European Russia. The area of analysis spans from the northern forest–tundra ecotone to the forest–steppe boundary in the south and includes a variety of boreal and temperate forest types. A total of 7,227 Landsat ETM+ images from 1999 to 2007 were selected based on cloud cover and growing season date criteria. Landsat image normalization was performed using a MODIS-derived pan-boreal coniferous forest mask as the normalization target. Normalized Landsat images were used to create time-sequential image composites for 2000 and 2005 and a set of spectral metrics describing reflectance variability within ±1 year of the target composite date. For places with persistent cloud cover and/or a limited number of observations, images that were acquired more than 1 year before or after the target year were used for compositing and metrics. To create the image composite, all selected cloud-free observation dates for each pixel were ranked based on band 4 values. The image date corresponding to the band 4 median was chosen as the composite date, and all reflective bands from this date were used to create a final ca. 2000 or ca. 2005 image composite. In addition to the band 4 median value composites, a set of spectral metrics was created on the basis of a band 5 ranking meant to capture reflectance variation within the growing season. Owing to the time-preferential compositing rule, more than 95% of the composite areas for the ca. 2000 and 2005 could be created from images acquired within ±1 year of the target year. Less than 0.5% of the total composite area had to be excluded from analysis due to lack of cloud-free observations. Due to the relatively slow reforestation within the boreal and temperate forests, we concluded that using the composite difference would be sufficient for 5-year forest cover loss mapping (Figure 8.2).

Forest cover for the year 2000 was mapped using Landsat composites and metrics for ca. year 2000 supplemented with pixel latitude and MODIS annual metrics. The MODIS annual metrics included mean red reflectance and NDVI value for the growing season and annual highest red and NIR reflectance representing the extent of snow cover during the winter. Forest cover within European Russia is generally easily defined and mapped as most of the natural or managed forests have high canopy densities. Additional MODIS metrics helped improve the forest/nonforest classification within wetland forests, the forest–tundra, and the forest–steppe interface. Gross forest cover loss from 2000 to 2005 was mapped within the resulting year 2000 forest mask. All stand-replacing events, whether caused by logging, road/pipeline construction, wind throws, stand-replacement forest fires,

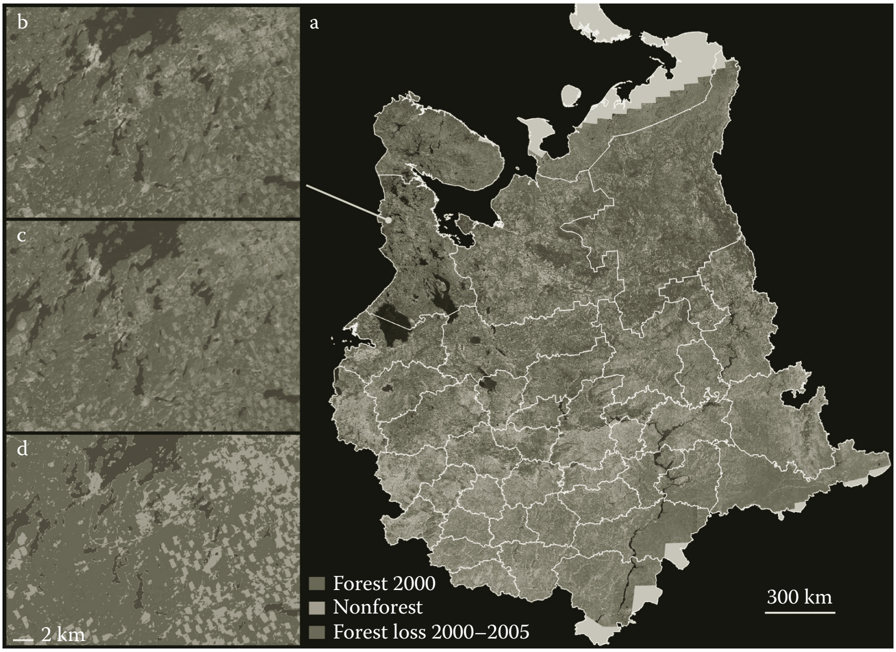

FIGURE 8.2
(See color insert.) Forest cover loss monitoring in European Russia. (a) The ca. 2000 region-wide Landsat ETM+ image composite. (b–d) Zoom-in example of forest cover and change mapping in the Republic of Karelia: b—the ca. year 2000 image composite; c—the ca. year 2005 image composite; d—classification result.

or severe insect outbreaks, were mapped together without any attempt to discriminate among them. Within low-intensity selective logging sites, only areas with significant forest impact (roads and clearings) were mapped.

The total forest area within analyzed regions of European Russia was estimated to be 150,228 thousand ha at the time around year 2000. The area of forest cover loss from 2000 to 2005 is 2,210 thousand ha, which represents a 1.5% of the year 2000 forest cover. Our forest extent estimate is within 1% difference with the latest available official forest cover area assessment for year 2003 (ROSLESINFORG 2003). At the regional level, our forest area estimates are well correlated (R^2 of 1.00) with official statistics. A per-pixel validation with independently derived forest cover mapping results for 23 blocks 20 km × 20 km in size within the boreal and temperate forests showed good agreement, with an overall forest cover accuracy of 89% (kappa of 0.78) and overall change detection accuracy of 98% (kappa of 0.71). A comparison at the individual sample block level, however, indicated relatively high forest cover classification uncertainty along the boreal forest's northern limit (overall accuracy of 87%) and low forest cover loss producer's accuracy (58%) within southern temperate forests featuring small-scale logging.

Forest cover loss was distributed unevenly within the administrative regions, reflecting several forest management issues. More than 60% of the total forest cover loss was found within the largest northern forest regions including Arkhangelsk, Kirov, Leningrad, and Vologda Oblast, Komi, and Karelia Republics. While regional forest cover loss is linearly related to forest area (R^2 of 0.84), the Leningrad region had the largest residual value, indicating a much higher rate of forest cover loss than the general trend within the area of study. One-third of the analyzed regions have a percent forest cover loss above the average and represent areas of intensive forest harvesting and frequent wildfires. These regions are located in the western and central parts of European Russia, close to large industrial cities and the Finnish border. Regions of eastern European Russia, the Urals, and northern forest–tundra transition have the lowest proportional gross forest loss. The three regions with the highest proportional forest cover loss are Vladimir, Leningrad, and Moscow Oblast (forest loss 3.7%, 3.5%, and 3.1% of year 2000 forest cover, respectively) (Figure 8.3).

The high forest cover loss within Leningrad region is thought to be a consequence of intensive forest harvesting. This is confirmed by official Russian forest use statistics for annual timber harvesting. The Leningrad region had

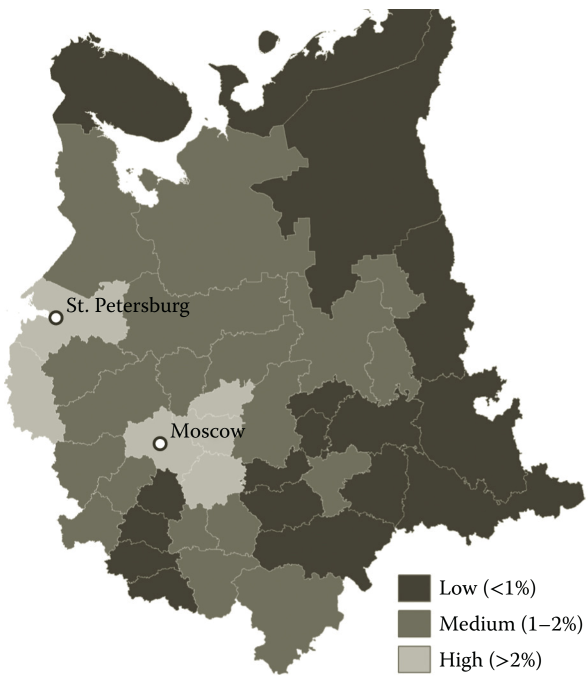

FIGURE 8.3
Forest cover loss intensity in European Russia (percent forest loss 2000–2005 of forest cover for year 2000 per administrative region).

the highest rate of timber removal of all analyzed administrative regions in the period from 2000 to 2005 (ROSSTAT 2008). The intensive felling in the Leningrad region and the neighboring Karelia Republic (gross forest cover loss 1.9% of year 2000 forest cover) is stimulated by the demand from the Nordic countries, particularly Finland, for timber from these border regions. The extensive gross forest cover loss due to industrial logging near the Russian–Finnish border could result in forest resource depletion and consequent environmental and social problems if not compensated by forest restoration.

While the gross forest cover loss in the Leningrad region was connected mainly with industrial timber harvesting, the forest loss in the Moscow and Vladimir regions is a consequence of several factors, including logging (partly illegal), insect outbreaks, human-caused fires, and expansion of settlements. The single largest forest cover loss event within these regions was due to the forest fires of year 2002. While in general wildfires play a comparatively small role in the forest dynamics within European Russia, severe drought conditions and human-induced fires led to extensive forest loss within the central regions of European Russia during the extreme fire season of 2002. According to official data, the area of burned forest in the Moscow region in 2002 was roughly 10 times higher than the mean annual burned area from 1992 to 2005 (ROSSTAT 2008). Another cause of forest cover loss around large cities is urban sprawl. For example, the expansion of settlements and industrial facilities around the city of Moscow led to the conversion of about 58 thousand ha of former forest and agriculture lands from 1998 to 2008 (Karpachevskiy et al. 2009). The forests that remain around large industrial cities provide ecological services (e.g., water and air purification, natural species refugee, recreation) that are important to urban populations. Our results raise concerns about the fate of the remaining forests in the most populated regions of European Russia.

8.3.2 Forest Cover Monitoring in the DRC

Information on forest cover extent and change is sparse or lacking for the DRC due to the vast extent of intact forest landscapes (IFLs), the lack of transportation infrastructure, and the continued political instability, all of which limit the possibilities to collect data on the ground. Satellite images are currently the only viable data source for national level mapping. We employed wall-to-wall Landsat imagery to map forest cover for the year 2000 and the gross forest cover loss between 2000 and 2010. The analysis was performed in partnership with Observatoire satellital des forêts d'Afrique central (OSFAC), a local nongovernmental organization supported by the Central Africa Regional Program for the Environment (CARPE) project of the United States Agency for International Development (USAID).

A total of 8,881 Landsat ETM+ images were selected, downloaded, and processed to create complete national-scale image composites and metrics.

About 99.6% of the country was covered by cloud-free Landsat observations. Gaps due to persistent cloud cover were located primarily in the coastal areas of the lower Congo River. The data gaps were mostly due to an insufficient number of cloud-free observations. Even though most of the available Landsat 7 observations (82%) were captured during the 11 years of observation in coastal areas, few of them were more than 50% cloud free for more than a quarter of a scene. This shows that data from a single sensor is often insufficient for monitoring forests in persistently cloudy tropical regions. A constellation of sensors with similar spectral and spatial resolution but varying overpass time and orbital cycle would be needed to provide sufficient observational coverage.

Forest cover and forest types were mapped for ca. year 2000. Forest cover classes included humid tropical forests (defined as having greater than 60% canopy cover) and woodlands (canopy cover between 30% and 60%). Humid tropical forests were additionally stratified into primary (mature) forests and secondary forests (regrowing after stand-replacement disturbance). A generic forest cover class category was mapped, and within this layer primary and secondary humid tropical forest classes were subsequently characterized. After mapping humid tropical forest classes, the remaining forest cover was assigned to the woodland class. Gross forest cover loss from 2000 to 2005 was mapped within the generic year 2000 forest mask, and forest cover loss 2005–2010 was mapped within the remaining forest area of 2005 (Figure 8.4).

The total forest cover extent in the DRC was estimated to be 159,529 thousand ha, which is within 1.5% of the FAO FRA estimate for year 2000. Primary and secondary humid tropical forests predominate (66% and 11% of total forest cover extent, respectively), with woodlands occupying the remaining 23%. The gross forest cover loss from 2000 to 2010 was 3,712 thousand ha or 2.3% of year 2000 forest area. About 57% of this loss occurred in secondary humid forests, 29% in primary humid forests, and 14% in woodlands. Secondary humid tropical forests experienced the most intensive loss (11.6% over 10 years), while the rate of loss in primary humid tropical forests and woodlands was considerably lower (1.0% and 1.4%, respectively). The gross forest cover increased by 14% between the 2000–2005 and the 2005–2010 periods. The increase was most prominent in primary humid tropical forests and woodlands (by 91% and 63%, respectively).

Visual examination of Landsat composite data suggests that almost all forest clearing was associated with the expansion of subsistence agriculture, local charcoal production, or mining. We found no evidence of major forest fires or windthrow events during the study period, with the exception of forest fires caused by the repeated eruptions of the Nyamuragira volcano. Clearings are common in secondary humid tropical forests due to the practice of rotational slash-and-burn agriculture. On the one hand, the fallow period between clearings (not quantified in this study) would be a useful indicator of land degradation. Clearing of primary forests, on the other hand, represents the expansion of agriculture into heretofore intact

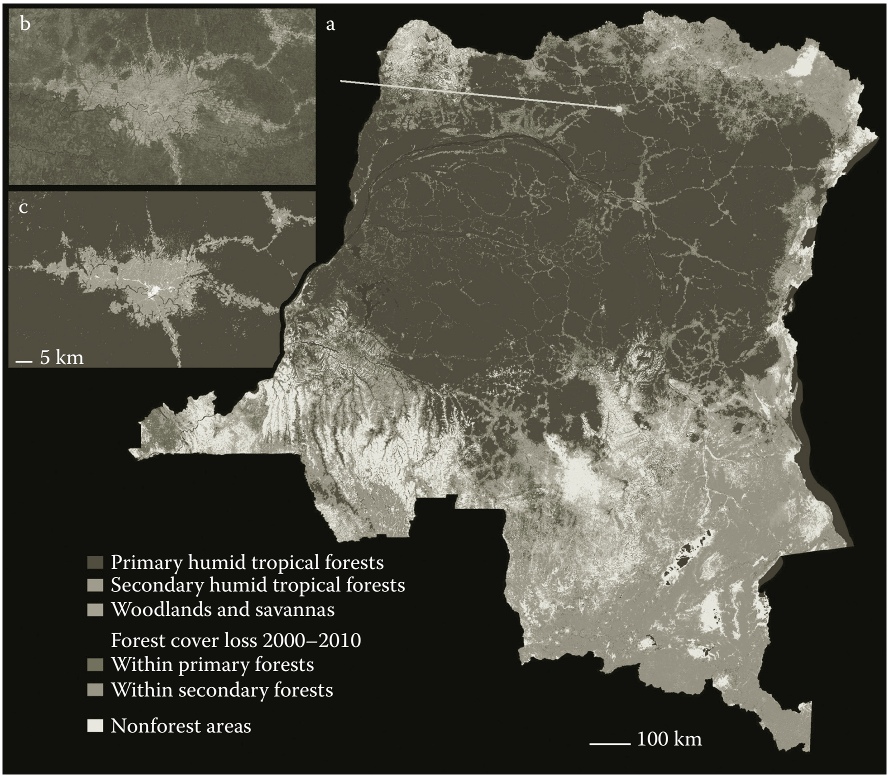

FIGURE 8.4
(See color insert.) Forest cover loss monitoring in the DRC. (a) Nation-wide forest cover and change mapping result. (b–c) Zoom-in example of forest cover and change mapping around Buta: b—ca. year 2010 image composite; c—classification result.

forests, triggering changes in ecosystem dynamics and loss of floristic and faunal biodiversity. Clearing generally occurs in belts around secondary forests and roads due to the nearly continuous distribution of population along transportation infrastructure (Figure 8.4). Since forest clearing is mainly a consequence of small-scale subsistence farming, the change patches are small and have a mean area of 1.4 ha.

Most of the clearing occurred in areas with high population density and growth rates, such as Kinshasa, Kasai-Occidental, Sud-Kivu, and Kasai-Oriental provinces. Large industrial (Tshikapa, Mbuji-Mayi, Kolwezi, Lubumbashi) and artisanal mining areas (Kisangani, Beni, Buta) also exhibited intensive forest loss. The intensive forest loss along the boundaries of Virunga National Park (NP) in the North Kivu province is related to ongoing political unrest. The Virunga NP has the highest loss of primary forest of all national parks in the country (0.9%, compared to the mean of 0.4%), making it one of the most threatened natural protection areas. The loss of primary forest in protected areas increased by 64% from 2000–2005 to 2005–2010, highlighting the pressures and the need to improve the protection and management of nature reserves across the country.

8.4 Global- and National-Scale Forest Degradation Monitoring

It is well known that forest degradation, including fragmentation of natural landscapes, has a negative effect on global climate change and biodiversity (Harris 1984). However, forest degradation is a complex concept that is difficult to define and even more difficult to map. Unlike forest cover extent that can be quantified using straightforward biophysical parameters, assessing and monitoring forest degradation is a complicated task due to the great variability in the forms, factors, and degrees of human impact. In the late 1990s, a group of nongovernmental organizations including Greenpeace and the World Resources Institute developed a simple yet straightforward approach for assessment and monitoring of forest degradation called the IFL method (Potapov et al. 2008). An IFL is an unbroken expanse of natural ecosystems that shows no signs of significant human activity and is large enough to maintain all native biodiversity, including viable populations of wide-ranging species. The essence of the IFL method is to use medium spatial resolution satellite imagery to locate IFLs, establish their boundaries, and use them as a baseline for monitoring. The IFL method provides a simple and feasible way to cope with the complexity of the forest degradation concept by using changes in forest intactness as a proxy for forest degradation (Potapov et al. 2009). In this context, forest degradation is defined as a reduction in the ecological integrity of a forest landscape below a certain threshold due to human influence (e.g., conversion, alteration, and fragmentation), and forest landscapes are treated as being either intact (undegraded) or nonintact (altered or degraded).

An IFL boundary is defined using a sequence of two sets of criteria specifically developed for visual interpretation of medium spatial resolution satellite imagery. These criteria are globally applicable and easily replicable, allowing for repeated assessments over time as well as verification by independent assessments. The first set of criteria is used to eliminate lands with evidence of significant human-caused alteration from IFL status. Such alteration includes (1) settlements and industrial objects; (2) infrastructure used for transportation between settlements or for industrial development of natural resources; (3) agriculture and forest plantations; (4) industrial activities (including logging, mining, oil and gas exploration or extraction) during the last 30–70 years; and (5) stand-replacing wildfires during the last 30–70 years if located in the vicinity of infrastructure or developed areas. Some alterations, notably low-intensity human impacts that tend to occur in the vicinity of settlements and roads (e.g., selective logging and overhunting), are not visible in medium spatial resolution imagery. We, therefore, removed such areas by applying a buffer zone around settlements and transportation infrastructure, adapting the buffer width to the expected extent of human influence. For the global IFL method, a 1 km wide buffer was used. The second set of criteria is used to eliminate fragmented lands from IFL status by identifying patches of otherwise IFLs that are smaller or narrower than a selected threshold value. For the global analysis, a patch needed to meet the following criteria to qualify as an IFL: (1) minimal area of 500 km^2, (2) minimal width of at least 10 km (measured as the diameter of the largest circle that can be fitted inside the patch), and (3) at least 2 km wide in corridors or appendages to areas that meet the above criteria.

The IFL method was used to assess the ecological integrity of the world's forest landscapes. First, the current global extent of the forest zone was determined, defined as lands with at least 20% tree canopy cover (Hansen et al. 2003) and including treeless areas that occur naturally within forest ecosystems, such as wetlands. The area under consideration was then reduced by identifying and eliminating developed areas and infrastructure through visual interpretation of Landsat imagery. The global IFL mapping was done before the Landsat data archive was opened, and the GeoCover Landsat orthorectified image collection was therefore used. A global coverage of Landsat TM data (representing an average date of 1990) and ETM+ data (representing an average date of 2000) was used to systematically assess candidate IFL areas for human-caused alteration and fragmentation and to delineate IFLs. Fine-scale geospatial datasets on roads and settlements were used where available to facilitate interpretation. Infrastructure buffering was performed simultaneously with the visual image analysis. Altered and fragmented patches were eliminated from the area of study and remaining areas, if meeting the criteria, were classified as IFLs.

The current extent of the world's forest zone is 5,588 million ha. IFLs make up 23.5% of the forest zone (1,313 million ha). The remainder of the forest zone is affected by development or fragmentation and thus is either managed or degraded. The vast majority of the world's remaining IFLs are found within humid tropical and boreal forests (45.3% and 43.8% of the total IFL area, respectively). The distribution of IFL within these biomes is heterogeneous, reflecting differences in the history and intensity of economic development. Tropical IFLs are found mainly in the large forest massifs of the Amazon and Congo basins, and in insular Southeast Asia. More than half of the IFL area in the humid tropics is in the Amazon basin, while IFLs are largely absent in the lowlands of continental Asia. In the boreal region, the highest proportion of IFL is in the North. IFLs occupy more than half of the forest zone in Canada but have nearly disappeared in Europe due to the long history of intensive agriculture and forest management.

A particular strength of the IFL method is that it can easily be applied to different points in time, making it suitable for regular reassessments, i.e., monitoring. The work is conducted through expert-based visual interpretation using the same criteria and the same type of data as in the baseline assessment (medium spatial resolution satellite imagery) but is much less time consuming as only remaining IFLs need to be monitored. We used the IFL method to assess change in IFLs from 2000 to 2010 (using two 5-year steps) for the three largest tropical forest countries: Brazil, the DRC, and Indonesia (Figure 8.5). For the DRC and Indonesia, national reassessments were performed using Landsat time-sequential image composites (see Section 8.2), individual Landsat scenes, and ASTER imagery. For Brazil, the forest cover loss monitoring results from PRODES (INPE 2002) were used to update the IFL map.

Our results show that a significant extent of intact areas has been lost within all three countries after year 2000. The total proportion of IFLs lost was 5.2%, 1.9%, and 10.0% in Brazil, the DRC, and Indonesia, respectively. The IFL loss in Brazil is mostly a consequence of agroindustrial development along the forest/agriculture boundary of "arc of deforestation." In the DRC, the loss of IFLs is unevenly distributed and located mostly within active timber

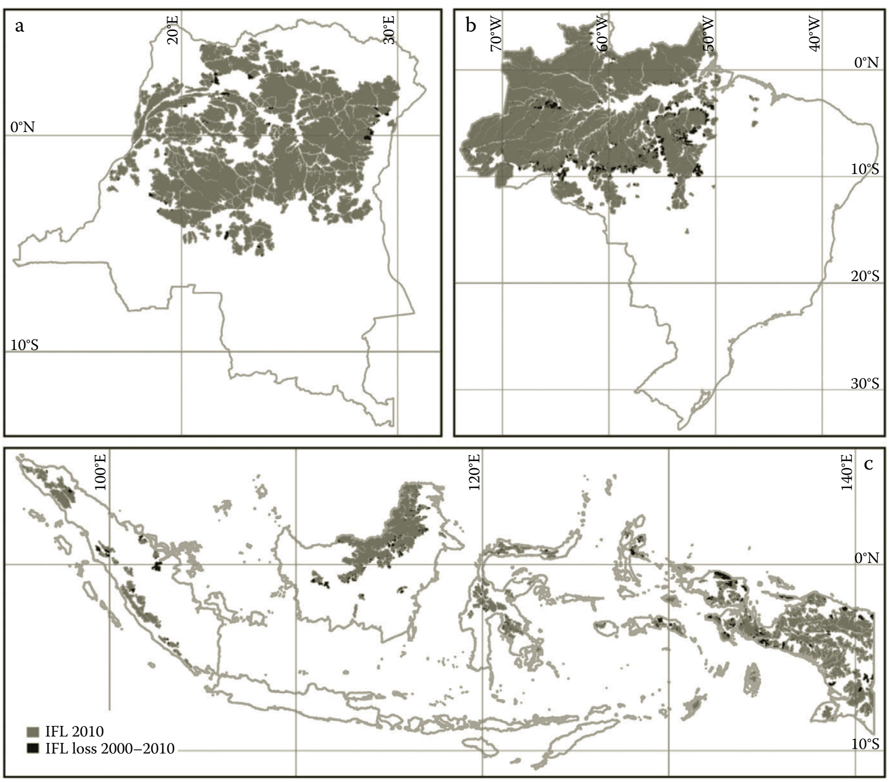

FIGURE 8.5
IFL decadal monitoring results for the DRC (a), Brazil (b), and Indonesia (c).

concessions (where selective logging is taking place) and in the vicinity of growing settlements (where subsistence agriculture, artisanal logging, and charcoal production are expanding). Conversion of IFLs to oil palm and timber plantations is common within the Indonesian lowlands of Sumatra and Kalimantan islands, while IFL loss in mountain areas is generally caused by selective logging.

While all analyzed countries experienced reductions of IFL area, the change trends are different, as approximated by IFL loss between 2000 and 2005 and 2006 and 2010. Brazil features a dramatic reduction in overall IFL loss from 4.1% during the first 5 years to 1.1% during the second half of the decade. In the DRC, the IFL loss rate was relatively stable (1.0% during 2000–2005 and 0.9% during 2006–2010). In contrast, the IFL loss rate in Indonesia increased from 4.2% to 5.8%. While no special analysis is available to explain these trends, we can speculate on their origins based on the global economy and the distribution of IFL loss. Undoubtedly, the global financial crisis that began in 2007 and followed by the recession during the end of the decade is a single most important factor behind the reduction of agroindustrial clearings and timber production worldwide. This crisis was more pronounced in Western countries but had consequences also for their main suppliers. Brazil was hit hardest of the three analyzed countries and experienced a negative GDP growth rate in 2009 (CIA 2011). The efforts by the Brazilian government to reduce forest clearing in the framework of the UN REDD+ program and the establishment of an effective deforestation monitoring system have likely also played a role. The situation was different in Asian countries, including Indonesia, where GDP either continued to grow or fell only slightly. Indonesia accelerated the conversion of remaining lowland forest areas to plantations and expanded selective logging in remote mountain forests, especially in the Papua island group. The IFL change dynamic is complicated in the DRC due to the combination of global economic drivers and local political instability. While economic stagnation and years of civil war have resulted in a low level of forest clearing in the country, an analysis of nature resources management (Endamana et al. 2010) highlighted that there was little change in conservation indicators in the Congo basin over the last decade. We may conclude that more favorable economic conditions may accelerate the loss of IFLs in the DRC, unless improved conservation policies are established.

8.5 Conclusion

Independent, satellite-based monitoring is an important tool for providing transparent information on forest change. Government officials, land managers, researchers, conservationists, and civil society groups can use such information to make better-informed decisions regarding the management of forest ecosystems. We have presented a novel, automated Landsat image processing approach that could be used for timely monitoring of forest cover change at national scales. This approach is a practical solution for examining trends in forest cover change at regional to national scales and could be implemented at a fraction of the cost of individual scene processing in terms of workload and processing time. Regional monitoring has the advantage of providing internally consistent, directly comparable results for assessing variation in the spatiotemporal trends of forest cover dynamics.

Landsat-based mapping of forest cover extent and change using supervised expert-driven classification is a well-established and accepted methodology, and reported accuracies for Landsat forest cover change detection range between 75% and 91% (Coppin and Bauer 1994). Our Landsat-based mapping algorithm has been tested for large forest regions, and our regional-scale Landsat forest cover change results are comparable with NFI data and individual scene supervised characterizations. The spatial accuracies of forest cover and change detection have not been rigorously validated, however, due to the lack of high spatial resolution imagery and field data. In the future, our approach can be validated using a series of high spatial resolution data sets. Our results can be used to target sampling with high spatial resolution imagery as part of a national-scale validation protocol.

The application of our forest monitoring approach in different biomes at the national/regional scales illustrate the possibility that it can be used also at the biome/global scales. Remaining challenges include possible gaps in future image availability, insufficient observation frequency for some areas, and the lack of a rigorous validation that uses high spatial resolution imagery along with field data. These concerns must be addressed before the proposed algorithm is implemented further. Yet having the technical ability to conduct satellite-based monitoring is not sufficient to detect and solve all environmental problems caused by inefficient and irresponsible forest management. First, only some components of ecosystem health can be monitored from space. Other components such as reductions in biodiversity due to overhunting and poaching, effects of chemical pollution, and global impact caused by human-induced climate change require a set of *in situ* measurements. Second, the forest management problems that are highlighted by monitoring data are sometimes a result of inadequate governmental control of natural resources exploitation and/or political and economic instability. Weak and/or corrupt governance precludes the maintenance of forest ecosystem services and protection of nature conservation areas. Integrating the drivers of forest cover change with satellite-based forest monitoring methods into national natural resource management systems and international conservational initiatives are important future steps for national-scale monitoring activities.

Acknowledgments

Support for this work was provided by the United States National Aeronautics and Space Administration's Land Cover and Land Use Change program and the USAID-supported CARPE project under Grants NNG06GD95G and NNX09AD26G.

About the Contributors

Peter Potapov received a diploma in botany from the Moscow State University, Moscow, Russia, in 2000, and a PhD in ecology and natural resources from the Russian Academy of Science, Moscow, Russia, in 2005. From 1998 to 2006, he was a GIS specialist at Greenpeace (Russian office) where he took part in developing an approach for mapping and monitoring forest degradation using the IFL method. He was a postdoctoral researcher from 2006 to 2011 at South Dakota State University, Brookings, South Dakota, and currently he is a research associate professor at the University of Maryland, College Park. His current research is focused on establishing a global operational forest monitoring algorithm using integration of Landsat and MODIS data.

Svetlana Turubanova received a BSc in geography from the Komi Pedagogical Institute, Syktyvkar, Russia (1996), an MSc in ecology from the Pushchino State University, Pushchino, Russia (1998), and PhD in ecology from the Russian Academy of Science, Moscow, Russia (2002). She started her career as a GIS specialist at Greenpeace Russia in 1999. Later, she was a postdoctoral researcher at South Dakota State University (from 2008 to 2011), Brookings, South Dakota. Currently she is a research associate at the University of Maryland, College Park, Maryland. Her current research interests are focused on national-scale Landsat-based forest mapping, deforestation monitoring, and forest degradation assessment.

Lars Laestadius holds a forest degree from the Swedish University of Agricultural Sciences, Uppsala, Sweden, and a PhD in forestry from the Virginia Polytechnic Institute and State University, Blacksburg, Virginia. He is a senior associate at the World Resources Institute, Washington, DC, and conducts forest policy research with a special interest in frontier forest landscapes assessment, forest landscape restoration, and the legality of forest management and trade. Prior to his current position, he served in the European Commission and was responsible for coordinating nationally funded European forestry and forest products research.

Alexey Yaroshenko received a diploma in botany in 1993 and a PhD in ecology and natural resources in 1997, both from Moscow State University, Moscow, Russia. From 1993 to 1997, he was a freelance researcher of forests of Central Russia and the Urals. Since 1997, he has been the head of the forest department in Greenpeace, Russia. His current work and main area of interest is related to forest policy and economics and boreal forest conservation. He is the founder (2004) and editor of the popular Russian portal for professional foresters and environmentalists—https://www.forestforum.ru.

Ilona Zhuravleva received her diploma in ecology from Tver State University, Tver, Russia in 2004. Since 2005, she has been working for Greenpeace Russia first as an assistant, and then as the head of the GIS unit. Her research interests are focused on IFL mapping, forest cover change analysis, forest fire monitoring, and conservation planning. Her current work is focused on developing Web applications to present deforestation mapping and IFL assessment results in tropics and boreal regions.

References

Achard, F. et al., Determination of deforestation rates of the world's humid tropical forests. *Science*, 297, 999–1002, 2002.

Breiman, L. et al., *Classification and Regression Trees*. Wadsworth and Brooks/Cole, Monterey CA, 1984.

Chander, G., Markham, B.L., and Helder, D.L., Summary of current radiometric calibration coefficients for Landsat MSS, TM, ETM+, and EO-1 ALI sensors. *Remote Sensing of Environment*, 113, 893–903, 2009.

CIA, *The World Factbook 2011*. CIA, Washington, DC, 2011 (https://www.cia.gov/library/publications/the-world-factbook/fields/2003.html). Accessed 12/14/2011.

Coppin, P.R. and Bauer, M.E., Processing of multitemporal Landsat TM imagery to optimize extraction of forest cover change features. *IEEE Transactions on Geoscience and Remote Sensing*, 32, 918–927, 1994.

Endamana, D. et al., A framework for assessing conservation and development in a Congo Basin Forest Landscape. *Tropical Conservation Science*, 3, 262–281, 2010.

FAO, *The 2010 Global Forest Resources Assessment Remote Sensing Survey: An Outline of the Objectives, Data, Methods and Approach*. FAO FRA Paper 155, FAO, Rome, 2009.

Hansen, M., Dubayah, R., and DeFries, R. Classification trees: An alternative to traditional land cover classifiers. *International Journal of Remote Sensing*, 17, 1075–1081, 1996.

Hansen, M., Stehman S., and Potapov P., Quantification of global gross forest cover loss. *Proceedings of the National Academy of Sciences of the USA*, 107, 8650–8655, 2010.

Hansen, M.C. et al., Global percent tree cover at a spatial resolution of 500 meters: First results of the MODIS vegetation continuous fields algorithm. *Earth Interactions*, 7, 1–15, 2003.

Hansen, M.C. et al., A method for integrating MODIS and Landsat data for systematic monitoring of forest cover and change and preliminary results for Central Africa. *Remote Sensing of Environment*, 112, 2495–2513, 2008.

Harris, L.D., *The Fragmented Forest: Island Biogeography Theory and the Preservation of Biotic Diversity*. The University of Chicago Press, Chicago, IL, 1984.

Holben, B., Characteristics of maximum-value composite images from temporal AVHRR data. *International Journal of Remote Sensing*, 7, 1417–1434, 1986.

INPE, *Deforestation Estimates in the Brazilian Amazon*. INPE, São José dos Campos, 2002.

Jin, S. and Sader, S.A., MODIS time-series imagery for forest disturbance detection and quantification of patch size effects. *Remote Sensing of Environment*, 99, 462–470, 2005.

Karpachevskiy, M.L. et al., *Natural Environment of Moscow Region: Losses 1992–2008 and Current Threats*. Biodiversity Conservation Center, Moscow, 2009.

Masek, J.G. et al., A Landsat surface reflectance dataset for North America, 1990–2000. *IEEE Geoscience and Remote Sensing Letters*, 3, 68–72, 2006.

Olthof, I. et al., Landsat ETM+ mosaic of northern Canada. *Canadian Journal of Remote Sensing*, 31, 412–419, 2005.

Potapov, P., Turubanova, S., and Hansen, M.C., Regional-scale boreal forest cover and change mapping using Landsat data composites for European Russia. *Remote Sensing of Environment*, 115, 548–561, 2011.

Potapov, P. et al., Mapping the World's intact forest landscapes by remote sensing. *Ecology and Society*, 13, 1–16, 2008.

Potapov, P. et al., *Global Mapping and Monitoring the Extent of Forest Alteration: The Intact Forest Landscapes Method*. FAO FRA Paper 166, FAO, Rome, 2009.

ROSLESINFORG, *Forest Fund of Russia (Data of State Forest Account, State by January 1, 2003).* VNIILM, Moscow, 2003.

ROSSTAT, *Regions of Russia: Social and Economic Indicators.* ROSSTAT, Moscow, 2008.

Tomppo, E., Multi-source national forest inventory of Finland. *The Finnish Forest Research Institute. Research Papers*, 444, 52–60, 1993.

Tucker, C.J. and Townshend, J.R.G., Strategies for monitoring tropical deforestation using satellite data. *International Journal of Remote Sensing*, 21, 1461–1471, 2000.

Willén, E., Rosengren, M., and Persson, A., Multiresolution satellite data for boreal forest change detection mapping and monitoring. *Proceedings of ForestSat 2005*, 1–6, 2005.

Williams, D.L., Goward, S., and Arvidson, T., Landsat: Yesterday, today, and tomorrow. *Photogrammetric Engineering and Remote Sensing*, 72, 1171–1178, 2006.

Wulder, M.A. et al., Monitoring Canada's forests. Part 1: Completion of the EOSD land cover project. *Canadian Journal of Remote Sensing*, 34, 549–562, 2008.

9

The Brazilian Amazon Monitoring Program: PRODES and DETER Projects

Yosio Edemir Shimabukuro, João Roberto dos Santos, Antonio Roberto Formaggio, Valdete Duarte, and Bernardo Friedrich Theodor Rudorff

Brazilian Institute for Space Research

CONTENTS

9.1 Introduction 153
9.2 Brazilian Amazon 155
9.3 Deforestation Monitoring in the BLA 158
  9.3.1 Digital PRODES Methodology 158
  9.3.2 DETER Methodology 161
9.4 Results 162
  9.4.1 Analog and Digital PRODES 162
  9.4.2 DETER Project 164
9.5 Discussion and Conclusion 166
About the Contributors 167
References 168

9.1 Introduction

The Amazonia region comprises the greatest rain forest of our planet where the largest continuous remaining tropical forest can be found. In Brazil, an accelerated anthropization process began at the end of the 1960s in response to governmental policies to integrate the vast Amazonian region with the rest of the country. This was to be achieved mainly through road construction and incentivized transmigration policies that consequently expanded the Brazilian agriculture frontier. The anthropization process has been most intense in the so-called *arc of deforestation* where the Amazon ecosystem meets with the savanna (*cerrado*) ecosystem. Since 1973, Brazil has had access to remote sensing imagery from the series of Landsat satellites, enabling the quantification of natural resource extent and modification over the Amazon region. Based on the availability of these images, the Brazilian government began monitoring of the Amazon forest to quantify deforestation at multiyear intervals. Quantitative data on deforestation could then be used to assess the human impacts of the development policies, with the objective of minimizing the negative effects of the man–biome interaction on renewable and nonrenewable resources.

Since 1988, the Brazilian government has performed annual monitoring of the Amazon forest using Landsat-type imagery through the PRODES (monitoring of Amazon forest) project carried out by the Brazilian Institute for Space Research (INPE). PRODES has quantified approximately 750,000 km^2 of deforestation in the Brazilian Amazon through the year 2010, a total that accounts for approximately 17% of the original forest extent. PRODES data have revealed the annual deforestation rates to vary significantly in response to domestic political, economic, and financial policies as well as foreign market demands.

PRODES information is based primarily on Landsat imagery. Medium spatial resolution (30 m) data such as Landsat have a relatively low temporal resolution of 16-day repeat coverage, allowing for annual monitoring of deforestation. More rapid updating of forest disturbance is not possible with Landsat as the infrequent repeat coverage coupled with the persistent cloud cover of the humid tropical Amazon basin limits the number of viable land surface observations. This fact prevents the government and environment control agencies from making fast and adequate interventions to stop illegal deforestation activities.

Near-real-time deforestation monitoring is possible using the almost daily images of the MODIS (MODerate resolution Imaging Spectroradiometer) sensor on board the Terra and Aqua satellite platforms. Thus, a new methodology based on MODIS images was developed for rapid detection of deforestation in the Amazon region through the DETER (real-time detection of deforestation) project (Shimabukuro et al. 2006). While MODIS is a coarse spatial resolution sensor, and not viable for area estimation of deforestation, MODIS data can be valuable as a change indicator, or alarm product in the service of land management policies and enforcement.

This chapter presents an overview of the PRODES and DETER projects for annual and monthly monitoring of deforestation in the Brazilian Amazon, respectively. Initially, the Brazilian Amazon region is characterized in terms of its soil, biodiversity, climate, and vegetation followed by the deforestation history and the description of the methodology developed at INPE for the deforestation monitoring activities based on remote sensing image-processing and geographic information system (GIS) techniques. Results from more than three decades of monitoring are presented and discussed, illustrating the rapid deforestation that occurred during this period in the Amazon region. The results have quantified the magnitude and trends of deforestation in the Brazilian Amazon. Results provide an invaluable input to decision makers in establishing public policies and enforcing environmental governance in the critical ecosystems of the Brazilian Amazon.

9.2 Brazilian Amazon

The Amazon rainforest is located in South America and covers an area of 6.4 million km². Most of the Amazon rainforest (63%) is found in the Brazilian Legal Amazon (BLA) (Figure 9.1), with the remaining part being distributed among the countries of Peru, Colombia, Bolivia, Venezuela, Guiana, Suriname, Ecuador, and French Guiana. Much attention has been given to this region due to its relevance in terms of biodiversity as well its unique environmental services at the global scale.

The BLA is a geopolitical unit, established in 1966 by the Brazilian government. The BLA is located between 5° N, 20° S and 44° W, 75° W and covers an area of approximately 5 million km². It encompasses the whole states of Acre, Amapá, Amazonas, Mato Grosso, Pará, Rondônia, Roraima, Tocantins, and the western part (44° W) of the state of Maranhão (IBGE 2000). The BLA is included in the Amazon river basin except for the

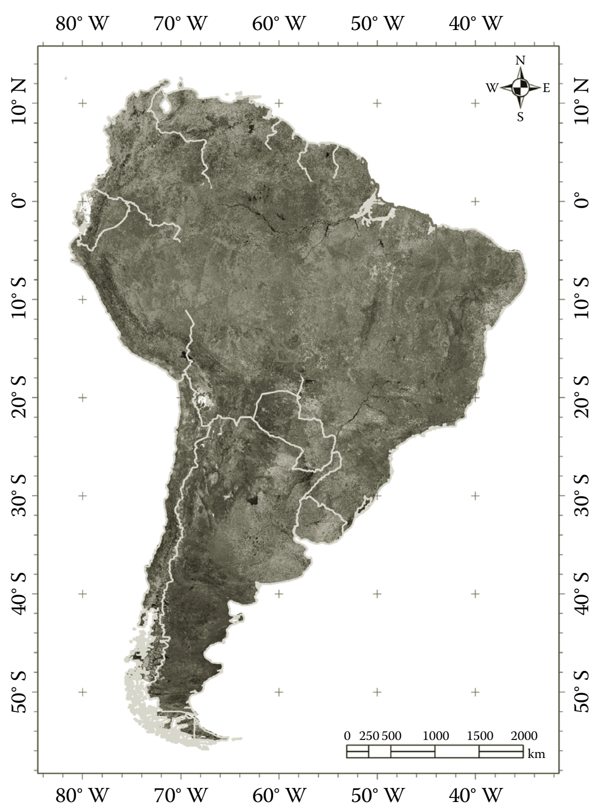

FIGURE 9.1
(See color insert.) The BLA (*red*) located in the South American continent.

southern part of Mato Grosso state (Paraguay river basin) and for part of Maranhão state (Parnaíba river basin).

Soils: The Amazon region includes varied soil classes formed under great geological diversity, exhibiting significant variation in relief and under the influence of high temperatures and precipitation typical for warm super humid or humid equatorial climates. The natural soil fertility is relatively low; however, the Amazon rainforest is a self-sustainable ecosystem due to its own nutrient cycles, making it vulnerable to anthropic interference (IBAMA 2009).

Biodiversity: The Amazon region comprises a large variety of ecosystems including upland forests (*terra firme*), swamp forests (seasonally flooded forest—*varzeas* and permanently flooded forest *igapós*), grasslands, and savannas (*cerrado*). An extremely rich biodiversity is found within the regions, including 1.5 million plant species; 3,000 fish species; 950 types of birds; and an enormous amount of insect, reptile, amphibian, and mammal species (IBAMA 2009).

Climate: The Amazon region is characterized by its enormous ability for water recycling. About 63%–73% of the water is lost through evapotranspiration, and approximately 50% of it is recycled within the region through precipitation (Salati 1985).

The average temperature varies from 25.8°C during the rainy season (May–September) to 27.9°C during the dry season (October–April). The duration of these seasons may vary due to the large extent of the Amazon region. The average annual precipitation is 2,250 mm, varying from 1,500 mm in the northern and southern regions to 3,000 mm in the northwestern region of the Amazon.

Vegetation: The Amazon region is covered by evergreen tropical rainforest comprised of three major classes of vegetation: (1) the evergreen tropical forest *stricto sensu*; (2) the semievergreen tropical forest; and (3) the semideciduous tropical forest (IBGE 1988). Evergreen tropical forests *stricto sensu* are mostly found in very moist regions where the annual precipitation is around 3,000 mm. They are composed of multilayered broadleaf evergreen trees that may reach 50 m in height, with a sparse substratum consisting mainly of herbaceous plants. Semievergreen tropical forests are spread along less humid areas, with annual precipitation varying from 2,000 to 3,000 mm. These forests are composed of three-layered formations of perennial and deciduous broadleaf trees, with the latter type being sparsely present and forming the top layer of the canopy. Semideciduous tropical forests differ from semievergreen ones by having a larger proportion of deciduous species.

The *cerrado* is a savanna-type ecosystem appearing mainly in the southern and eastern portions of the Amazon region. It is composed of broadleaf, semideciduous, or evergreen short trees typically growing in well-drained soils that are poor in nutrients, in a region where the average annual temperature ranges from 20°C to 26°C and annual precipitation ranges from 1,250 to 2,000 mm with marked influence of the austral winter dry season (May through September). In general terms, five structural types of *cerrado* are acknowledged to exist (Oliveira-Filho and Ratter 2002): *cerradão*—dominated by arboreous vegetation (8–12 m tall) whose canopy covers 50%–90% of the area; *cerrado* (*stricto sensu*)—dominated by trees and shrubs (3–8 m tall), with a more sparse canopy cover (above 30%); *campo cerrado*—formed by dispersed trees and shrubs, with a high density of herbaceous vegetation; *campo sujo*—dominated by herbaceous vegetation, with shrubs and small dispersed trees; and *campo limpo*—which is different from the *campo sujo* because it has no shrubs nor trees. *Cerrado* may also be associated with seasonally flooded areas. In total, the Amazon region has approximately 10%–15% of worldwide biomass (Houghton et al. 2001).

Deforestation in the BLA: Deforestation in the BLA has been a concern of several governmental and nongovernmental agencies, especially over the last three decades (Moran 1981; Skole and Tucker 1993). Although there is a longer history of human occupation in the BLA, nearly 90% of the deforestation for pasture and agriculture occurred between 1970 and 1988, as indicated by estimates based on satellite images (Skole et al. 1994).

Historically, the Brazilian territory was occupied along the coastline, with most of its population concentrated in this region. In an attempt to change this occupation pattern by increasing inland settlement, the federal capital was moved from the coast (Rio de Janeiro) to the Central region of Brazil (Brasília) in the mid-1950s (Mahar 1988). This occupation policy required major infrastructure investments to connect Brasília to the other regions of Brazil. The construction of the Belém-Brasília road (BR-010) in 1958 was the main factor that triggered major deforestation activities in the BLA (Moran et al. 1994; Nepstad et al. 1997). Subsequent events such as the construction of the BR-364 across the states of Mato Grosso, Rondônia, and Acre and the PA-150 in the state of Pará encouraged even more deforestation activities, converting forest into pasture and agriculture land (Moran 1993).

To introduce governance in the BLA, the SUDAM (Superintendência do Desenvolvimento da Amazônia) and the BASA (Banco da Amazônia) were established in 1966. Small producers were granted with incentives to invest in agriculture projects (Moran et al. 1994). Large producers were also granted tax incentives in exchange for converting forest to pasture land (Moran 1993). The incentives granted to large producers were the major drivers of deforestation; small producers had a lesser impact on deforestation due to the comparatively smaller scale practices of subsistence agriculture (Fearnside 1993).

Other activities with high economic value such as mining and selective logging also contributed to deforestation in the BLA (Cochrane et al. 1999).

Major deforestation in the BLA has been concentrated in the so-called *arc of deforestation,* located in the Southern and Eastern parts of the BLA from Acre to Maranhão states (Cochrane et al. 1999; Achard et al. 2002).

9.3 Deforestation Monitoring in the BLA

Since the late 1970s, INPE has performed deforestation assessments in the BLA using remotely sensed imagery. These assessments were carried out together with the former IBDF (Instituto Brasileiro de Desenvolvimento Florestal) that was later incorporated with IBAMA (Instituto Brasileiro do Meio Ambiente e dos Recursos Naturais Renováveis). The first assessments were carried out with the use of images acquired by the MSS sensor (four spectral bands with spatial resolution of 80 m) on board the Landsat-1, -2, and -3 satellites, during the periods of 1973–1975 and 1975–1978 using visual interpretation techniques (Tardin et al. 1980).

From 1988 onward, annual deforestation assessments were provided for the entire BLA using images from the TM sensor (six spectral bands with spatial resolution of 30 m) on board the Landsat-5 satellite, with improved mapping quality due to its improved spatial and spectral resolutions as compared to the MSS data. The methodology applied to map the deforested areas was based on visual interpretation of color composites (5R-4G-3B) of TM images in hard copy format at the scale of 1:250,000. The visually interpreted polygons of the deforested areas were summed up to compute the total deforested land for each state and presented in tabular format. This method, known as analog PRODES, was performed until 2001.

By the end of the 1990s, an automated methodology began to be developed and was named digital PRODES (Shimabukuro et al. 1998). However, the deforestation information provided by PRODES was not sufficient for the more frequent monitoring surveillance needs of various Brazilian government agencies. Therefore, the DETER project was developed based on the high temporal resolution images of the MODIS sensor to provide geospatial information on deforestation activities in near real time and has been in operation since 2004.

9.3.1 Digital PRODES Methodology

Digital PRODES is the world's largest remote sensing project for monitoring deforestation activities in tropical rain forests. It has the objective to survey all deforested areas within the 5 million km^2 of the BLA, an area covered by 229 Landsat scenes (Figure 9.2).

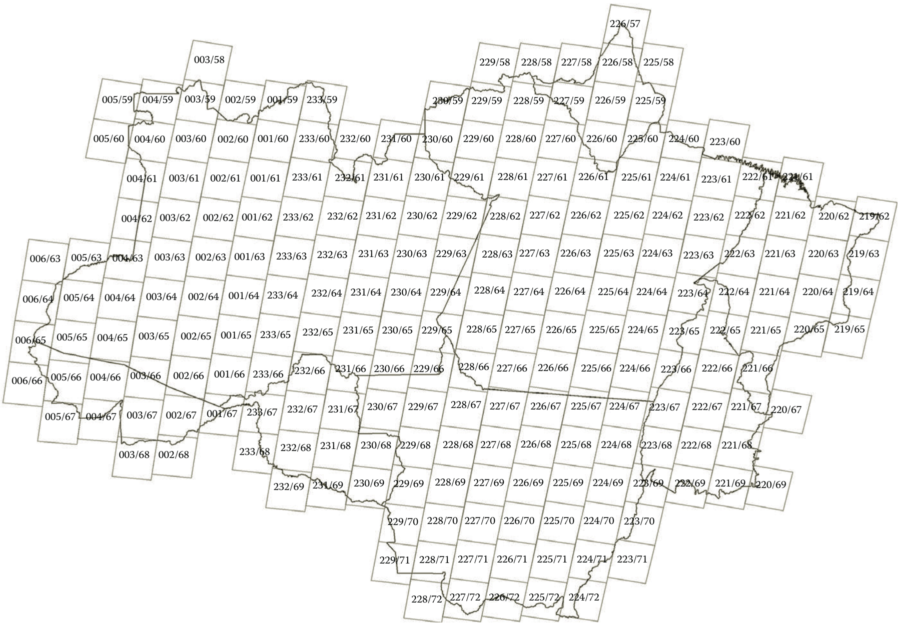

FIGURE 9.2
The BLA covered by 229 TM or ETM+/Landsat images for the annual survey of deforestation. (From INPE, *Monitoramento da cobertura florestal da Amazônia por satélites: Sistemas PRODES, DETER, DEGRAD E QUEIMADAS 2007–2008*, Instituto Nacional de Pesquisas Espaciais, São José dos Campos, SP, Brazil, 2008; Mahar, D., *Government Policies and Deforestation in Brazil's Amazon Region*, World Bank, Washington, DC, 1988.)

PRODES depicts deforestation within the BLA. A mask of nominally intact forest is annually updated by identifying new deforestation events to the exclusion of nonforest vegetation type and other change dynamics such as the clearing of secondary regrowth. Input Landsat TM images are selected from July, August, and September acquisitions. This period is within the *arc of deforestation's* local dry season and represents an atmospheric window where cloud-free images are typically available. These images are rectified using nearest neighbor sampling to a UTM projection, resulting in a cartographic product with 50 m internal error. For PRODES, TM 3 (red), TM 4 (NIR), and TM 5 (MIR) bands are used to generate the fraction images. The legend for the maps contains the following classes: forest, non-forest *cerrado arbustivo, campo limpo de cerrado, campinarana*, etc.), accumulated deforestation from previous years, deforestation from the current year, hydrography, and cloud.

Digital PRODES consists of the following methodological steps: (1) generation of per pixel vegetation-, soil-, and shade-fractional images; (2) segmentation based on growing regions' algorithm; (3) classification based on nonsupervised classifier; (4) mapping the classes based on the following legend: forest, nonforest (vegetation that is not characterized by a forest structure), deforestation (accumulated deforestation up to the previous year), hydrography, and clouds; and (5) editing of classified map based on visual interpretation to minimize omission and commission errors from the automatic classification to produce the final deforestation map in digital format. PRODES products are available at the official PRODES website (http://www.obt.inpe.br/prodes/index.html).

A linear spectral mixture model (LSMM) is used to produce fraction images of vegetation, soil, and shade applied to the TM spectral bands (Shimabukuro and Smith 1991). This method reduces data dimensionality and enhances the specific targets of interest. A vegetation-fraction image enhances the green vegetation, a soil-fraction image enhances bare soil, and a shade-fraction image enhances water bodies and burned land. The shade-fraction image was used to characterize the total previously deforested land in the BLA (Shimabukuro et al. 1998) up to 2001. The soil-fraction image is used to classify the annual deforested increment based on the contrast between forested and deforested land.

The LSMM can be written as:

$$r_i = a \times \text{vege}_i + b \times \text{soil}_i + c \times \text{shade}_i \times e_i,$$

where

r_i is the response for the pixel in band i of TM image
a, b, and c are the proportion of vegetation, soil, and shade in each pixel
vege_i, soil_i, and shade_i correspond to the spectral responses of each component
e_i is the error term for each band i

Landsat TM bands 3, 4, and 5 are used to form a linear equation system that can be solved by any developed algorithm (e.g., weighted least square). The resulting fraction images are resampled to a 60 m spatial resolution in order to minimize computer processing time and disk space, without losing information compatible with the 1:250,000 final product map scale.

Image segmentation is a technique to group the data into contiguous regions having similar spectral characteristics. Two thresholds are required to perform image segmentation: (a) *similarity*, that is the minimum value defined by the user to be considered as similar to form a region and (b) *area*, that is the minimum size given in number of pixels in order to be individualized. The unsupervised classification (ISOSEG) method is used to classify the segmented fraction images. It uses the statistical attributes (mean and covariance matrix) derived from the polygons of the image segmentation.

After the unsupervised classification, it is necessary to check the resulting maps. This task is performed by interpreters using interactive image editing tools. Color composites of Landsat bands 5, 4, and 3 are displayed in red–green–blue videos. Expert-identified omission and commission errors are manually corrected in order to improve the classification result. Then the individually classified images are mosaicked to generate the final maps per state and for the entire BLA. For the state mosaics, the spatial resolution is kept at 60 m and the scale for presentation is 1:500,000, while for the BLA the spatial resolution is degraded to 120 m and the scale for presentation is 1:2,500,000.

9.3.2 DETER Methodology

Starting in 2004, the DETER project was implemented to provide a near-real-time monitoring and detection of deforestation activities to support the Federal Government Action Plan for the Prevention and Control of Deforestation in the BLA. The procedure mimics the PRODES method but is meant to detect deforestation activities in near real time by exploiting the high temporal resolution of the MODIS sensor.

The first step in the method of the DETER project is to mask the intact forest based on the PRODES evaluation of the previous year. The map of intact forest is used as a reference for identifying new deforestation events in near real time throughout the current year. The monitoring activity with MODIS imagery begins in January, but becomes more active after March due to less cloud cover in the BLA. This does not significantly impact results as there is comparatively little deforestation occurring during the rainy season (November through March).

Daily MODIS images (surface reflectance—MOD09) used to identify deforestation spots are selected based on two criteria: (a) amount of cloud cover and (b) swath within sensor view zenith angle less than 35° (~1,400 km). The amount of cloud cover is evaluated based on quick-look images and, if deemed viable, a follow-on full spatial resolution assessment. The entire BLA is covered by 12 MODIS tiles from V09 to V11 and H10 to H13.

The images from the MOD09 product are delivered as HDF (hierarchical data format) files projected in a sinusoidal projection (WGS84 datum). All data are converted to a GeoTIFF format and reprojected to the geographic coordinate system for use in the SPRING software image-processing package.

From the set of seven reflective bands of the MOD09 product, bands 1 (red), 2 (NIR), and 6 (MIR) are used to generate the vegetation-, soil-, and shade-fraction images, respectively, using the linear spectral mixing model as previously described in the digital PRODES method. The soil-fraction images are then segmented, classified, mapped, and eventually edited by interpreters following the digital PRODES protocol.

The above procedure is carried out for every daily MODIS image acquired over the BLA. The results of the deforestation activities detected by DETER can be accumulated for different intervals such as weekly, biweekly, or monthly and are available in a digital format at the DETER website (http://www.obt.inpe.br/deter/index.html).

9.4 Results

9.4.1 Analog and Digital PRODES

Tardin et al. (1980) reported that deforestation in the BLA had reached a figure of 152,200 km^2 in 1978, which included the deforested land prior to 1960. Since that period, the average rate of deforestation has undergone significant changes. For example, from 1978 to 1988, the average deforestation rate was 21,130 km^2 $year^{-1}$ while it gradually decreased to 11,130 km^2 in 1991. After 1991, it began to increase again, reaching a rate of 27,423 km^2 in 2004. However, an abnormally high rate of 29,059 km^2 was also observed in 1995. From 2004 on, a significant decrease in deforestation rates was observed, with a minimum rate of 7,000 km^2 in 2010 (Tables 9.1 and 9.2). This period is coincident with the implementation of the DETER project as part of the Federal Government Action Plan for the Prevention and Control of Deforestation in BLA.

Since the implementation of the digital PRODES method in 2002, the deforestation results are immediately provided to government agencies to implement policies that enforce the reduction of illegal deforestation. The PRODES results are available to the public at the Web site, and the main data on deforestation over the last 8 years are shown in Table 9.2.

Figure 9.3 illustrates the annual deforestation rates from 1988 to 2010 for the BLA.

Figure 9.4 presents the thematic map of the PRODES classes, showing the spatial distribution of the deforested areas up to 2010; note the concentration of forest loss in the *arc of deforestation*.

The remote sensing images acquired since the early 1970s proved to be an important tool for monitoring the deforestation in the entire BLA and largely coincide with enactment of policies by the Brazilian government to promote the occupation of the region. Spatiotemporal data on deforestation rates have significantly contributed not only to government policies in reducing illegal deforestation activities, but also to the scientific community and the study of human impacts on biodiversity, greenhouse gases emission, and regional and global climate change.

TABLE 9.1

Deforestation Estimates (km^2) from the Analog PRODES Method from 1988 to 2001

States/Year	1988[a]	1989	1990	1991	1992	1993[b]	1994[b]	1995	1996	1997	1998	1999	2000	2001
Acre	620	540	550	380	400	482	482	1,208	433	358	536	441	547	419
Amazonas	1,510	1,180	520	980	799	370	370	2,114	1,023	589	670	720	612	634
Amapá	60	130	250	410	36	–	–	9	–	18	30	–	–	7
Maranhão	2,450	1,420	1,100	670	1,135	372	372	1,745	1,061	409	1,012	1,230	1,065	958
Mato Grosso	5,140	5,960	4,020	2,840	4,674	6,220	6,220	10,391	6,543	5,271	6,466	6,963	6,369	7,703
Pará	6,990	5,750	4,890	3,780	3,787	4,284	4,284	7,845	6,135	4,139	5,829	5,111	6,671	5,237
Rondônia	2,340	1,430	1,670	1,110	2,265	2,595	2,595	4,730	2,432	1,986	2,041	2,358	2,465	2,673
Roraima	290	630	150	420	281	240	240	220	214	184	223	220	253	345
Tocantins	1,650	730	580	440	409	333	333	797	320	273	576	216	244	189
Brazilian Amazon	21,050	17,770	13,730	11,030	13,786	14,896	14,896	29,059	18,161	13,227	17,383	17,259	18,226	18,165

[a] Average between 1978 and 1988.
[b] Average between 1993 and 1994.

TABLE 9.2
Deforestation Estimates (km²) from the Digital PRODES from 2002 to 2009

States/Year	2002	2003	2004	2005	2006	2007	2008	2009
Acre	883	1,078	728	592	398	184	254	211
Amazonas	885	1,558	1,232	775	788	610	604	406
Amapá	–	25	46	33	30	39	100	–
Maranhão	1,014	993	755	922	651	613	1,272	980
Mato Grosso	7,892	10,405	11,814	7,145	4,333	2,678	3,258	1,047
Pará	7,324	6,996	8,521	5,731	5,505	5,425	5,606	3,687
Rondônia	3,099	3,597	3,858	3,244	2,049	1,611	1,136	505
Roraima	84	439	311	133	231	309	574	116
Tocantins	212	156	158	271	124	63	107	56
Brazilian Amazon	21,394	25,247	27,423	18,846	14,109	11,532	12,911	7,008

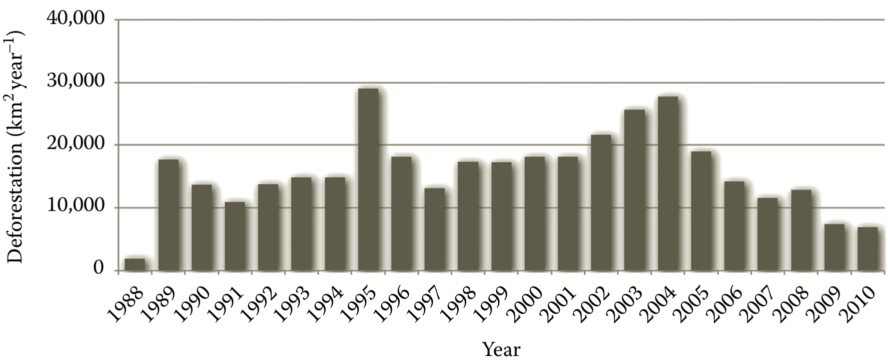

FIGURE 9.3
Variation of deforested areas during 1988–2010 time period for the Brazilian Amazonia region.

9.4.2 DETER Project

Figure 9.5 presents an example of the DETER monitoring results, showing the spatial distribution of the deforestation activities detected on a monthly basis for 2004.

The DETER system provides a near-real-time monitoring procedure to support the Federal Government Action Plan for the Prevention and Control of Deforestation in BLA since 2004, when a significant reduction in the deforestation rate started to be observed (Figure 9.3). DETER products are not used to estimate areas of deforestation but as an alarm to inform government agencies on potential illegal forest-clearing activities in the BLA. The availability of the high temporal resolution images from the MODIS sensor enables monthly reporting of forest loss alarms and has contributed to slowing illegal deforestation activities in the BLA.

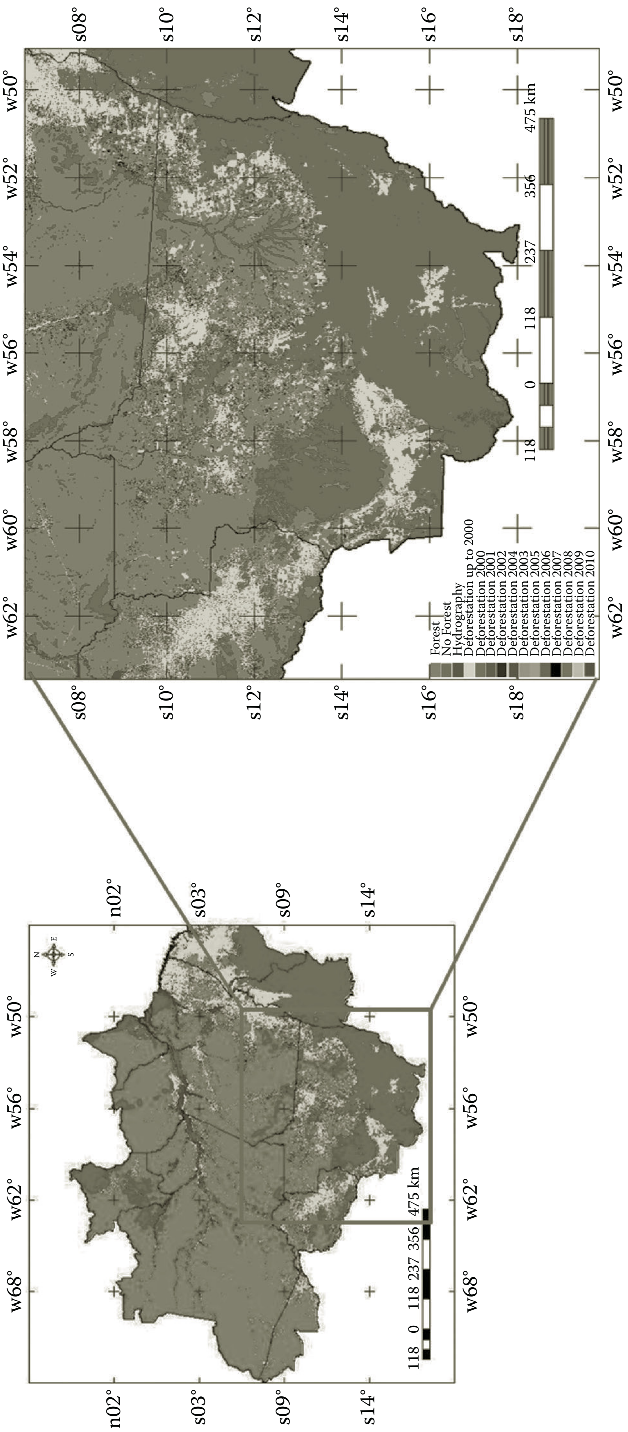

FIGURE 9.4
(See color insert.) Mosaic of digital PRODES mapping over the period 2000–2010.

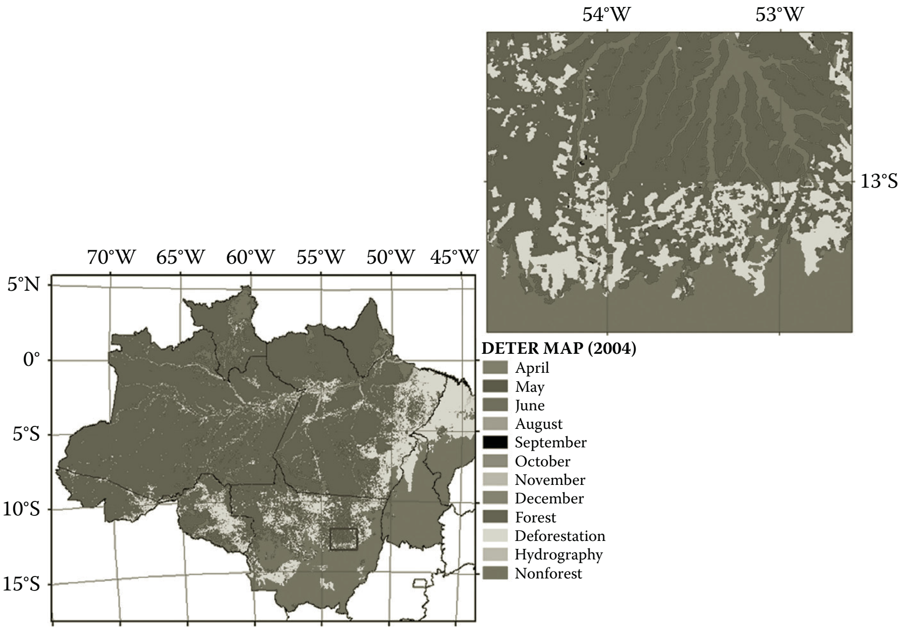

FIGURE 9.5
(See color insert.) Illustration of the example of DETER project results, showing the deforested areas detected during the year 2004.

9.5 Discussion and Conclusion

The initial monitoring of deforestation activities in BLA was performed by the analog PRODES product that was based on visual interpretation of hard copies of Landsat scenes at the scale of 1:250,000. This was an expensive and tedious procedure carried out by numerous interpreters on a yearly basis. However, it produced valuable information on deforestations rates until the 2001.

In 2002, the analog PRODES was replaced by the digital PRODES product that employs a semiautomatic method based on digital image-processing techniques and minor visual interpretation to correct for classification errors. The great advantage of digital PRODES is the provision of deforestation information in a compatible format for use in GIS for ecosystem and land use and cover change modeling. However, the annual frequency of deforestation estimates was insufficient to support other government needs, specifically that of reducing illegal deforestation activities.

As a consequence, the DETER project was implemented in 2004 to reinforce public policies that have helped to reduce the deforestation rates from 27,423 km^2 in 2004 to 7,000 km^2 in 2010. It is important to mention that the DETER does not replace but complements the digital PRODES monitoring procedure. The DETER detects deforestation activities in its initial stage without providing an area estimate, while the digital PRODES evaluates the total annual deforested area (INPE 2008).

The long-term history of the images acquired by the sensors on board the Landsat satellites proved to be an essential tool for monitoring the annual deforestation of the BLA. The Landsat record covers the majority of the period since the Brazilian government initially incentivized settlement of the BLA. The high temporal resolution of the MODIS sensor on board the Terra and Aqua platforms was also highly relevant to support government policies in stopping illegal deforestation. The result has been a consequent reduction of deforestation rates aided by the combined information from both the DETER and PRODES projects.

About the Contributors

Yosio Edemir Shimabukuro is a senior researcher at the Brazilian Institute of Space Research (INPE), São Paulo, Brazil. His fields of interest are use of satellite remote sensing data for studying vegetation cover and use of GIS techniques and models for environmental change detection over different biomes in Brazil.

João Roberto dos Santos is a senior researcher at the Brazilian Institute of Space Research (INPE), São Paulo, Brazil, and his fields of interest are optical and synthetic aperture radar (SAR) data for inventory and monitoring of forest typologies.

Antonio Roberto Formaggio is a researcher and postgraduation teacher/advisor in remote sensing for environment and agriculture at the Brazilian Institute of Space Research (INPE), São Paulo, Brazil. His research interests include impacts of agriculture in the Brazilian savannas and Amazonia biomes and environmental modeling and radiative transfer models for the retrieval of vegetation biophysical variables.

Valdete Duarte is a researcher in change detection and monitoring of forest by multisensor remote sensing satellite data. He contributed to establish the methodologies of PRODES (monitoring of Amazon forest) and DETER (real-time detection of deforestation) projects and is currently the principal investigator of the Panamazonia-II project to monitor the tropical forests in South America.

Bernardo Friedrich Theodor Rudorff is a researcher at the Remote Sensing Division of the Brazilian Institute of Space Research (INPE), São Paulo, Brazil, working with the assessment of agricultural production using remote sensing techniques and agrometeorological models. He is currently coordinating the soy moratorium project (monitoring of soy plantation in recent deforested land in the Amazon biome) and the Canasat project (monitoring of sugarcane for ethanol production).

References

Achard, F. et al., Determination of deforestation rates of the world's humid tropical forests. *Science*, 297, 999–1002, 2002.

Cochrane, M.A. et al., Positive feedbacks on the fire dynamic of closed canopy tropical forests. *Science*, 284, 1832–1835, 1999.

Fearnside, P.M., Deforestation in Brazilian Amazonia: The effect of population and land tenure. *Ambio*, 22(8), 537–545, 1993.

Houghton, R.A. et al., The spatial distribution of forest biomass in the Brazilian Amazon: A comparison of estimates. *Global Change Biology*, 7, 731–746, 2001.

IBAMA (Instituto Brasileiro do Meio Ambiente), Ecossistemas brasileiros: Amazônia. Disponível online: http://www.ibama.gov.br/ecossistemas/amazonia.htm. Consulta em 30 de novembro de 2009.

IBGE (Fundação Instituto Brasileiro de Geografia e Estatística), Brasil, Ministério da Agricultura, Instituto Brasileiro de Desenvolvimento Florestal, Secretária de Planejamento e Coordenação da Presidência da Republica, Mapa de Vegetação do Brasil, escala 1:5000000. Brasília, 1988.

INPE (Instituto Nacional de Pesquisas Espaciais), *Monitoramento da cobertura florestal da Amazônia por satélites: Sistemas PRODES, DETER, DEGRAD E QUEIMADAS 2007–2008*. São José dos Campos, SP, Brazil: Instituto Nacional de Pesquisas Espaciais, 47 p., 2008.

Mahar, D., *Government Policies and Deforestation in Brazil's Amazon Region*. Washington, DC: World Bank, 1988.

Moran, E.F., *Developing the Amazon*. Bloomington, IN: Indiana University Press, 1981.

Moran, E.F., Deforestation and land use in the Brazilian Amazon. *Human Ecology*, 21(1), 1–21, 1993.

Moran, E.F. et al., Integrating Amazonian vegetation, land-use, and satellite data. *Bioscience*, 44(5), 329–338, 1994.

Nepstad, D.C. et al., Land-use in Amazonia and the Cerrado of Brazil. *Ciência e Cultura Journal of the Brazilian Association for the Advancement of Science*, 49(1/2), 73–86, 1997.

Oliveira-Filho, A.T. and Ratter, J.A., Vegetation physiognomies and woody flora of the cerrado biome. In: P.S. Oliveira and R.J. Marquis (Eds.). *The Cerrados of Brazil*. New York: Columbia University Press, 91–120, 2002.

Salati, E., The climatology and hydrology of Amazonia. In: G.T. Prance and T.E. Lovejoy (Eds.). *Amazonia*. New York: Pergamon, 18–48, 1985.

Shimabukuro, Y.E. and Smith, J.A., The least-squared mixing models to generate fraction images derived from remote sensing multispectral data. *IEEE Transactions on Geoscience and Remote Sensing*, 29, 16–20, 1991.

Shimabukuro, Y.E. et al., Using shade fraction image segmentation to evaluate deforestation in Landsat Thematic Mapper images of the Amazon region. *International Journal of Remote Sensing*, 19(3), 535–541, 1998.

Shimabukuro, Y.E. et al., Near real time detection of deforestation in the Brazilian Amazon using MODIS imagery. *Ambiente e Água*, 1, 37–47, 2006.

Skole, D. and Tucker, C., Tropical deforestation and habitat fragmentation in the Amazon: Satellite data from 1978 to 1988. *Science*, 260, 1905–1910, 1993.

Skole, D.L. et al., Physical and human dimensions of deforestation in Amazonia. *Bioscience*, 44(5), 14–32, 1994.

Tardin, A.T. et al., Subprojeto Desmatamento. Convênio IBDF/CNPq/INPE, Rel. Técnico INPE-1649-RPE/103, 1980.

10

Monitoring of Forest Degradation: A Review of Methods in the Amazon Basin

Carlos Souza, Jr.
Amazon Institute of People and the Environment

CONTENTS

10.1 Introduction 171
10.2 Field Characterization of Forest Degradation 173
10.2.1 Definition 173
10.2.2 Types of Degraded Forests 174
10.2.3 Attributes of Degraded Forests Detectable Using Remote Sensing 175
10.2.4 Ecological Impacts 177
10.3 Remote Sensing of Forest Degradation 178
10.3.1 Remote Sensing Approaches to Mapping Selective Logging ... 179
10.3.1.1 Visual Interpretation 179
10.3.1.2 Combining Remote Sensing and GIS 182
10.3.1.3 SMA 183
10.3.2 Classification of Forest Degradation 185
10.4 Forest Monitoring for REDD+ 188
10.5 Conclusions 190
Acknowledgments 191
About the Contributor 191
References 191

10.1 Introduction

Forest degradation is an anthropogenic process that can lead to significant carbon loss from forests to the atmosphere. Measuring and mapping of forest degradation have become important tasks for advancing carbon payment negotiations through the reducing emissions from deforestation and degradation (REDD+) process (Herold et al. 2011). The forests of the Brazilian Amazon are significantly impacted by forest degradation due to three main processes: selective logging, forest fires, and forest fragmentation.

These degradation dynamics operate synergistically and recurrently, resulting in the loss of original carbon stocks of intact forests. In extreme cases, forest degradation can lead to a complete conversion of forests to other land cover types (i.e., pasture or agriculture lands). However, it is more common for forests to remain nominally as forests, but with a reduced carbon stock and altered biodiversity and forest structure.

The annual area of selectively logged forest in the Brazilian Amazon is as large as that cleared by deforestation (Nepstad et al. 1999; Asner et al. 2005). Due to the significance of this disturbance dynamic to forest structure in the Amazon basin, several remote sensing techniques have been tested and developed to detect, measure, and map the areal extent of forest degradation (Souza and Barreto 2000; Asner et al. 2002; Souza et al. 2005a; Matricardi et al. 2007). Selective logging has also been studied in the Brazilian Amazon in terms of its ecological impacts, including changes in carbon stocks, biodiversity loss, soil compaction, forest microclimate, and biogeochemical cycles (Verissimo et al. 1992, 1995; Johns et al. 1996; Pereira et al. 2002).

Forest fires (Cochrane et al. 1999; Alencar et al. 2004) and forest fragmentation (Laurance et al. 2000, 2002) have also received great scientific attention, including studies of the synergism between these two processes (Cochrane 2001; Cochrane and Laurance 2002). The synergism between selective logging and forest fires is also well understood (Holdsworth and Uhl 1997; Nepstad et al. 1999). Remote sensing techniques to map forest fragments (FFs) have been developed since the early 1990s (Skole and Tucker 1993). However, mapping burned area extent is more challenging as ground fires result only in degradation of forest understory. Moreover, fire is often related to forests that have been previously logged, further complicating their quantification and unique contribution to emissions.

A host of ecological and remote sensing studies of forest degradation have been conducted in the Brazilian Amazon, making the region a suitable area for a review and evaluation of optical remote-sensing techniques for REDD+ projects. Presenting a review of these remote-sensing techniques is the first objective of this chapter. By definition, REDD+ includes both forest conversion as well as forest degradation, and the Brazilian Amazon is the only tropical forest where both deforestation and forest degradation have been studied in great detail. The second objective of this chapter is to demonstrate how remote sensing techniques can be integrated with forest biomass field measurements to construct reliable baselines of carbon emissions associated with forest degradation. In order to achieve these objectives, the chapter is divided into three sections. The first section presents a summary of forest degradation processes and their impacts on forest carbon stocks and includes an evaluation of those attributes of forest degradation that can be quantified using remotely sensed data. In the second section, the optical remote sensing techniques available for detecting and mapping forest degradation are presented in detail, including a discussion of their strengths and limitations when applied to mapping changes in forest carbon stocks. The last session presents a framework for integrating deforestation and forest degradation monitoring activities in developing baselines for REDD+.

10.2 Field Characterization of Forest Degradation

10.2.1 Definition

Forest degradation is a temporary or permanent change in density, composition, or structure of natural forest attributes caused by anthropogenic factors. Forest degradation differs from forest changes caused by natural phenomena, such as natural tree falls, windthrows, and lightning strikes, as these changes in forest attributes are not human induced (Lambin 1999). Several ecological field studies conducted in the Brazilian Amazon have shown that selective logging, forest fires, and forest fragmentation are the main processes responsible for forest degradation (Verissimo et al. 1992; Barros and Uhl 1995; Holdsworth and Uhl 1997; Cochrane et al. 1999; Cochrane and Laurance 2002). Forest degradation processes operate at different intensities and time scales, creating a continuum from intact forests to degraded forests to complete stand replacement and conversion (Figure 10.1). Defining the types of forest attributes affected by degradation processes is important, as is assessing the capabilities of remote sensing in measuring changes to these attributes.

In the Brazilian Amazon, logging creates small clearings, known as log landings or logging decks, varying in size from 40 to 190 m^2. Log landings are connected by primary logging roads that can be 6–15 m wide and account for additional clearings of 60–567 m^2 per hectare. These roads give access to harvesting areas through secondary roads and/or skid trails. Tree fall gaps are commonly found in forest areas where commercial tree species are harvested, given that vine cutting is not a widespread practice in this region. High tree diameters (i.e., diameter at breast height [DBH] > 45 cm) are usually taken in the first harvesting cycle, but recurrent logging cycles can occur as smaller trees are successively harvested (i.e., 15 < DBH < 45 cm) (Figure 10.1). The harvesting intensity varies from 1 to 9 trees per hectare (Verissimo et al. 1992, 1995; Barros and Uhl 1995; Johns et al. 1996; Pereira et al. 2002).

It is well established that logging leads to favorable conditions for burning forests. Logging creates canopy gaps that allow penetration of more incoming solar radiation into the understory environment. As result, understory humidity is reduced, drying out remaining logging debris or slash. Agriculture fires can unintentionally escape to adjacent logged forests (Holdsworth and Uhl 1997). Similar to logging, forest fires can also reoccur in the same forest, creating a positive feedback in increasing forest degradation (Cochrane et al. 1999; Cochrane and Schulze 1999) (Figure 10.1).

Several logging cycles and fire events can drastically deplete forest carbon stocks to carbon density levels similar to those of a deforested area. However,

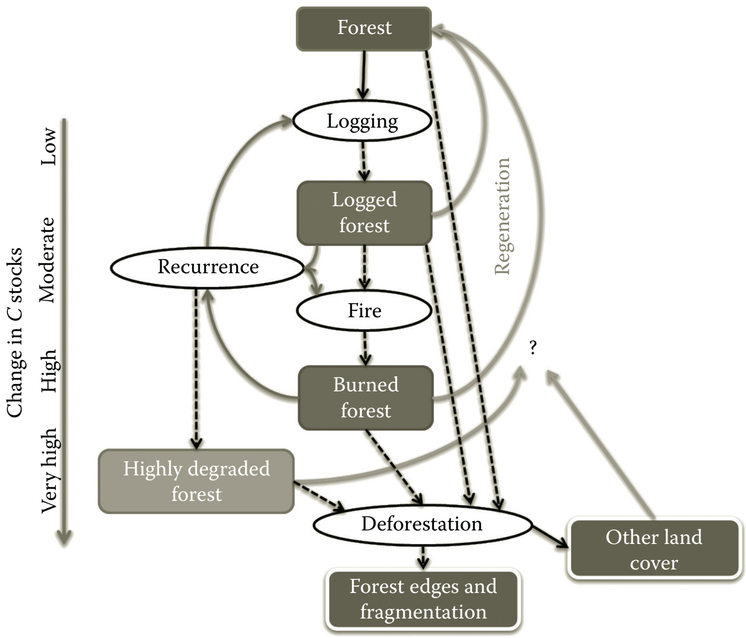

FIGURE 10.1
(See color insert.) Forest degradation processes and interactions commonly found in the Brazilian Amazon. Pristine forests can be subject to selective logging, creating favorable conditions for burning when fires from adjacent agriculture fields unintentionally escape. Logging and fires can be recurrent, creating highly degraded forests. Eventually, degraded forests can be converted by deforestation, increasing forest edges and landscape fragmentation. If degraded forests are not cleared, vegetation regeneration processes can prevail given the high resiliency of forests.

before this occurs, it is more common for degraded forests to be cleared. The fate of degraded forests in the Brazilian Amazon varies across the region. In areas close to deforestation frontiers, degraded forests are more likely to be cleared within 5–10 years, a process that increases forest edges and landscape fragmentation (Asner et al. 2005) (Figure 10.1). The degraded forests that are not converted by deforestation may regenerate, returning to their original carbon stocks after several decades. However, the original species composition may not be restored due to local extinctions (Figure 10.1).

10.2.2 Types of Degraded Forests

As discussed above, forest degradation creates a continuum from intact forest to clearings. But, for mapping purposes a typology of classes is required. Here, degraded forests are classified in terms of the processes and intensities associated with degradation (Souza et al. 2009). The first type of degraded forests in the Brazilian Amazon is logged forests. Three types of selectively logged forests have been identified in this region: nonmechanized logging (NML), managed logging (ML), and conventional logging (CL). Agricultural fires are more likely to burn forests that experienced CL. CL forests have favorable conditions for burning due to a greater amount of slash and collateral canopy damage. Fires in logged forests lead to a new class of forest degradation named burned forest (BF). Finally, forest patches of different sizes can be isolated due to landscape fragmentation. The resulting FF class has often been subject to logging and/or fire. Thus, a suitable classification scheme to characterize forest degradation in the Brazilian Amazon based on field ecological studies, associated with different processes and their interactions (Figure 10.1), and covering a spectrum of intensity, can be proposed as follows:

- Undisturbed forest (UF): Old-growth intact forest dominated by shade-tolerant tree species and original carbon stocks.
- NML: Logged forest without the use of heavy vehicles such as skidders and trucks, also known as traditional logging. Logging infrastructure (log landings, roads, and skid trails) are not built.
- ML: Planned selective logging where a tree inventory is conducted, followed by road and log landing planning to reduce harvesting impacts.
- CL: Conventional unplanned selective logging using skidders and trucks. Log landings, roads, and skid trails are built causing extensive canopy damage. Low-intensity understory burning may occur, but forest canopy is not burned.
- BF: Either NML or logged forests (ML and CL) where forest canopy has been intensively burned.
- FF: Isolated forest patches created by deforestation with abrupt changes on edges to pasture and agriculture lands, or with partial transitional edges to secondary forests. Fragments in the study area are usually subject to recurrent NML and fires.

10.2.3 Attributes of Degraded Forests Detectable Using Remote Sensing

At the field scale, logged forests are composed of three main environments: (1) forest islands that were not disturbed due to poor access imposed by difficult topography and rivers, or a lack of commercial timber species; (2) areas where the forest has been cleared to create roads for machine movements (skidders and trucks) and log landings to store the harvested timber; and (3) canopy-damaged forests (i.e., harvested areas and areas damaged by tree falls and machine movements) (Souza and Roberts 2005) (Figure 10.2). All of these environments can be found in the ML and CL classes, but the difference is that in ML, reduced impact logging practices are conducted to reduce direct and collateral damages (Johns et al. 1996; Pereira et al. 2002).

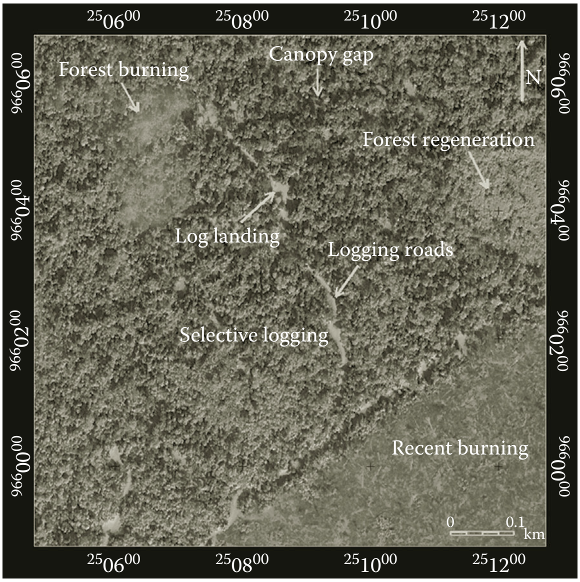

FIGURE 10.2
(See color insert.) Very high spatial resolution false-color infrared IKONOS image showing the different environments commonly found in logged and burned (LB) forests in the eastern Brazilian Amazon. At 1 m spatial resolution, log landings, logging roads, tree fall canopy gaps, and forest edges can be identified as well as "islands" of UFs and signs of regeneration. Signs of forest erosion along the edges between the LB forest and the recently slashed-and-burned forest can also be observed. (From Souza, C.M. and Roberts, D., *Int. J. Remote Sens.*, 26, 425, 2005.)

For these two classes, logging harvesting intensity varies from 30 to 40 m^3 of logs per hectare (Verissimo et al. 1992; Johns et al. 1996). The NML class does not feature the various logging environments described above as no heavy machinery is used to harvest trees and a low harvest intensity is practiced (i.e., 5–10 m^3 of logs per hectare). When fires penetrate logged forests, undetected damage under the canopy is expected. Prolonged and more intense fires can damage the tree canopy, exposing tree branches and trunks and making remote sensing detectability possible (Souza and Roberts 2005).

Tree inventories and forest impact measurements have been conducted to characterize forest degradation caused by selective logging (Verissimo et al. 1992; Johns et al. 1996; Pereira et al. 2002). Gerwing's (2002) was the first study in the Brazilian Amazon that proposed an all-encompassing approach to characterize the biophysical properties of a range of degraded forests. Slightly different forest degradation classes were proposed for this study. For example, repeated logging and burning were placed in separate classes. Our research group has adjusted Gerwing's method to characterize classes of forest degradation that can be easily integrated with remotely sensed measurements (Souza et al. 2005a, 2009).

The forest survey proposed by Gerwing (2002) consisted of measuring all trees with DBH >10 cm along transects of 10 m × 500 m (i.e., 0.5 ha).

Moreover, subparcels (10 m × 10 m; 0.1 ha) were established at every 50 m along transects, and all trees <10 cm DBH were surveyed. Logging and/or burning impacts were measured in the subparcels, including ground cover, and canopy gaps were estimated using a hemispherical lens and densitometer. Aboveground live and dead biomass pools were estimated for trees >10 cm DBH for each transect using tree inventory data and available allometric equations. Ancillary information about land use and disturbance history (i.e., time since last disturbance, number of times the area was disturbed) was collected during the field surveys. The forest transects were randomly defined in the field, and more than three must be conducted per class of degraded forest.

10.2.4 Ecological Impacts

Field ecological studies have provided the foundation for understanding the structural and compositional changes caused by forest degradation processes on pristine UFs. For remote sensing detection of forest degradation impacts, the following attributes are relevant: (1) ground cover comprised of intact vegetation, wood debris, and disturbed soils; (2) canopy cover; and (3) aboveground live biomass (AGLB). Our research group has conducted more than 100 transects in the Brazilian Amazon using an adaptation of Gerwing's methodology to link field measurements with remotely sensed data (Souza et al. 2005b, 2009). We have observed that for a single degradation event, intact vegetation and canopy cover decrease with an increase in forest degradation intensity by 20% and 60%, respectively. Conversely, soil disturbance and wood debris increase by 10% and 40%, respectively. However, when repeated degradation events are considered, these impacts tend to be more drastic. For example, repeated logging in the eastern Amazon region can disturb up to 70% of the original vegetation and deplete up to 40% of the original canopy cover (Gerwing 2002).

The forest structure changes caused by the forest degradation processes described above affect species composition and carbon stocks of UFs. The mean AGLB of UF obtained for our transect measurements was 377 Mg per hectare, with minimum biomass for the Ji-Paraná site (273 Mg per hectare) and maximum for Santarém (497 Mg per hectare). This result is compatible with field AGLB estimates using very large forest plots (Keller et al. 2001) and within the range of average values reported for the Brazilian Amazon region (Malhi et al. 2006; Saatchi et al. 2007). Using the mean AGLB obtained with our transects and assuming that carbon makes up 50% of the forest biomass, we can then demonstrate how carbon stocks vary with degradation intensity (Figure 10.3). A trend of reduced carbon stocks in pristine UF undergoing forest degradation processes has been observed. The more significant change is when UF is fragmented or burned, leading to respective 28% and 30% reductions in carbon stocks relative to original UF stocks. NML, ML, and CL degradation classes each experienced a <10% carbon loss. The carbon

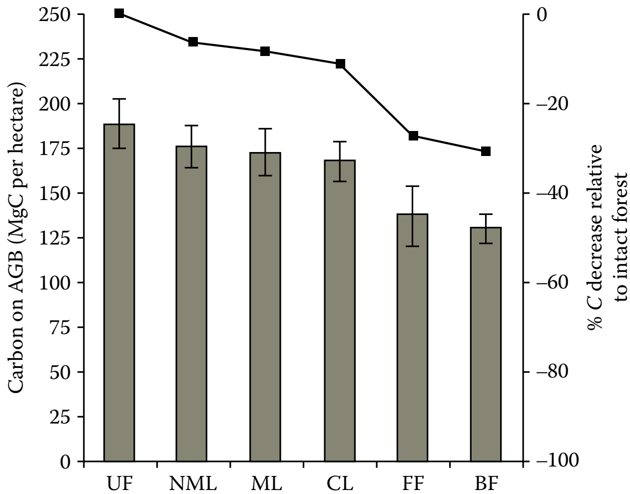

FIGURE 10.3
Change in aboveground live biomass as a function of degradation intensity. Bars represent standard error of the mean value and lines represent the percent change of *C* mean relative to intact forest. (From Souza, C. et al., Integrating forest transects and remote sensing data to quantify carbon loss due to forest degradation in the Brazilian Amazon. In *Case Studies on Measuring and Assessing Forest Degradation*. Forest Resources Assessment Working Paper 161, FAO, Rome, 20 p., 2009.)

stock changes presented in Figure 10.3 are for one event of forest degradation only. When considering recurrent forest degradation events, carbon stocks can be reduced by up to 50% (Gerwing 2002).

10.3 Remote Sensing of Forest Degradation

Detecting and mapping forest degradation with optical remotely sensed data is more complicated than mapping forest clearings by deforestation because degraded forest "pixels" are complex environments with mixtures of different land cover materials (i.e., vegetation, dead trees, bark, tree branches, soil, shade; Figure 10.1 [Souza and Roberts 2005]). Furthermore, signs of forest degradation disappear within 1–2 years due to rapid canopy closure and understory revegetation, making spectral characteristics of degraded forests similar to that of UFs (Stone and Lefebvre 1998; Asner et al. 2004a,b; Souza et al. 2005a, 2009).

The first attempts to map degraded forests in the Brazilian Amazon focused on detecting the processes responsible for degradation. Mapping selective logging received considerable attention, given its large extent and negative ecological impacts. The annual logged area in this region has been considered as large as the annually deforested area, with first estimates coming from socioeconomic field surveys (Nepstad et al. 1999) and the following ones based on satellite imagery (Asner et al. 2005; Matricardi et al. 2007). Techniques to map forest fire scars have also been developed, and forest fragmentation can be mapped with traditional techniques used to map deforestation. More recently, an all-encompassing approach for mapping forest canopy damage caused by these degradation processes has been proposed. Techniques for doing so are discussed in the following sections.

10.3.1 Remote Sensing Approaches to Mapping Selective Logging

Several remote sensing techniques were tested and applied to local and regional scale studies in the Amazon region to map selectively logged forests (Table 10.1). These techniques can be grouped in terms of mapping goals and methods utilized. In terms of mapping goals, some techniques were developed to map the total forest area affected by logging, which includes forest canopy damage and forest clearings created by log landings and roads, and to map intact forest islands surrounded by logging infrastructure and canopy-damaged areas. The second mapping goal focused on the mapping of areas with forest canopy damage only (i.e., intact forest islands were not included). In terms of methods for mapping logging, visual interpretation, semiautomated, and automated techniques have been tested (Table 10.1), and most of them can be applied to different spatial and spectral resolution sensors.

At high spatial resolutions (i.e., <5 m pixel size), images acquired by either space-borne or aerial platforms are viable for small-area analyses. Most of the features found in logging environments (i.e., roads, log landings, tree fall gaps, and UF islands) can be easily identified at this scale (Figure 10.1). Fusion techniques of panchromatic and multispectral images are commonly applied to enhance the imagery (Read et al. 2003; Souza and Roberts 2005), and visual interpretation is the most common mapping technique used. However, given the cost for image acquisition and interpretation, their use in mapping and monitoring logging is limited. For these reasons, the methods presented in the following sections focus only on medium spatial resolution imagery (i.e., 10–60 m pixel size). These data are freely available and are regularly acquired, unlike higher spatial resolution commercial data sets.

10.3.1.1 Visual Interpretation

Watrin and Rocha (1992) pioneered the use of satellite images to map selective logging in the Amazon region. Their work focused on Paragominas municipality, which was the most important logging center of the Brazilian Amazon from 1985 to 1995 (Verissimo et al. 1992). This study used printouts

TABLE 10.1

Remote Sensing Methods Most Often Used to Detect Forest Degradation Caused by Selective Logging in the Amazon Region

Mapping Approach	Studies	Sensor	Spatial Extent	Objective	Advantages	Disadvantages
Visual interpretation	Watrin and Rocha (1992)	Landsat TM	Local	Map total logging area	Does not require sophisticated image-processing techniques	Labor intensive for large areas and may be user biased to define the boundaries of logged forest
	Stone and Lefebvre (1998)	Landsat TM	Local			
	Matricardi et al. (2001)	Landsat TM	Brazilian Amazon			
	Santos et al. (2002)	Landsat TM	Brazilian Amazon			
Combining remote sensing and GIS (detection of logging landings + buffer)	Souza and Barreto (2000) Matricardi et al. (2001) Monteiro et al. (2003) Silva et al. (2003) Graça et al. (2005)	Landsat TM and ETM+	Local	Map total logging area (canopy damage, clearings, and undamaged forest)	Relatively simple to implement and satisfactory for estimating the total potential logging area	Logging buffers vary across the landscape and do not reproduce the actual shape of the logged area
Textural analysis	Matricardi et al. (2007)	Landsat TM	Brazilian Amazon	Map logging infrastructure	Implementation is straightforward and fully automated	Less sensitive to detect canopy damage created by tree falling
Decision tree	Souza et al. (2003)	SPOT 4	Local	Map forest canopy damage associated with logging and burning	Simple and intuitive classification rules	Has not been tested in very large areas, and classification rules may vary across the landscape

Change detection	Souza Jr. and Roberts (2002)	Landsat TM and ETM+	Local	Map forest canopy damage associated with logging and burning	Enhances forest canopy-damaged areas	Requires two pairs of images and does not separate natural and anthropogenic forest changes
Image segmentation	Graça et al. (2005)	Landsat TM	Local	Map total logging area (canopy damage, clearings, and undamaged forest)	Relatively simple to implement and satisfactorily estimate the total logging area. Free software available	Has not been tested in very large areas and segmentation rules may vary across the landscape
CLAS	Asner et al. (2005, 2006)	Landsat TM and ETM+	Five states in the Brazilian Amazon	Map total logging area (canopy damage, clearings, and undamaged forest)	Highly automated and standardized to very large areas	Requires high computation power and pairs of images for forest change detection
NDFI+CCA	Souza et al. (2005)	Landsat TM and ETM+	Local	Map forest canopy damage associated with logging and burning	Enhances forest canopy-damaged areas	Has not been tested in very large areas and does not separate logging from burning damages

of Landsat TM5 bands 4 and 5 acquired in 1988 to first visually identify and trace on overlay paper the boundaries of selectively logged areas. Next, the resulting polygons were hand digitized using a geographic information system (GIS) at 1:100,000 scale. The authors used the boundaries of forest scars created by roads, log landings, and canopy-damaged areas as the criteria for defining logged areas. Stone and Lefebvre (1998) also used visual interpretation of Landsat TM5 data to map logged forests in Paragominas for 1986, 1988, 1991, and 1995. In 2001, a large-scale study was conducted to map selective logging of the Brazilian Amazon using visual interpretation of Landsat TM5 digital imagery. In this study, Santos et al. (2001) mapped logged forests at a 1:250,000 scale and estimated an average of 1,580 km^2 per year for the period 1988–1998.

There are drawbacks to the use of visual interpretation for mapping selective logging. First, defining the boundary of logged and UFs is not always straightforward, even when using more detailed imagery such as IKONOS (Read et al. 2003; Souza and Roberts 2005). Second, there is some level of subjectivity in defining forest degradation created by logging and forest fires; none of the studies that used visual interpretation methods define rigorous criteria for separating these two causes of forest degradation. Third, visual interpretation is labor intensive and may be cost prohibitive for operational forest monitoring projects (Table 10.1).

10.3.1.2 Combining Remote Sensing and GIS

The need for a faster, cheaper, and replicable method to detect and map selective logging has driven the development of automated techniques. The first attempt combined automated detection of log landings from soil fraction derived from a spectral mixture analysis (SMA; covered in detail later) applied to Landsat images followed by the application of buffer regions (Souza and Barreto 2000). This technique requires field measurements to estimate harvesting radius from log landings in order to define the buffer radius. For tropical dense forest of the eastern Amazon and open forests of the central–southern region, buffer sizes were 180 m (Souza and Barreto 2000) and 350 m (Monteiro et al. 2003), respectively; both are considered local studies. Matricardi et al. (2001) used this buffer approach (with fixed radius of 180 m) to estimate selective logging impact over the Brazilian Amazon, differing with the use of texture measures applied to Landstat TM5 bands 3–5 to detect log landings. This large-scale study estimated an annual average area affected by logging of 4,690 km^2 per year for the period 1992–1999. This result is almost three times the one obtained by visual interpretation (Santos et al. 2001), though the product is at a more detailed scale (1:50,000) (Table 10.1).

The buffer technique for estimating logging areas also has limitations. Logging buffers are not fixed, and neither circular (Souza and Barreto 2000) nor squared buffers (Monteiro et al. 2003) adequately capture logged areas. The area affected by logging in most cases did not follow the contours of the buffer regions, resulting in commission and omission classification errors. To overcome this problem, a technique that uses region growth algorithms from log landings was proposed (Graça et al. 2005) to map canopy-damaged areas (Table 10.1).

10.3.1.3 SMA

Studies in the Brazilian Amazon have shown that Landsat reflectance data have limited the capacity for detecting logged forests, with bands 3 and 5 providing the best spectral contrast between logged and intact forests (Stone and Lefebvre 1998; Asner et al. 2002; Souza et al. 2005a). Vegetation indices and texture filters also showed some potential for detection of canopy damage created by logging (Asner et al. 2002; Souza et al. 2005a), but are more useful for enhancing logging infrastructure using Landsat band 5 (i.e., roads and log landings; Matricardi et al. 2007) (Table 10.1).

Alternatively, SMA has been proposed to overcome the challenge of using whole-pixel information to detect and classify logged forests. Landsat pixels typically contain a mixture of land cover components (Adams et al. 1995). In logged forests (and also in BF and forest edges), mixed pixels predominate and are expected to have a combination of green vegetation (GV), soil, nonphotosynthetic vegetation (NPV), and shade-covered materials. Therefore, fractional images derived from SMA analyses have the potential to enhance the detectability of logging infrastructure and canopy damage within degraded forests. For example, soil fractions enhance log landings and logging roads (Souza and Barreto 2000), while NPV fractions enhance forest-damaged areas (Cochrane and Souza 1998; Souza et al. 2003), and GV highlights forest canopy gaps (Asner et al. 2004a).

In SMA, the Landsat TM/ETM+ reflectance data of each pixel can be broken down into GV, NPV, soil, and shade fractions, which are the expected materials found in pixels within areas of forest degradation. The SMA model assumes that the image spectra are formed by a linear combination of n pure spectra, referred to as endmembers (Adams et al. 1995), such that:

$$R_b = \sum_{i=1}^{n} F_i R_{i,b} + \varepsilon_b \tag{10.1}$$

for

$$\sum_{i=1}^{n} F_i = 1 \tag{10.2}$$

where

R_b is the reflectance in band b

$R_{i,b}$ is the reflectance for endmember i, in band b

F_i the fraction of endmember i

ε_b is the residual error for each band

The SMA model error is estimated for each image pixel by computing the root mean square (RMS) error, given by:

$$\mathrm{RMS} = \left[n^{-1} \sum_{b=1}^{n} \varepsilon_b \right]^{1/2} \tag{10.3}$$

The identification of the nature and number of pure spectra (i.e., endmembers) in the image scene is an important step in obtaining correct SMA models. Two approaches have been proposed to define endmembers. First, reflectance spectra can be acquired at the field level with a handheld spectrometer (Roberts et al. 2002). The pure spectra measured on the ground are named reference endmembers and need to be well calibrated to the image data. The second approach uses image endmembers obtained directly from the images (Small 2004). This approach does not require spatial and radiometric calibration between endmembers and image data since their acquisition is from the same sensor and scale. SMA automation is also required to make this technique useful for monitoring large areas. A Monte Carlo unmixing technique using reference endmember bundles was proposed for that purpose (Bateson et al. 2000) and applied to map selective logging with Landsat images over the Brazilian Amazon (Asner et al. 2004a, 2005). An alternative approach using generic image endmembers (Small 2004) was implemented for the same application (Souza et al. 2005b), avoiding the need for collecting reference field spectra.

A novel spectral index applicable combines SMA fractions to derive the normalized difference fraction index (NDFI) (Souza et al. 2005b). The NDFI was developed to more accurately map selective logging. The NDFI is computed as:

$$\mathrm{NDFI} = \frac{\mathrm{GV}_{\mathrm{Shade}} - (\mathrm{NPV} + \mathrm{Soil})}{\mathrm{GV}_{\mathrm{Shade}} + \mathrm{NPV} + \mathrm{Soil}} \tag{10.4}$$

where $\mathrm{GV}_{\mathrm{shade}}$ is the shade-normalized GV fraction given by

$$\mathrm{GV}_{\mathrm{Shade}} = \frac{\mathrm{GV}}{100 - \mathrm{Shade}} \tag{10.5}$$

NDFI values range from –1 to +1. For intact forests, NDFI values are expected to be high (i.e., about 1) due to the combination of high $\mathrm{GV}_{\mathrm{shade}}$ (i.e., high GV and canopy shade) and low NPV and soil values. As forest becomes degraded, the NPV and soil fractions are expected to increase, lowering NDFI values relative to intact forest. Cleared forests are expected to exhibit low GV and shade, and high NPV and soil, making it possible to distinguish them from degraded forests as well (Figure 10.4).

Fraction images obtained with the subpixel estimation of forest endmembers through SMA enhanced the detection of forest degradation caused by

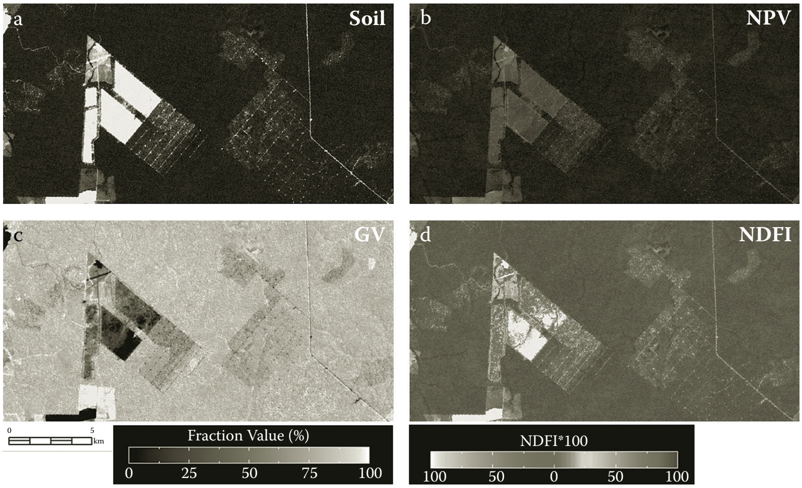

FIGURE 10.4
(See color insert.) Subset of a Landsat TM image showing fractions obtained from SMA and NDFI. (a) High soil fraction shows logging infrastructure (log landings and roads); (b) NPV shows higher fraction values for canopy-damaged areas along infrastructure relative to the surrounding intact forest; (c) canopy damage is also identified with lower GV fraction values (dark colors); and (d) all the fraction information are combined to enhance the detection of logged forest.

logging. As a result, spatial and contextual classifiers were developed and applied to fraction images improving detection and mapping of selectively logged forests. The techniques varied from simple GV change detection (Souza et al. 2002) and contextual–spectral classifiers (Souza et al. 2005b) to more sophisticated and computer-intensive spectral and spatial pattern recognition techniques (Asner et al. 2005) (Table 10.1). As a result, selective logging, initially considered cryptic to Landsat-like images (Nepstad et al. 1999), became visible and measurable over large forest areas of the Brazilian Amazon. Subsequent analyses proved that this type of degradation was affecting areas as large as those cleared by deforestation, as indicated by field survey estimates (Nepstad et al. 1999).

10.3.2 Classification of Forest Degradation

The remote sensing techniques described in Section 10.3.1 represent a considerable contribution toward mapping selective logging, which is one of the processes responsible for forest degradation. However, the application of these techniques has also revealed challenges in separating logging damage from that created by forest fires. For example, SMA fractions have been used to map fire scars of previously logged forests of the eastern Amazon (Cochrane and Souza 1998; Cochrane et al. 1999); the large-area mapping studies of selective logging did not take into account the associated fire impacts on forests (Asner et al. 2005; Matricardi et al. 2007), assuming that the forest damage was created only by logging. Therefore, new classification algorithms were needed to account for the different change dynamics created by logging and fires.

Morton et al. (2011a) proposed a technique, also applied to SMA fractions, to detect the spatial and temporal pattern of forest burn damage and recovery (BDR) in order to distinguish forest degradation from logging and forest fires. The BDR technique was applied to Landsat and MODIS data, with the latter more suitable for mapping large burn scars (i.e., >50 ha). This technique requires robust time series including a postdisturbance recovery signal, meaning that the result is always 1 year out-of-date. An alternative to this method is to use spatial–contextual classifiers to separate logged forest from BFs based on the size and shape of the forest damage (Souza et al. 2005b) or the burn scar index (BSI) (Alencar et al. 2011), which is an SMA fraction-based approach to map BFs. However, these methods do not eliminate all spatial and temporal overlaps between the different degradation processes. Therefore, it is more appropriate to map canopy damage without regard to the cause of forest degradation (either logging or forest fire), and then use contextual information to distinguish the process responsible for the impact.

For example, Figure 10.5 shows the result of a time-series (1984–2010) analysis of deforestation and forest degradation for a Landsat TM scene (226/68) covering Sinop municipality, in Mato Grosso state, southern Amazon region. A decision tree classifier was built and applied to fractions (GV, NPV, soil, and shade) and NDFI derived from SMA to map forest canopy damage caused by selective logging and forest fires every year. Then, forest degradation age and frequency were obtained from these annual maps. Moreover, a carbon emission simulator (CES) (Morton et al. 2011a) model was used to estimate carbon emissions associated with deforestation and forest degradation and associated uncertainty. Forest degradation frequency enables the CES model to keep track of carbon stock reduction; forest degradation age is important to track carbon sequestration due to forest regeneration.

Because CES is based on a Monte Carlo simulation approach, emission factors from deforestation and forest degradation and model parameters are defined as ranges of possible values. For example, forest carbon stock changes due to forest degradation in this region range from 10% to 30% (Figure 10.3). CES runs several times (i.e., at least 100 times), and in each simulation carbon stock changes associated with forest degradation can have any possible value between this range. Here, we assumed a uniform distribution since we do not have sufficient data to define the actual statistical distribution of carbon stock changes in degraded forests. Then, uncertainty of carbon emissions associated with deforestation and forest degradation can be estimated with CES.

The CES results showed that the carbon emissions for the 226/62 Landsat scene covering the Sinop region in Mato Grosso totaled 46.7–82 MgC (i.e., tons of C) from 1984 to 2010 (Figure 10.5). The average total carbon

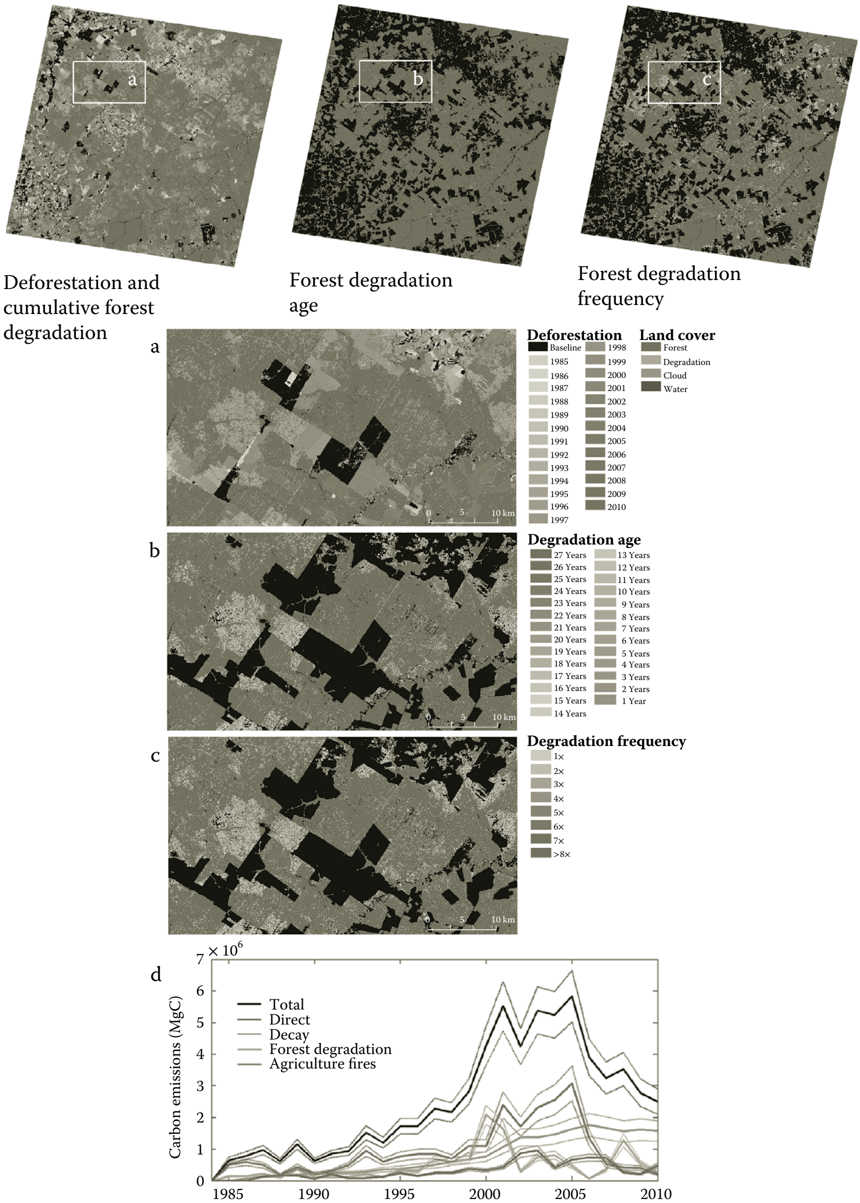

FIGURE 10.5
(See color insert.) In this example, a long time series (i.e., >25 years) of Landsat TM/ETM+ data from Sinop, Mato Grosso state, was used to track deforestation and forest degradation. Forest degradation age and frequency maps are obtained from the annual maps and used together with the forest degradation and deforestation maps in a CES model to estimate carbon emissions associated with these processes. More reliable and consistent baseline scenarios for REDD+ can be obtained with this type of model because information about forest degradation is included and associated uncertainty estimated.

emissions were 66.5 MgC (with 95% CI). Forest degradation contributed 19% (i.e., 8.7–16.3 MgC; average of 8.7 MgC) of the carbon emissions over this 26-year period. However, in 2000, 2007, and 2008, carbon emissions from forest degradation were higher than emissions from direct forest conversion. These results reinforce the need to measure carbon emissions associated with forest degradation (Figure 10.5).

10.4 Forest Monitoring for REDD+

In a recent study conducted in the forests of Mato Grosso state, the sources of uncertainties for carbon emission estimates from deforestation, forest degradation, and forest carbon stocks were identified for the period 1990–2008 (Morton et al. 2011b). The sources of deforestation data showed good agreement for multiyear periods (i.e., 5-year interval), but annual deforestation rates differed by >20%. Data sources of forest carbon stocks ranged more significantly, between 99 and 192 MgC per hectare. Even though there were several ecological studies of the impacts of forest degradation in this region and remote sensing techniques for mapping forest degradation were available, existing maps of forest degradation were scarce. Additionally, the available forest biomass maps did not account for changes in forest carbon stocks due to forest degradation. As a result, full carbon accounting for REDD+ is compromised. The remote sensing techniques described in this chapter can be used to reduce this uncertainty by quantifying annual transitions involving degraded forest and their relation to deforestation and reduction of forest carbon stocks (Figures 10.1 and 10.6).

Selective logging, forest fires, and forest fragmentation are the major sources of depletion of forest carbon stocks in the Amazon region through forest degradation, even though less carbon-impacting forest degradation processes have been recognized (Peres et al. 2006). Therefore, the lessons from the Amazon region regarding characterization of forest degradation through ecological and remote sensing measurements can be useful for establishing a framework for the spatially explicit estimation of carbon emissions and their sources of uncertainty for REDD+ (Figure 10.6). The proposed framework is that of the United Nations Framework Convention on Climate Change (UNFCCC) Approach 3 and Tier 3 forest area change and carbon stocks estimates (Herold et al. 2011).

First, the baseline period for the project must be defined. In our study in Mato Grosso, we concluded that a long (>15 years) historic assessment could help reduce uncertainty in remote sensing data sources. In the example provided in Figure 10.5, 1984 was defined as the baseline year for mapping forest changes. For mapping deforestation, there are several well-established remote sensing techniques and operational monitoring systems in place in

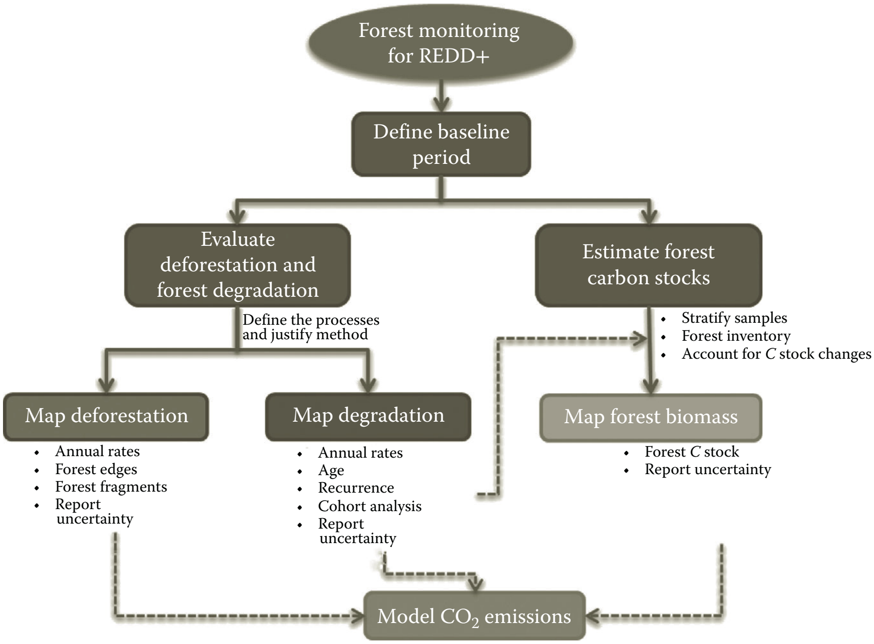

FIGURE 10.6
(See color insert.) Integrating deforestation and forest degradation information to estimate forest carbon stock changes for REDD+ projects.

the Amazon region. For forest degradation, Table 10.1 offers several options to map forest canopy-damaged areas. The reported map accuracy for the methods used to map logging and forest fires ranged from 89% to 93%. However, it is important to previously characterize the processes responsible for degradation in order to support the selection of the remote sensing method.

Deforestation maps over the REDD+ baseline period allow estimation of annual deforestation rates. Additionally, deforestation maps can also inform the length of forest edges and the extent of forest fragmentation. For example, in 1999 and 2002, more than 32,000 km and 38,000 km of new forest edges were created, respectively, as a result of deforestation and selective logging (Broadbent et al. 2008). Information on forest fragmentation and edge effects has not been taken into account in REDD+ projects, but can be a major source of carbon emissions (Numata et al. 2010, 2011). Forest degradation maps are important for providing information on annual rates of degradation and on forest degradation age and recurrence (i.e., frequency). Age and recurrence histories of forest degradation are necessary for updating forest carbon stock maps. Moreover, this information can aid in designing forest inventory sampling stratification schemes to estimate carbon stocks of degraded forests at field level. For example, forest inventories can be conducted in areas that have undergone several cycles of carbon depletion by degradation processes.

Annual maps of forest degradation derived from remote sensing offer a reliable spatiotemporal data set to account for forest carbon stock changes in preparing a REDD+ baseline. Once forest inventories are conducted, spatial interpolation methods can be used to derive forest biomass information over large areas. Kriging interpolation is an approach that has been successfully tested in the Brazilian Amazon to estimate spatially explicit unbiased averages of forest biomass and their associated uncertainty (Sales et al. 2007). Integration of krigged forest biomass maps with maps of deforestation and forest degradation has already been conducted and proven to be useful in reporting carbon emissions associated with these processes (Morton et al. 2011a; Numata et al. 2011).

These results are promising and support the proposed framework (Figure 10.6) for monitoring REDD+ projects. The challenges to applying this framework to other tropical forest regions include the lack of technical capacity for both remote sensing and forest inventory activities. However, options for monitoring forest degradation and deforestation going from a less to more rigorous approach/tier are available (Herold et al. 2011). Nonetheless, there is no technical reason to exclude carbon emissions estimates by forest degradation from REDD+ MRV activities.

10.5 Conclusions

Selective logging, forest fires, and forest fragmentation are the main processes responsible for forest degradation in the Brazilian Amazon. These processes can lead to significant reduction of forest carbon stocks, especially when recurrent forest degradation occurs. Additionally, significant change in forest structure also happens, allowing detection and mapping of forest degradation scars with optical remotely sensed data. A range of 1–30 m of spatial resolution imagery has been tested in the Amazon region for mapping forest degradation, using different techniques. But high spatial resolution imagery such as Landsat has been the most important source of data to map forest degradation in this region. Landsat imagery is important because it covers very large areas and allows to construct very long (i.e., >15 years) historical deforestation and forest degradation credible baseline for REDD+. In terms of techniques, subpixel information derived from SMA offers a better way to enhance forest degradation scars relative to whole-pixel classifiers or textural metrics (which is based on pixel neighborhood information). Moreover, forest change detection algorithms must be designed to track history and recurrent events of forest degradation to better estimate carbon emissions associated with these processes. Therefore, because of the large area affected and high impact on forest carbon stocks, baseline for REDD+ projects in the Amazon region must include annual forest area change and associated carbon emissions due to forest degradation, as demonstrated in this chapter.

Acknowledgments

My research activities on mapping forest degradation in the Brazilian Amazon have been funded by several organizations in the past 10 years. I am grateful to the LBA Research Program funded by NASA and the Brazilian government. I am also thankful to the Gordon and Betty Moore Foundation, the Packard Foundation, and the Avina Foundation for having supported my research and operational projects in Brazil. I would also like to thank Imazon for providing the work conditions to conduct this review. Antônio Victor Fonseca, Marcio Sales, and João Victor Siqueira helped to prepare some figures for this chapter and I would like to thank them.

About the Contributor

Carlos Souza, Jr. is a senior researcher at Imazon, Belém, Pará, Brazil. He received his PhD in geography from the University of California, Santa Barbara, in 2005, and got the Skoll Award for Social Entrepreneurship in 2010 for his contributions on monitoring deforestation and forest degradation in the Brazilian Amazon. His research focuses on development of methods for mapping forest changes with satellite images and modeling carbon emissions associated with forest and land use changes.

References

Adams, J.B. et al., Classification of multispectral images based on fractions of endmembers: Application to land-cover change in the Brazilian Amazon. *Remote Sensing of Environment*, 52, 137, 1995.

Alencar, A. et al., Modeling forest understory fires in an eastern Amazonian landscape. *Ecological Applications*, 14, S139, 2004.

Alencar, A. et al., Temporal variability of forest fires in eastern Amazonia. *Ecological Applications*, 21, 2397, 2011.

Asner, G.P. et al., Remote sensing of selective logging in Amazonia: Assessing limitations based on detailed field observations, Landsat ETM+, and textural analysis. *Remote Sensing of Environment*, 80, 483, 2002.

Asner, G.P. et al., Canopy damage and recovery after selective logging in Amazonia: Field and satellite studies. *Ecological Applications*, 14, S280, 2004a.

Asner, G.P. et al., Spatial and temporal dynamics of forest canopy gaps following selective logging in the eastern Amazon. *Global Change Biology*, 10, 765, 2004b.

Asner, G.P. et al., Selective logging in the Brazilian Amazon. *Science*, 310, 480, 2005.

Asner, G.P. et al., Condition and fate of logged forests in the Brazilian Amazon. *Proceedings of the National Academy of Sciences (PNAS)*, 103 (34), 12947–12950, doi: 10.1073/pnas.0604093103, 2006.

Barros, A.C. and Uhl, C., Logging along the Amazon River and estuary: Patterns, problems and potential. *Forest Ecology and Management*, 77, 87, 1995.

Bateson, C.A. et al., End-member bundles: A new approach to incorporating endmember variability into spectral mixture analysis. *IEEE Transactions on Geoscience and Remote Sensing*, 38, 1083, 2000.

Broadbent, E.N. et al., Forest fragmentation and edge effects from deforestation and selective logging in the Brazilian Amazon. *Biological Conservation*, 141, 1745, 2008.

Cochrane, M.A., Synergistic interactions between habitat fragmentation and fire in evergreen tropical forests. *Conservation Biology*, 15, 1515, 2001.

Cochrane, M.A. and Laurance, W.F., Fire as a large-scale edge effect in Amazonian forests. *Journal of Tropical Ecology*, 18, 311, 2002.

Cochrane, M.A. and Schulze, M.D., Fire as a recurrent event in tropical forests of the eastern Amazon: Effects on forest structure, biomass, and species composition. *Biotropica*, 31, 2, 1999.

Cochrane, M.A. and Souza, C.M., Linear mixture model classification of burned forests in the Eastern Amazon. *International Journal of Remote Sensing*, 19, 3433, 1998.

Cochrane, M.A. et al., Positive feedbacks in the fire dynamic of closed canopy tropical forests. *Science*, 284, 1832, 1999.

Gerwing, J.J., Degradation of forests through logging and fire in the eastern Brazilian Amazon. *Forest Ecology and Management*, 157, 131, 2002.

Graça, P.M.L.A., Santos, J.R., Soares, J.V. and Souza, P.E.U., Desenvolvimento metodológico para detecção e mapeamento de áreas florestais sob exploração madeireira: estudo de caso, região norte do Mato Grosso. In: SIMPÓSIO BRASILEIRO DE SENSORIAMENTO REMOTO, 12. (SBSR), Goiânia. Anais, São José dos Campos: INPE, 1555–1562. CD-ROM, On-line. ISBN 85-17-00018-8. (INPE-12649-PRE/7941). Disponível em: <http://urlib.net/ltid.inpe.br/sbsr/2004/11.16.13.56>. Acesso em: 03 Jul. 2012, 2005.

Herold, M. et al., Options for monitoring and estimating historical carbon emissions from forest degradation in the context of REDD+. *Carbon Balance and Management*, 6, 13, 2011.

Holdsworth, A.R. and Uhl, C., Fire in Amazonian selectively logged rain forest and the potential for fire reduction. *Ecological Applications*, 7, 713, 1997.

Johns, J.S. et al., Logging damage during planned and unplanned logging operations in the eastern Amazon. *Forest Ecology and Management*, 89, 59, 1996.

Keller, M. et al., Biomass estimation in the Tapajos National Forest, Brazil: Examination of sampling and allometric uncertainties. *Forest Ecology and Management*, 154, 371, 2001.

Lambin, E.F., Monitoring forest degradation in tropical regions by remote sensing: Some methodological issues. *Global Ecology and Biogeography,* 8, 191, 1999.

Laurance, W.F., et al., Forest loss and fragmentation in the Amazon: Implications for wildlife conservation. *Oryx,* 34, 39, 2000.

Laurance, W.F. et al., Ecosystem decay of Amazonian forest fragments: A 22-year investigation. *Conservation Biology,* 16, 605, 2002.

Malhi, Y., et al., The regional variation of aboveground live biomass in old-growth Amazonian forests. *Global Change Biology,* 12, 1107, 2006.

Matricardi, E.A.T., Skole, D.L., Chomentowski, W., and Cochrane, M.A., Multi-temporal detection and measurement of selective logging in the Brazilian Amazon using Landsat data. BSRSI/RA03-01/w. Michigan State University, East Lansing, Michigan, 2001.

Matricardi, E. et al., Multi-temporal assessment of selective logging in the Brazilian Amazon using Landsat data. *International Journal of Remote Sensing*, 28, 63, 2007.

Monteiro, A.L. et al., Detection of logging in Amazonian transition forests using spectral mixture models. *International Journal of Remote Sensing*, 24, 151, 2003.

Morton, D.C. et al., Historic emissions from deforestation and forest degradation in Mato Grosso, Brazil: 1) source data uncertainties. *Carbon Balance and Management,* 6, 18, 2011a.

Morton, D.C. et al., Mapping canopy damage from understory fires in Amazon forests using annual time series of Landsat and MODIS data. *Remote Sensing of Environment*, 115, 1706, 2011b.

Nepstad, D.C. et al., Large-scale impoverishment of Amazonian forests by logging and fire. *Nature,* 398, 505, 1999.

Numata, I. et al., Biomass collapse and carbon emissions from forest fragmentation in the Brazilian Amazon. *Journal of Geophysical Research,* 115, G03027, 2010.

Numata, I. et al., Carbon emissions from deforestation and forest fragmentation in the Brazilian Amazon. *Environmental Research Letters*, 6, 044003, 2011.

Pereira, R. et al., Forest canopy damage and recovery in reduced-impact and conventional selective logging in eastern Para, Brazil. *Forest Ecology and Management*, 168, 77, 2002.

Peres, C.A. et al., Detecting anthropogenic disturbance in tropical forests. *Trends in Ecology & Evolution*, 21, 227, 2006.

Read, J.M. et al., Application of merged 1-m and 4-m resolution satellite data to research and management in tropical forests. *Journal of Applied Ecology,* 40, 592, 2003.

Roberts, D.A. et al., Large area mapping of land-cover change in Rondonia using multitemporal spectral mixture analysis and decision tree classifiers. *Journal of Geophysical Research-Atmospheres,* 107, D20, 2002.

Saatchi, S.S. et al., Distribution of aboveground live biomass in the Amazon basin. *Global Change Biology*, 13, 816, 2007.

Sales, M.H. et al., Improving spatial distribution estimation of forest biomass with geostatistics: A case study for Rondonia, Brazil. *Ecological Modelling,* 205, 221, 2007.

Santos, J.R. et al., *Dados multitemporarais TM/Landsat aplicados ao estudo da dinâmica de exploração madeireira na Amazônia*. Simpósio Brasileiro de Sensoriamento Remote, 2001.

Santos, J.R. et al., Change vector analysis technique to monitor selective logging activities in Amazon. Geoscience and Remote Sensing Symposium, IGARSS '03. *Proceedings, 2003 IEEE International,* 4, 2580–2582, doi: 10.1109/IGARSS.2003.1294515, 2003.

Skole, D. and Tucker, C., Tropical deforestation and habitat fragmentation in the Amazon: Satellite data from 1978 to 1988. *Science*, 260, 1905, 1993.
Small, C., The Landsat ETM+ spectral mixing space. *Remote Sensing of Environment*, 93, 1, 2004.
Souza, C. and Barreto, P., An alternative approach for detecting and monitoring selectively logged forests in the Amazon. *International Journal of Remote Sensing*, 21, 173, 2000.
Souza Jr., C. and Roberts, D., Multi-temporal analysis of canopy change due to logging in Amazonian transitional forests with green vegetation fraction images. *Second LBA Scientific Conference*, Manaus, Brazil, July 7–10, 2002 (http://lba.cptec.inpe.br/lba-conf-manaus02-en/accept_abstracts.htm), 2002.
Souza, C.M. and Roberts, D., Mapping forest degradation in the Amazon region with Ikonos images. *International Journal of Remote Sensing*, 26, 425, 2005.
Souza, C. et al., Mapping forest degradation in the Eastern Amazon from SPOT 4 through spectral mixture models. *Remote Sensing of Environment*, 87, 494, 2003.
Souza, C.M. et al., Multitemporal analysis of degraded forests in the southern Brazilian Amazon. *Earth Interactions*, 1–25, 2005a.
Souza, J. et al., Combining spectral and spatial information to map canopy damage from selective logging and forest fires. *Remote Sensing of Environment*, 98, 329, 2005b.
Souza, C. et al., Integrating forest transects and remote sensing data to quantify carbon loss due to forest degradation in the Brazilian Amazon. In *Case Studies on Measuring and Assessing Forest Degradation*. Forest Resources Assessment WorkingPaper161, FAO, Rome, 20 p., 2009.
Stone, T.A. and Lefebvre, P., Using multi-temporal satellite data to evaluate selective logging in Para, Brazil. *International Journal of Remote Sensing*, 19, 2517, 1998.
Verissimo, A. et al., Logging impacts and prospects for sustainable forest management in an old Amazonian frontier: The case of Paragominas. *Forest Ecology and Mana*gement, 55, 169, 1992.
Verissimo, A. et al., Extraction of a high-value natural resource in Amazonia: The case of mahogany. *Forest Ecology and Management*, 72, 39, 1995.
Watrin, O.S. and Rocha, A.M.A., Levantamento da vegetação natural e do uso da terra no Município de Paragominas (PA) utilizando imagens TM/Landsat. *Belém, Boletim de Pesquisa*, n. 124, 40 p. (EMBRAPA/CPATU), 1992.